International Journal of Biomaterials

Dental Implants

Guest Editors: Carlos Nelson Elias, Paulo G. Coelho, and Yoshiki Oshida

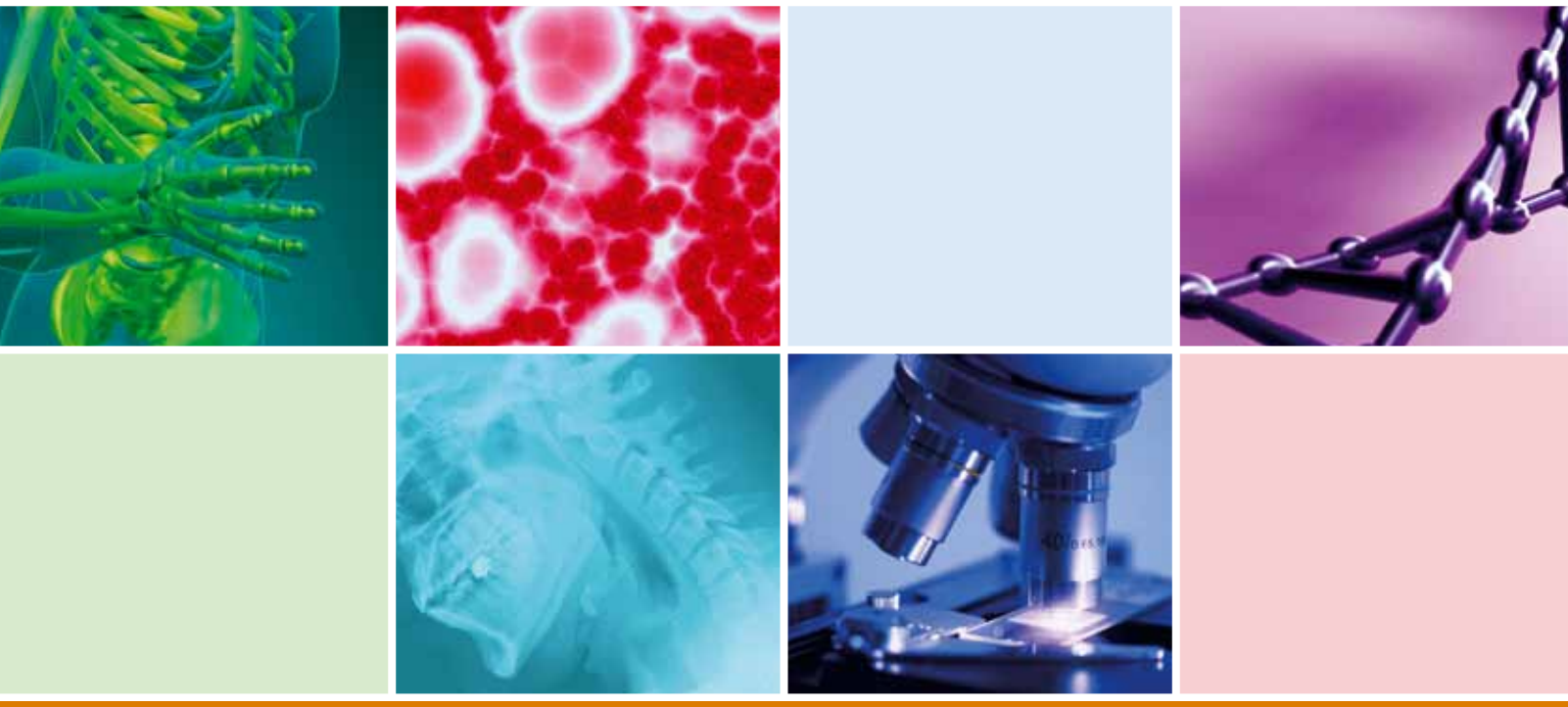

Dental Implants

International Journal of Biomaterials

Dental Implants

Guest Editors: Carlos Nelson Elias, Paulo G. Coelho, and Yoshiki Oshida

Editorial Board

Contents

Dental Implants, Carlos Nelson Elias and Paulo G. Coelho
Volume 2013, Article ID 838565, 2 pages

The Effect of Simplifying Dental Implant Drilling Sequence on Osseointegration: An Experimental Study in Dogs, Gabriela Giro, Nick Tovar, Charles Marin, Estevam A. Bonfante, Ryo Jimbo, Marcelo Suzuki, Malvin N. Janal, and Paulo G. Coelho
Volume 2013, Article ID 230310, 6 pages

Plasma Treatment Maintains Surface Energy of the Implant Surface and Enhances Osseointegration, Fernando P. S. Guastaldi, Daniel Yoo, Charles Marin, Ryo Jimbo, Nick Tovar, Darceny Zanetta-Barbosa, and Paulo G. Coelho
Volume 2013, Article ID 354125, 6 pages

The Effect of Laminin-1-Doped Nanoroughened Implant Surfaces: Gene Expression and Morphological Evaluation, Humberto Osvaldo Schwartz-Filho, Kostas Bougas, Paulo G. Coelho, Ying Xue, Mariko Hayashi, Rafael Silveira Faeda, Rosemary Adriana Chiérici Marcantonio, Daisuke Ono, Fumio Kobayashi, Kamal Mustafa, Ann Wennerberg, and Ryo Jimbo
Volume 2012, Article ID 305638, 9 pages

Bone Morphometric Evaluation around Immediately Placed Implants Covered with Porcine-Derived Pericardium Membrane: An Experimental Study in Dogs, Ryo Jimbo, Charles Marin, Lukasz Witek, Marcelo Suzuki, Nick Tovar, Ioana Chesnoiu-Matei, Irina Florentina Dragan, and Paulo G. Coelho
Volume 2012, Article ID 279167, 7 pages

Preparation of Bioactive Titanium Surfaces via Fluoride and Fibronectin Retention, Carlos Nelson Elias, Patricia Abdo Gravina, Costa e Silva Filho, and Pedro Augusto de Paula Nascente
Volume 2012, Article ID 290179, 7 pages

Novel Implant Coating Agent Promotes Gene Expression of Osteogenic Markers in Rats during Early Osseointegration, Kostas Bougas, Ryo Jimbo, Ying Xue, Kamal Mustafa, and Ann Wennerberg
Volume 2012, Article ID 579274, 9 pages

In Vitro Osteogenic Properties of Two Dental Implant Surfaces, Marta Monjo, Christiane Petzold, Joana Maria Ramis, Staale Petter Lyngstadaas, and Jan Eirik Ellingsen
Volume 2012, Article ID 181024, 14 pages

Effects of Surface Charges on Dental Implants: Past, Present, and Future, Cecilia Yan Guo, Jukka Pekka Matinlinna, and Alexander Tin Hong Tang
Volume 2012, Article ID 381535, 5 pages

Hindawi Publishing Corporation
International Journal of Biomaterials
Volume 2013, Article ID 838565, 2 pages
http://dx.doi.org/10.1155/2013/838565

Editorial
Dental Implants

Carlos Nelson Elias[1] and Paulo G. Coelho[2]

[1] *Department of Mechanical Engineering and Materials Science, Military Institute of Engineering, Rio de Janeiro, RJ, Brazil*
[2] *Department of Biomaterials and Biomimetics, College of Dentistry, New York University, New York, NY 10010, USA*

Correspondence should be addressed to Carlos Nelson Elias; elias@ime.eb.br

Received 16 January 2013; Accepted 16 January 2013

Osseointegration is a major factor influencing the success of dental implants. To achieve rapid and strong durable osseointegration, biomaterial researchers have investigated various surface treatment methods for titanium dental implants. Current dental implant research has studied the interaction between bone and implant surface in order to understand the osseointegration process. This special dental implant issue addresses the role of titanium dental implant surface treatment, chemical or topographic modification, and cells interactions. All these parameters can affect bone healing, promote accelerated osteogenesis, and increase bone-implant contact and bond strength.

The themes include a relevant interest about the properties of dental implant surfaces, analysis of molecular mechanisms which occur at the interface between bone and dental implant, evaluation of the biological behavior of the host's tissues at the interface with the implant, and considerations of implant micro- and nanotopography and its superficial chemical structure. Researchers present their results of investigation of various surface treatment methods for dental titanium implants, show the biological basis for successful implant therapy, and analyzed the effect of plasma fibronectin.

In F. P. S. Guastaldi et al.'s paper, the authors propose a novel plasma treatment for dental implant surfaces. Their results suggested that even after 30 days of plasma treatment, the biological responses were better than those of nontreated surfaces.

In M. Monjo et al.'s paper, the authors compared the cytotoxicity, cell morphology and proliferation, alkaline phosphatase activity, gene expression, and the release of a wide array of osteoblast markers of two commercial titanium (Ti) surfaces (OsseoSpeed and TiOblast). They observed changes in cell shape and BMP-2 secretion after 2 days between the surfaces, and this was followed by increased IGF-I, BSP, osterix gene expression and mineralization after 14 days.

In C. N. Elias et al's paper, the authors research the effects of dental implant surface treatment with fluoride and fibronectin adsorption on the adhesion of osteoblasts. They investigated the biofunctionalization of titanium surfaces and examine their effects on the interaction with osteoblastic cells. They observed that the association indexes of osteoblastic cells in fibronectin-treated samples were significantly higher than those in samples without fibronectin. The radioactivity values suggested that fibronectin incorporation is an important determinant of the *in vitro* cytocompatibility of the surfaces. They concluded that the preparation of bioactive titanium surfaces via fluoride and FN retention proved to be a useful treatment to optimize and to accelerate the osseointegration process of dental implants.

In C. Y. Guo et al.'s paper, the authors focus on surface charge modification on the surface of titanium dental implants. They make an overview on both theoretical explanations on how surface charge affects the implants' osseointegration, as well as a potential surface charge modification method. Additionally, they discuss the insights into the important factors affecting the effectiveness of surface charge modification methods and point out several interesting directions for future investigations on this topic.

In H. O. Schwartz-Filho et al.'s study, they observe the morphological and molecular effect of laminin-1 doping to nanostructured implant surfaces in a rabbit model. They concluded that the protein-doped surface showed higher gene expression of typical genes involved in the osseointegration

cascade than that of the control surface. They observed that the osseointegration cascade begins immediately after the implant is placed in the bone, where the blood contiguously interacts with the implant surface.

We hope that this special issue would attract a major attention of the research community. We would like to express our appreciation to all the authors, reviewers, and the Editor-in-Chief Dr. Mohamed Abdel Razek for the great support that made this special issue possible.

Carlos Nelson Elias
Paulo G. Coelho

Hindawi Publishing Corporation
International Journal of Biomaterials
Volume 2013, Article ID 230310, 6 pages
http://dx.doi.org/10.1155/2013/230310

Research Article

The Effect of Simplifying Dental Implant Drilling Sequence on Osseointegration: An Experimental Study in Dogs

Gabriela Giro,[1] Nick Tovar,[1] Charles Marin,[2] Estevam A. Bonfante,[2] Ryo Jimbo,[3] Marcelo Suzuki,[4] Malvin N. Janal,[5] and Paulo G. Coelho[1,6]

[1] *Department of Biomaterials and Biomimetics, New York University, 345E 24th Street, Room 813A, New York, NY 10010, USA*
[2] *Postgraduate Program in Dentistry, School of Health Sciences, UNIGRANRIO University, Rua Professor José de Souza Herdy, 1.160-25 de Agosto, 25071-202 Duque de Caxias, RJ, Brazil*
[3] *Department of Prosthodontics, Faculty of Odontology, Malmö University, Smedjegatan 16, 214 2 Malmö, Sweden*
[4] *Department of Operative Dentistry and Prosthodontics, Tufts University School of Dental Medicine, One Kneeland Street, Boston, MA 02111, USA*
[5] *Department of Epidemiology and Health Promotion, New York University College of Dentistry, New York, NY 10010, USA*
[6] *Department of Periodontology and Implant Dentistry, New York University College of Dentistry, 345E 24th Street, New York, NY 10010, USA*

Correspondence should be addressed to Estevam A. Bonfante; estevamab@gmail.com

Received 9 October 2012; Accepted 15 December 2012

Academic Editor: Carlos Nelson Elias

Objectives. To test the hypothesis that there would be no differences in osseointegration by reducing the number of drills for site preparation relative to conventional drilling sequence. *Methods*. Seventy-two implants were bilaterally placed in the tibia of 18 beagle dogs and remained for 1, 3, and 5 weeks. Thirty-six implants were 3.75 mm in diameter and the other 36 were 4.2 mm. Half of the implants of each diameter were placed under a simplified technique (pilot drill + final diameter drill) and the other half were placed under conventional drilling where multiple drills of increasing diameter were utilized. After euthanisation, the bone-implant samples were processed and referred to histological analysis. Bone-to-implant contact (BIC) and bone-area-fraction occupancy (BAFO) were assessed. Statistical analyses were performed by GLM ANOVA at 95% level of significance considering implant diameter, time *in vivo,* and drilling procedure as independent variables and BIC and BAFO as the dependent variables. *Results*. Both techniques led to implant integration. No differences in BIC and BAFO were observed between drilling procedures as time elapsed *in vivo*. *Conclusions*. The simplified drilling protocol presented comparable osseointegration outcomes to the conventional protocol, which proved the initial hypothesis.

1. Introduction

Osseointegration has been defined as the intimate contact between bone tissue and implanted biomaterial in the optical microscopy level, and such phenomenon has rendered dental implantology as one of the most successful treatment modalities in both dentistry and medicine [1, 2]. However, while high success rates have been reported (often higher than 90% over a decade), the early failure of the osseointegration has been associated with endogenous factors such as quantity and quality of bone, smoking habits, and host systemic impairment, as well as nutritional status and osteometabolic disorders that may impair bone healing or affect the maintenance of osseointegration. On the other hand, especially in cases where endogenous factors are not present, failure of dental implants has also been attributed to exogenous factors such as implant design (including macro- and microgeometry), surgical technique (excessive surgical trauma), overload, misfit of suprastructures, or surgical site infection [3, 4].

Albrektsson et al. (1981) suggested that there are 6 factors that determine the success of osseointegration, that is, biocompatibility, design, surface, state of the host bed, surgical technique, and loading conditions [5]. Needless to say, the

proposal advocated some 3 decades ago still remains the gold standard for success, and a great number of researches have been conducted on these factors. However, compared to the plethora of studies concerning the implant biocompatibility, design, surface, and loading conditions, the number of studies focusing on the host bed and surgical technique is limited. Especially the effect of surgical procedures such as the drilling protocol has been sparsely explored, and clinicians basically follow the given instructions from the manufacturers.

Previous research has shown that the osteotomy preparation may result in a region of necrotic bone surrounding the inserted implant and that the extent of this region is potentially influenced by the relationship between the drilling speed and heat generated at these sites [6–8]. Thus, it is expected that the amount of damage incurred to bone due to instrumentation, and subsequently its ability to heal around implants may depend on the drill material, design, whether irrigation is external or internal and if at all utilized, the rate which the drilling site diameter is incrementally increased (the number of iteration from initial drill and final drill diameter prior to implant placement). Different drilling parameters have been currently evaluated in laboratory bench studies, where variations in drilling speed have been shown to be potentially beneficial to implant integration [9, 10]. In addition, heat production during drilling has also been evaluated as a function of drill design [11–14], repeated utilization of drill units [15], and irrigation method [16, 17].

With regard to the determination of drilling efficiency and temperature profile as a function of different variables, most investigations are bench studies [9–14, 16, 18], and few represent the osseointegration assessment of implants placed in sites drilled under various conditions [19]. While useful when a numeric control temperature reference is given, these bench studies have not been appropriately validated *in vivo* and such studies are highly desirable.

Even though there are studies investigating the effect of different drilling protocols on osseointegration, little or no data is available regarding the rate in which the drilling site diameter is incrementally increased prior to implant placement, as anecdotally, this procedure has been performed in an incremental drill diameter fashion in an attempt to minimize bone damage during its instrumentation. It is a fact that there is no evidence in the literature whatsoever on the optimal drilling protocol that would result in successful osseointegration in clinical reality. At times, there are drilling protocols that require so many time-consuming steps. It is of great interest to investigate if reducing the number of drills used would provide comparable results to the conventional drilling sequence. Thus, this study tested the hypothesis that no difference in implant osseointegration occurs by reducing the number of drills used for site preparation (pilot drill + final diameter drill) relative to the conventional incremental site preparation.

2. Materials and Methods

This study utilized 72 screw root form endosseous Ti-6Al-4V implants of 3.75 mm ($n = 36$) and 4.2 mm ($n = 36$) in diameter and 10 mm in length (C1, MIS, BarLev Industrial Park, Israel). Half of the implants of each diameter were placed under a simplified technique (pilot drill + final diameter drill) and the other half were placed under the conventional drilling technique where multiple drills of increasing diameter were utilized. Previous atomic force microscopy based texture analysis of the alumina-blasted/acid-etched surface used in the present study were made showing an Sa of 0.35 μm and Sq of 0.5 ± 0.54 μm [20].

Eighteen beagle dogs approximately 1.5 years of age in good health were used in this study under approval of the bioethics committee for animal experimentation at the Ecole Veterinaire D'Alfort, France.

The surgical site was the proximal tibia, a region with a type 2 bone density, and two implants were placed per limb. The right and left limbs provided 3.75 mm and 4.2 mm diameter implants that were placed under the simplified and conventional drilling techniques, respectively (each limb provided samples from the simplified or conventional drilling techniques).

The conventional drilling sequence for the 3.75 mm diameter implants started from the pilot drill (2.4 mm diameter), an intermediate drill (3.0 mm diameter), and then ended with the final drill (3.6 mm maximum diameter provided with each implant). The conventional drilling sequence for the 4.2 mm diameter implants started from the pilot drill (2.4 mm diameter), two intermediate drills (3.0 mm and 3.5 mm in diameter), and then ended with the final drill (4.0 mm in diameter). The simplified drilling sequence for the 3.75 mm and 4.2 mm diameter implants started with the pilot and then the final burs (3.6 mm and 4.0 mm for the 3.75 mm and 4.2 mm diameter implants, resp.). All drilling procedures were conducted at 900 rpm under abundant irrigation.

3. Surgical Procedure

All surgical procedures were performed under general anesthesia. The preanesthetic procedure comprised of an intramuscular administration of atropine sulfate (0.044 mg/kg) and xylazine chlorate (8 mg/kg). General anesthesia was then obtained following an intramuscular injection of ketamine chlorate (15 mg/kg).

Following hair shaving, skin exposure, and antiseptic cleaning with iodine solution at the surgical and surrounding area, a 5 cm incision at the skin level was performed. Then, the flap and muscle layers were reflected and the proximal tibia was exposed.

Two osteotomies were produced at least 10 mm from each other from proximal to distal, and the implants were placed with a torque wrench. Standard layered suture techniques were utilized for wound closure (4–0 Vicryl, internal layers; 4–0 nylon, the skin, Ethicon, Johnson & Johnson, Somerville, NJ). Postsurgical medication included antibiotics (penicillin, 20,000 UI/kg) and analgesics (ketoprofen, 1 mL/5 kg) for a period of 48 h postoperatively.

Euthanasia was performed by an anesthesia overdose ($n = 6$ animals at 1, 3, and 5 weeks after surgery). At necropsy, the limbs were retrieved by sharp dissection, the soft tissue was

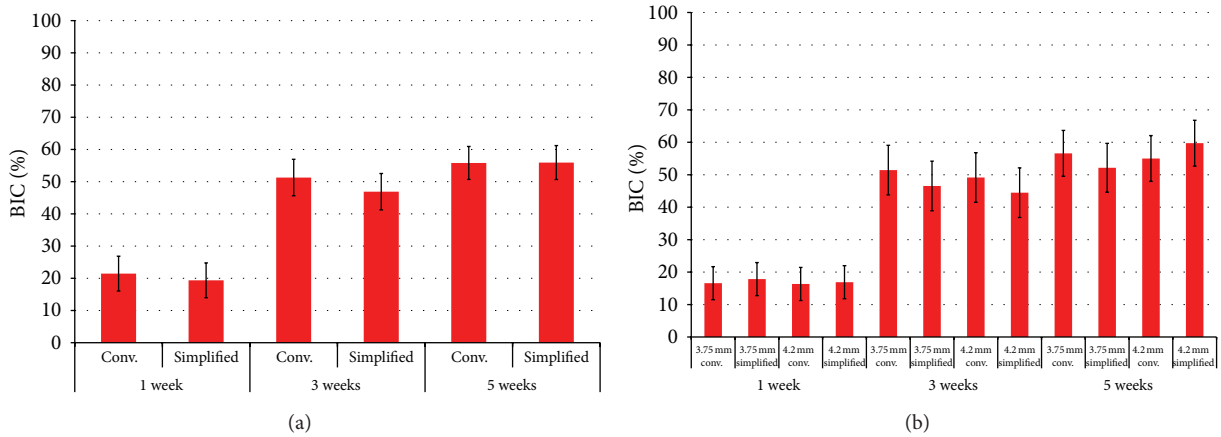

Figure 1: (a) Results for bone-to-implant (BIC) (mean ± 95% CI) as a function of drilling technique and time *in vivo* where no significant differences were observed between groups for each time point *in vivo*. (b) Results for BIC (mean ± 95% CI) as a function of drilling technique, time *in vivo*, and implant diameter. No significant differences were observed between groups for each time point *in vivo*.

removed with surgical blades, and initial clinical evaluation was performed.

4. Hard Tissue Histology Preparation

The specimens were fixed in 10% buffered formalin solution for 24 h, washed in tap water for 24 h, and gradually dehydrated in a series of alcohol solutions ranging from 70% to 100% ethanol. Following dehydration, the samples were embedded in a methacrylate-based resin (Technovit 9100, Heraeus Kulzer GmbH, Wehrheim, Germany) according to the manufacturer's instructions. The blocks were then cut aiming at the center of the implant along its long axis with a precision diamond saw (Isomet 2000, Buehler Ltd., Lake Bluff, IL, USA), glued to acrylic slides with an acrylate-based resin, and a 24 h setting time was allowed prior to grinding and polishing. The sections were then reduced to a final thickness of approximately 30 μm by means of a series of SiC abrasive papers (Buehler Ltd., Lake Bluff, IL, USA) in a grinding/polishing machine (Metaserv 3000, Buehler, Lake Bluff, IL, USA) under water irrigation. The sections were then stained in 1% toluidine blue and referred to light microscopy evaluation.

Measurements of the percentages of bone-to-implant contact (BIC) and bone-area-fraction occupancy (BAFO) between threads [21] were performed at 1001x magnification (Leica DM2500M, Leica Microsystems GmbH, Wetzlar, Germany) by using the National Institutes of Health image analyzer software (ImageJ 1.41o, National Institutes of Health, USA).

The effects of drilling technique, implant diameter, and time *in vivo* on BIC and BAFO were evaluated by a GLM ANOVA. Statistical significance was set at 5% ($\alpha = 0.05$).

5. Results

Bone healing around implants was uneventful following implant placement for all 72 sites. No signs of inflammation or infection were observed during the experimental period.

The statistical summary concerning the effects of drilling technique as a function of time for BIC is presented in Figure 1(a). While a significant increase was observed from 1 to 3 weeks ($P = 0.02$), this difference was not significant from 3 to 5 weeks ($P = 0.82$). The statistical summary for the effect of drilling technique, implant diameter, and time (Figure 1(b)) did not show significant differences in BIC as a function of drilling technique and implant diameter for each time point evaluated.

The statistical summary concerning the effects of drilling technique as a function of time for BAFO is presented in Figure 2(a). While a significant increase in BAFO was observed from 1 to 3 weeks ($P < 0.01$), this difference was not significant from 3 to 5 weeks ($P = 0.85$). The statistical summary concerning the effect of drilling technique, implant diameter, and time (Figure 2(b)) did not depict significant differences in BAFO as a function of drilling technique and implant diameter for each time point evaluated.

No morphologic differences were observed between implants placed with either conventional or simplified techniques, and initial evaluation of the histologic sections at all time points evaluated showed direct contact between implant and bone in cortical and trabecular regions (Figure 3). In general, the histologic evaluation showed that at 1 week, initial woven bone formation occurred in the regions between threads and in direct contact with the implant surface (Figure 4(a)). At three weeks (Figure 4(b)), an increase in the amounts of bone between threads was evident, and ongoing replacement of woven bone by lamellar bone was observed for all groups evaluated at 5 weeks (Figure 4(c)).

6. Discussion

The present study design allowed the evaluation of osseointegration measurable parameters in implants placed in sites that were prepared in an incremental diameter fashion (conventional) or in a two-step fashion (pilot drill + final drill) to final diameters of 3.6 mm and 4.0 mm at 900 rpm under abundant irrigation. Previous research has pointed

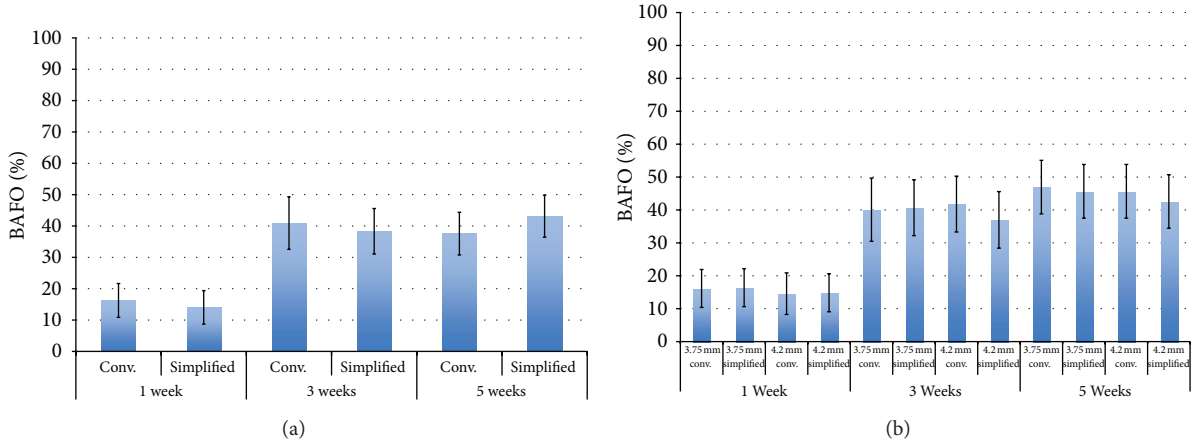

FIGURE 2: (a) Results for bone area fraction occupancy (BAFO) (mean ± 95% CI) as a function of drilling technique and time *in vivo* where no significant differences were observed between groups for each time point *in vivo*. (b) Results for BAFO (mean ± 95% CI) as a function of drilling technique, time *in vivo*, and implant diameter. No significant differences were observed between groups for each time point *in vivo*.

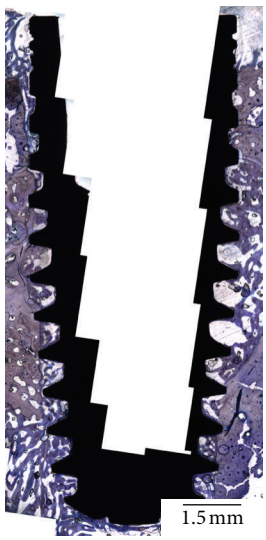

FIGURE 3: No morphologic differences were observed between implants placed with either conventional or simplified techniques. The evaluation of the histologic sections at all time points showed direct contact between implant and bone in cortical and trabecular regions, as showed in this section of a 4.2 mm diameter implant at 5 weeks of healing.

that a region of necrotic bone surrounding the implant exists following surgery and that the extent of this region is influenced by drilling speed [9, 10], design [11–14], and irrigation mode (or absence of irrigation) [14, 15]. For most of the research concerning drills and drilling technique variations, the most commonly measured outcome concerns the heat generated at these sites as a function of different variables always referenced by a suitable control group. Thus, while useful when a numeric control temperature reference is given, these studies and the present study hypothesized that no difference in implant osseointegration occurs by reducing the number of drills for site preparation (pilot drill + final diameter drill) relative to the conventional drilling sequence.

It is known that rises in bone temperature during rotary instrumentation are expected to be higher as a function of diametric differences between drills due to the amount of pressure and cutting necessary for site preparation being proportional to this difference. In fact, thermal osteonecrosis is inexorable if the temperature rises higher than 47°C in the bone [22], which has been reported clinically to be one of the causes of implant periapical lesions [23] or otherwise of a delay in bone regenerative process [24]. Intriguingly, not only did our results depict no differences in BIC and BAFO between drilling techniques when implant diameter information was collapsed from statistical analyses, but also showed no difference in BIC and BAFO as a function of implant diameter and time *in vivo*. Further, the histological observation presented no visible differences for both groups, showing no signs of excessive inflammation, osteoclastic activity, or noticeable necrosis. This is an indication that the temperature elevation, if any created by the simplified procedure, did not have any negative effects as compared to the conventional protocol, and the irrigation was probably sufficient enough to keep the temperature below the osteonecrosis threshold of 47°C. If the temperature exceeded 47°C, the healing probably would have delayed for the simplified protocol group, which would have been evident in the histology or in the histomorphometry as reported by Yoshida et al. [24]. Thus, it is highly desirable that future studies combine methods where correlative statistical inferences between temperature rise and osseointegration/biomechanical measurable parameters are possible in order to allow an informed platform for future surgical drilling protocols.

Since a simplified surgical drilling procedure did not negatively affect the biological response of the implants placed in these sites and was comparable to the conventional drilling sequence, our initial hypothesis that no difference in implant osseointegration occurs by reducing the number of drills for bone site preparation relative to the conventional

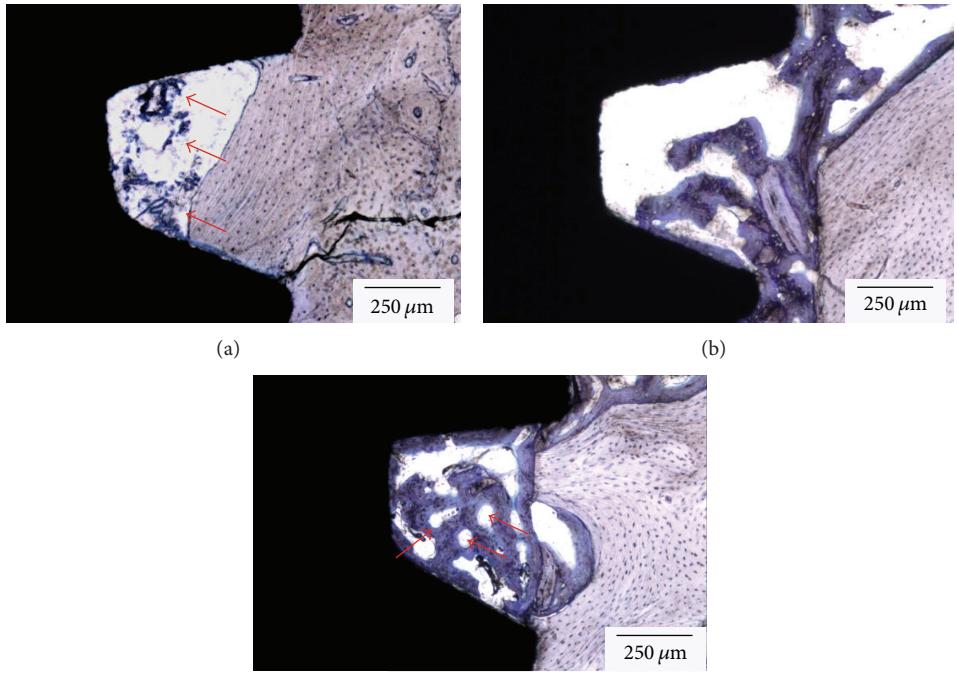

(a) (b)

(c)

Figure 4: Histologic evaluation showed that at (a) 1 week, initial woven bone formation occurred in the regions between threads and in direct contact with the implant surface (arrows). (b) At three weeks, an increase in the amounts of bone between threads was evident, and the (c) onset of replacement of woven bone by lamellar bone was observed for all groups evaluated at 5 weeks (arrows).

drilling sequence was accepted. The results of this study strongly suggest that the osteotomy preparation may be simplified and be less time consuming; however, constant irrigation will always be necessary to avoid the deleterious effect of temperature elevation in the bone, specially in high density bone, such as the mandibular anterior region. Lastly, a precise drilling orientation is required in the first drills, as in other techniques, but with fewer opportunities for angulation corrections, which may demand a steeper learning curve for the less experienced professional.

Conflict of Interests

The authors of this work declare no conflict of interests.

Acknowledgment

This study was partially funded by MIS Implants, Israel.

References

[1] M. Esposito, J. M. Hirsch, U. Lekholm, and P. Thomsen, "Biological factors contributing to failures of osseointegrated oral implants. (I). Success criteria and epidemiology," *European Journal of Oral Sciences*, vol. 106, no. 1, pp. 527–551, 1998.

[2] P. I. Brånemark, R. Adell, U. Breine, B. O. Hansson, J. Lindström, and A. Ohlsson, "Intra-osseous anchorage of dental prostheses. I. Experimental studies," *Scandinavian Journal of Plastic and Reconstructive Surgery*, vol. 3, no. 2, pp. 81–100, 1969.

[3] T. Albrektsson, J. Brunski, and A. Wennerberg, "'A requiem for the periodontal ligament' revisited," *International Journal of Prosthodontics*, vol. 22, no. 2, pp. 120–122, 2009.

[4] M. Esposito, J. M. Hirsch, U. Lekholm, and P. Thomsen, "Biological factors contributing to failures of osseointegrated oral implants: (II). Etiopathogenesis," *European Journal of Oral Sciences*, vol. 106, no. 3, pp. 721–764, 1998.

[5] T. Albrektsson, P. I. Branemark, H. A. Hansson, and J. Lindstrom, "Osseointegrated titanium implants. Requirements for ensuring a long-lasting, direct bone-to-implant anchorage in man," *Acta Orthopaedica Scandinavica*, vol. 52, no. 2, pp. 155–170, 1981.

[6] S. Iyer, C. Weiss, and A. Mehta, "Effects of drill speed on heat production and the rate and quality of bone formation in dental implant osteotomies. Part I: relationship between drill speed and heat production," *International Journal of Prosthodontics*, vol. 10, no. 5, pp. 411–414, 1997.

[7] G. Augustin, S. Davila, K. Mihoci, T. Udiljak, D. S. Vedrina, and A. Antabak, "Thermal osteonecrosis and bone drilling parameters revisited," *Archives of Orthopaedic and Trauma Surgery*, vol. 128, no. 1, pp. 71–77, 2008.

[8] Y. Reingewirtz, S. Szmukler-Moncler, and B. Senger, "Influence of different parameters on bone heating and drilling time in implantology," *Clinical Oral Implants Research*, vol. 8, no. 3, pp. 189–197, 1997.

[9] M. Sharawy, C. E. Misch, N. Weller, and S. Tehemar, "Heat generation during implant drilling: the significance of motor speed," *Journal of Oral and Maxillofacial Surgery*, vol. 60, no. 10, pp. 1160–1169, 2002.

[10] S. J. Kim, J. Yoo, Y. S. Kim, and S. W. Shin, "Temperature change in pig rib bone during implant site preparation by low-speed

drilling," *Journal of Applied Oral Science*, vol. 18, no. 5, pp. 522–527, 2010.

[11] G. E. Chacon, D. L. Bower, P. E. Larsen, E. A. McGlumphy, and F. M. Beck, "Heat production by 3 implant drill systems after repeated drilling and sterilization," *Journal of Oral and Maxillofacial Surgery*, vol. 64, no. 2, pp. 265–269, 2006.

[12] M. Sumer, A. F. Misir, N. T. Telcioglu, A. U. Guler, and M. Yenisey, "Comparison of heat generation during implant drilling using stainless steel and ceramic drills," *Journal of Oral and Maxillofacial Surgery*, vol. 69, no. 5, pp. 1350–1354, 2011.

[13] H. J. Oh, U. M. Wikesjö, H. S. Kang, Y. Ku, T. G. Eom, and K. T. Koo, "Effect of implant drill characteristics on heat generation in osteotomy sites: a pilot study," *Clinical Oral Implants Research*, vol. 22, no. 7, pp. 722–726, 2011.

[14] A. Scarano, A. Piattelli, B. Assenza et al., "Infrared thermographic evaluation of temperature modifications induced during implant site preparation with cylindrical versus conical drills," *Clinical Implant Dentistry and Related Research*, vol. 13, no. 4, pp. 319–323, 2011.

[15] A. C. Carvalho, T. P. Queiroz, R. Okamoto, R. Margonar, I. R. Garcia Jr., and O. M. Filho, "Evaluation of bone heating, immediate bone cell viability, and wear of high-resistance drills after the creation of implant osteotomies in rabbit tibias," *International Journal of Oral and Maxillofacial Implants*, vol. 26, no. 6, pp. 1193–1201, 2011.

[16] I. C. Benington, P. A. Biagioni, J. Briggs, S. Sheridan, and P. J. Lamey, "Thermal changes observed at implant sites during internal and external irrigation," *Clinical Oral Implants Research*, vol. 13, no. 3, pp. 293–297, 2002.

[17] D. Flanagan, "Osteotomy irrigation: is it necessary?" *Implant Dentistry*, vol. 19, no. 3, pp. 241–249, 2010.

[18] A. Rashad, A. Kaiser, N. Prochnow, I. Schmitz, E. Hoffmann, and P. Maurer, "Heat production during different ultrasonic and conventional osteotomy preparations for dental implants," *Clinical Oral Implants Research*, vol. 22, no. 12, pp. 1361–1365, 2011.

[19] G. Giro, C. Marin, R. Granato et al., "Effect of drilling technique on the early integration of plateau root form endosteal implants: an experimental study in dogs," *Journal of Oral and Maxillofacial Surgery*, vol. 69, no. 8, pp. 2158–2163, 2011.

[20] C. Marin, R. Granato, M. Suzuki et al., "Biomechanical and histomorphometric analysis of etched and non-etched resorbable blasting media processed implant surfaces: an experimental study in dogs," *Journal of the Mechanical Behavior of Biomedical Materials*, vol. 3, no. 5, pp. 382–391, 2010.

[21] G. Leonard, P. Coelho, I. Polyzois, L. Stassen, and N. Claffey, "A study of the bone healing kinetics of plateau versus screw root design titanium dental implants," *Clinical Oral Implants Research*, vol. 20, no. 3, pp. 232–239, 2009.

[22] G. Augustin, S. Davila, T. Udilljak, T. Staroveski, D. Brezak, and S. Babic, "Temperature changes during cortical bone drilling with a newly designed step drill and an internally cooled drill," *International Orthopaedics*, vol. 36, no. 7, pp. 1449–1456, 2012.

[23] G. M. Reiser and M. Nevins, "The implant periapical lesion: etiology, prevention, and treatment," *Compendium of Continuing Education in Dentistry*, vol. 16, no. 8, pp. 768–772, 1995.

[24] K. Yoshida, K. Uoshima, K. Oda, and T. Maeda, "Influence of heat stress to matrix on bone formation," *Clinical Oral Implants Research*, vol. 20, no. 8, pp. 782–790, 2009.

Hindawi Publishing Corporation
International Journal of Biomaterials
Volume 2013, Article ID 354125, 6 pages
http://dx.doi.org/10.1155/2013/354125

Research Article

Plasma Treatment Maintains Surface Energy of the Implant Surface and Enhances Osseointegration

Fernando P. S. Guastaldi,[1,2] Daniel Yoo,[1] Charles Marin,[3] Ryo Jimbo,[4] Nick Tovar,[1] Darceny Zanetta-Barbosa,[5] and Paulo G. Coelho[1]

[1] *Department of Biomaterials and Biomimetics, College of Dentistry, New York University, Room 813a, 345 East 24th Street, New York, NY 10010, USA*
[2] *Department of Surgery and Integrated Clinic, São Paulo State University, 16015 Araçatuba, SP, Brazil*
[3] *Department of Postgraduate Dentistry, UNIGRANRIO, 25071 Duque de Caxias, RJ, Brazil*
[4] *Department of Prosthodontics, Faculty of Odontology, Malmö University, 205 06 Malmö, Sweden*
[5] *Department of Oral & Maxillofacial Surgery and Implantology, University of Uberlândia, 38408 Uberlândia, MG, Brazil*

Correspondence should be addressed to Paulo G. Coelho; pc92@nyu.edu

Received 31 October 2012; Accepted 25 November 2012

Academic Editor: Carlos Nelson Elias

The surface energy of the implant surface has an impact on osseointegration. In this study, 2 surfaces: nonwashed resorbable blasting media (NWRBM; control) and Ar-based nonthermal plasma 30 days (Plasma 30 days; experimental), were investigated with a focus on the surface energy. The surface energy was characterized by the Owens-Wendt-Rabel-Kaelble method and the chemistry by X-ray photoelectron spectroscopy (XPS). Five adult beagle dogs received 8 implants ($n = 2$ per surface, per tibia). After 2 weeks, the animals were euthanized, and half of the implants ($n = 20$) were removal torqued and the other half were histologically processed ($n = 20$). The bone-to-implant contact (BIC) and bone area fraction occupancy (BAFO) were evaluated on the histologic sections. The XPS analysis showed peaks of C, Ca, O, and P for the control and experimental surfaces. While no significant difference was observed for BIC parameter ($P > 0.75$), a higher level for torque ($P < 0.02$) and BAFO parameter ($P < 0.01$) was observed for the experimental group. The surface elemental chemistry was modified by the plasma and lasted for 30 days after treatment resulting in improved biomechanical fixation and bone formation at 2 weeks compared to the control group.

1. Introduction

The interaction between the implant surface and the living body begins soon after the placement of the biomaterial in the body, and it has always been a challenge to determine the optimal modification to accelerate the biologic events which lead to faster osseointegration [1–3].

Since it has been proven that moderately rough surfaces outperform the turned surfaces [4–8], recent research has focused on further modifications that could possibly increase the bioactivity of the implant [9]. Thus, some of the state-of-the-art research has shifted to chemically modify moderately rough surfaces, which have been indicated to generate synergetic effects [10, 11]. Furthermore, the surface energy is another important factor involved in the regulation of osteogenesis. It has been said that depending on the surface energy, the surface state can either be hydrophilic or hydrophobic [12]. The energy state of the implant depends on the type of biomaterial, the handling during manufacturing, the mode of cleaning, sterilization, and needless to say, the handling of the implant during surgical procedure [13, 14]. In general, when the surface is positively charged, the surface turns hydrophilic and some of the plasma proteins essential for the initial osteogenic interactions adsorb to hydrophilic surfaces [15–17]. It has been suggested that the charge of the implant surface can be altered by oxidization [18], chemical and topographical modification [19, 20], and by plasma treatment [3, 14].

Plasma treatment is an interesting method to modify the implant surface. Not only can this treatment alter the

surface charge, but this treatment can also alter the chemistry and the topography [21–23]. Thermal plasma treatment has been traditionally used as a method to utilize hydroxyapatite coatings on implant surfaces (plasma spraying) [24, 25]. Another form of plasma treatment, the atmospheric pressure (cold) plasmas, has shown to alter the surface energy and the chemistry due to the generation of high concentration of reactive species that are generated [21, 22]. This has been reported to be beneficial for the enhancement of osteogenic responses, as Duske et al. reported that surfaces treated with atmospheric plasma significantly enhanced the wettability and improved the initial cellular interaction [23].

The application of atmospheric plasma is increasing in numerous situations especially in the biomedical field due to their practical capability to low temperature providing plasmas that are not spatially bound or confined by electrodes [26, 27]. Moreover, this efficient and cost-effective process presents a potential benefit to any commercially available implant surface and has shown positive host-to-implant response when implants were plasma treated immediately prior to placement in the surgical sites [3]. While promising results have been achieved by the atmospheric treatment of endosseous implants prior to placement, it is also of interest to evaluate whether such surface modification is effective over longer periods of time, since the surface may be contaminated when the implant is reexposed to air [14, 28]. Stachowski et al. has reported that there is a possibility to maintain the high surface energy state of the titanium implant for at least 30 days, depending on various factors such as storage conditions [29]. The reason for 30 days storage of plasma-treated implants is to simulate a scenario of large-scale production by dental implants manufacturers, where the storage after surface modification may occur for several days prior to reaching the dental practitioner.

Thus, the objective of the present study was to investigate whether the biologic effect of an argon-based nonthermal plasma-treated dental implant surface stored for 30 days before the placement is still effective in terms of surface charge as compared to its untreated counterpart.

2. Materials and Methods

This study utilized 3.75 mm in diameter by 10 mm length nonwashed resorbable blasting media surface implants (Touareg with Osseofix Surface, Adin Dental Implants Systems Ltd., Afula, Israel). Half of the samples utilized were plasma treated 30 days prior to implantation (20 implants; experimental group), and the other half were placed as provided by the manufacturer (20 implants; control group). In summary, the control surface is fabricated by grit-blasting the surface with a proprietary bioactive ceramic powder prior to cleaning and sterilization, resulting in a textured surface with amounts of Ca and P close to 10% of the implant surface area.

The plasma was applied with a KinPen device (length = 155 mm, diameter = 20 mm, weight = 170 g) (INP-Greif-Swald, Germany). The KinPen was used for the generation of a plasma jet at atmospheric pressure connected to a high-frequency power supply (1.5 MHz, 2–6 kV peak-to-peak, system power 230 V, 65 W), and the gas supply unit was connected to a gas controller (Multi Gas Controller 647C, MKS Instruments, Andover, MA). Argon tanks were attached to the gas controller with gas flow set at 5 standard liters per minute (slm). The plasma-treated implants were stored in their original vials before surgery for a period of thirty days.

Six implants of each treatment (plasma 30 days prior to placement, plasma immediately prior to surface characterization, and control) were referred to physicochemical characterization. The surface morphology was observed by scanning electron microscopy (SEM, Philips XL 30, Eindhoven, The Netherlands) at ×5000 magnification and an acceleration voltage of 20 kV ($n = 3$ per surface).

In order to assess the surface energy of the surfaces, the Owens-Wendt-Rabel-Kaelble method was utilized [30]. For this purpose, 500 μL droplets of distilled water, ethylene glycol, and diiodomethane were deposited on the surface of each implant group with a micropipette (OCA 30, Data Physics Instruments GmbH, Filderstadt, Germany). Images were captured and analyzed using software (SCA30, version 3.4.6 build 79). The relationship between the contact angle and surface energy was determined and was calculated by $\gamma_L = \gamma_L^D + \gamma_L^P$, where γ_L is the surface energy, γ_L^D is the disperse component, and γ_L^P is the polar component.

Surface-specific chemical assessment was performed by X-ray photoelectron spectroscopy (XPS). The implants ($n = 3$, each group) were inserted in a vacuum transfer chamber and degassed to 10^{-7} torr. The samples were then transferred under vacuum to a Kratos Axis 165 multitechnique XPS spectrometer (Kratos Analytical, Chestnut Ridge, NY). Survey and high-resolution spectra were obtained using a 165 mm mean radius concentric hemispherical analyzer operated at constant pass energy of 160 eV for survey and 80 eV for high resolution scans. The take-off angle was 90°, and a spot size of 150 μm × 150 μm was used. The implant surfaces were evaluated at various locations.

Five male adult beagle dogs (approximately 1.5 years of age) were used for the study under approval of the bioethics committee for animal experimentation (CEUA 172/11) at the Universidade Federal de Uberlandia, Brazil. The pre anesthetic procedure comprised an intramuscular administration of atropine sulfate (0.044 mg/Kg) and xylazine chlorate (8 mg/Kg). General anaesthesia was then obtained following an intramuscular injection of ketamine chlorate (15 mg/Kg). Surgical procedures for bone access and wound closure have been described in detail elsewhere [31, 32].

The different implant surfaces were alternately placed from proximal to distal at distances of 1 cm from each other along the central region of the bone, and the start surface site (control and experimental) was alternated between animals. The implant distribution resulted in an equal number of implants for the 2-week comparison for both surfaces.

Postsurgical medication included antibiotics (penicillin, 20.000 UI/Kg) and analgesics (ketoprofen, 1 mL/5 Kg) for a period of 48 hours postoperatively. The animals were euthanized after a postsurgical period of 2 weeks by anesthesia overdose and the tibiae were retrieved by sharp dissection. Half of the implants were removal torqued and the other

half were referred to nondecalcified histology processing as reported previously.

Histomorphometric analyses were carried out for each implant with the measurement of bone-to-implant contact (BIC) and bone area fraction occupancy (BAFO). The bone-to-implant contact (BIC) was determined at 50X–200X magnification (Leica DM2500 M, Leica Microsystems GmbH, Wetzlar, Germany) by means of computer software (Leica 8 Application Suite, Leica Microsystems GmbH, Wetzlar, Germany). The regions of bone-to-implant contact along the implant perimeter were subtracted from the total implant perimeter, and calculations were performed to determine the BIC percentage. The bone area fraction occupancy (BAFO) between threads in both cortical and trabecular bone regions was determined at 100X magnification (Leica DM2500 M, Leica Microsystems GmbH, Wetzlar, Germany) by means of computer software (Leica Application Suite, Leica Microsystems GmbH, Wetzlar, Germany). The areas occupied by bone were subtracted from the total area between threads, and calculations were performed to determine the BAFO (reported in percentage values of bone area fraction occupancy) [33].

Following the data normality check, statistical analysis was performed by paired t-tests at 95% level of significance.

3. Results

The scanning electron micrographs of the implant surface revealed a textured microstructure (Figure 1(a)). The surface energy assessment showed a substantial increase in both polar and disperses components immediately after plasma treatment and a slight decrease in both components 30 days after plasma treatment. Relative to untreated surfaces (control), the 30-day plasma-treated surfaces (experimental) presented higher polar and disperse components and an overall higher surface energy (Figure 1(b)).

The XPS analysis showed peaks of Ti, V, Al, C, Ca, O, and P for both groups tested. The control surface presented atomic percent values of 32.9, 9.8, 41.3, and 8.3 for C, Ca, O, and P, respectively, while the surface analyzed immediately after plasma treatment presented atomic percent values of 15.3, 12.2, 50.3 and 9.3 for C, Ca, O, and P, respectively. Relative to the control surface, the experimental surface presented increases in Ca, O, and P atomic percent levels at 10.4, 46.8, and 8.4, respectively, in addition to a decrease in C content at 24.6 atomic percent (Table 1).

No complications during animal surgical procedures and followup were observed, and all implants were clinically stable immediately after euthanasia. While no significant difference was observed for BIC parameter ($P > 0.75$), significantly higher levels of BAFO ($P < 0.01$) and torque ($P < 0.02$) were observed for the experimental group (Figures 2(a)–2(c)).

The histologic sections of the experimental group showed initial bone formation adjacent to the implant surface and the presence of layers of early connective tissue filling the region threads in a more intimate fashion than the control implants (Figure 3). In addition, the bone filled the region between implant threads in proximity to the implant inner diameter for the experimental group. Such observation could not be identified for the control group, where the bone formed

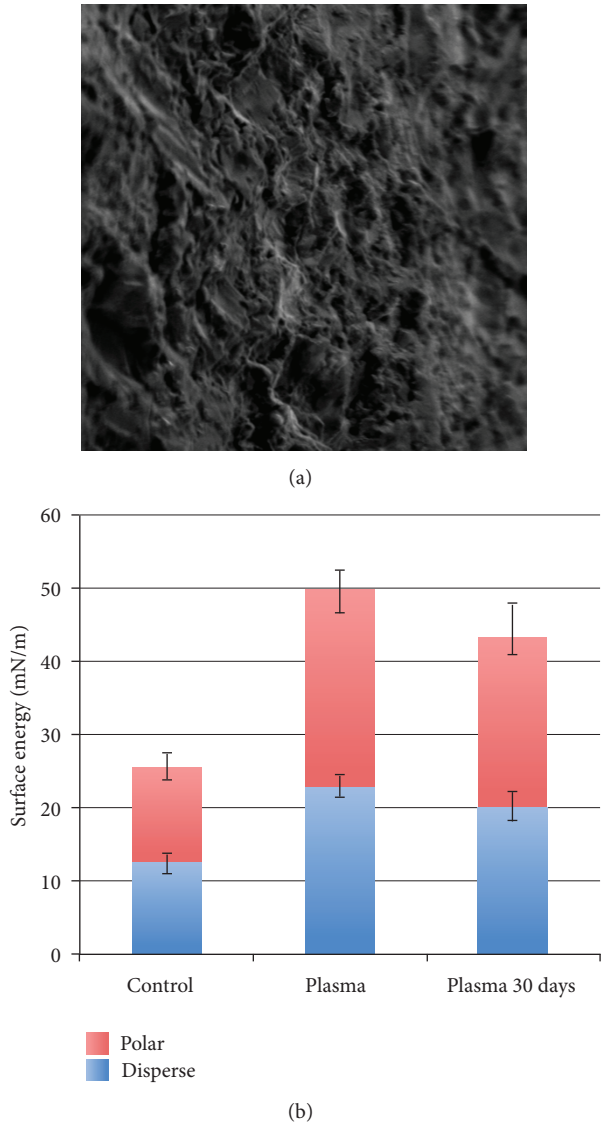

Figure 1: (a) Scanning electron microscopy micrograph (1000X) of the NWRBM implant surface and (b) surface energy measurements of the different groups (mean ± SD).

Table 1: X-ray photoelectron spectroscopy (XPS) spectra for both NWRBM, immediately treated plasma (Plasma), and Plasma 30 days surfaces (mean ± SD).

Chemical element (%)	NWRBM	Plasma	Plasma 30 days
Al2p	1.04 (0.2)	3.94 (1.2)	2.8 (1.5)
C1s	32.91 (2.1)	15.25 (1.6)	24.6 (3.3)
Ca2p	9.84 (1.1)	12.2 (2.1)	10.4 (2.4)
o1s	41.27 (3.2)	50.3 (3.7)	46.8 (5.2)
P2p	8.28 (0.8)	9.3 (1.6)	8.4 (2.7)
Ti2p	3.01 (0.4)	5.2 (1.4)	4.6 (2.3)
V2p3	0.16 (0.2)	0.9 (0.5)	0.7 (0.5)

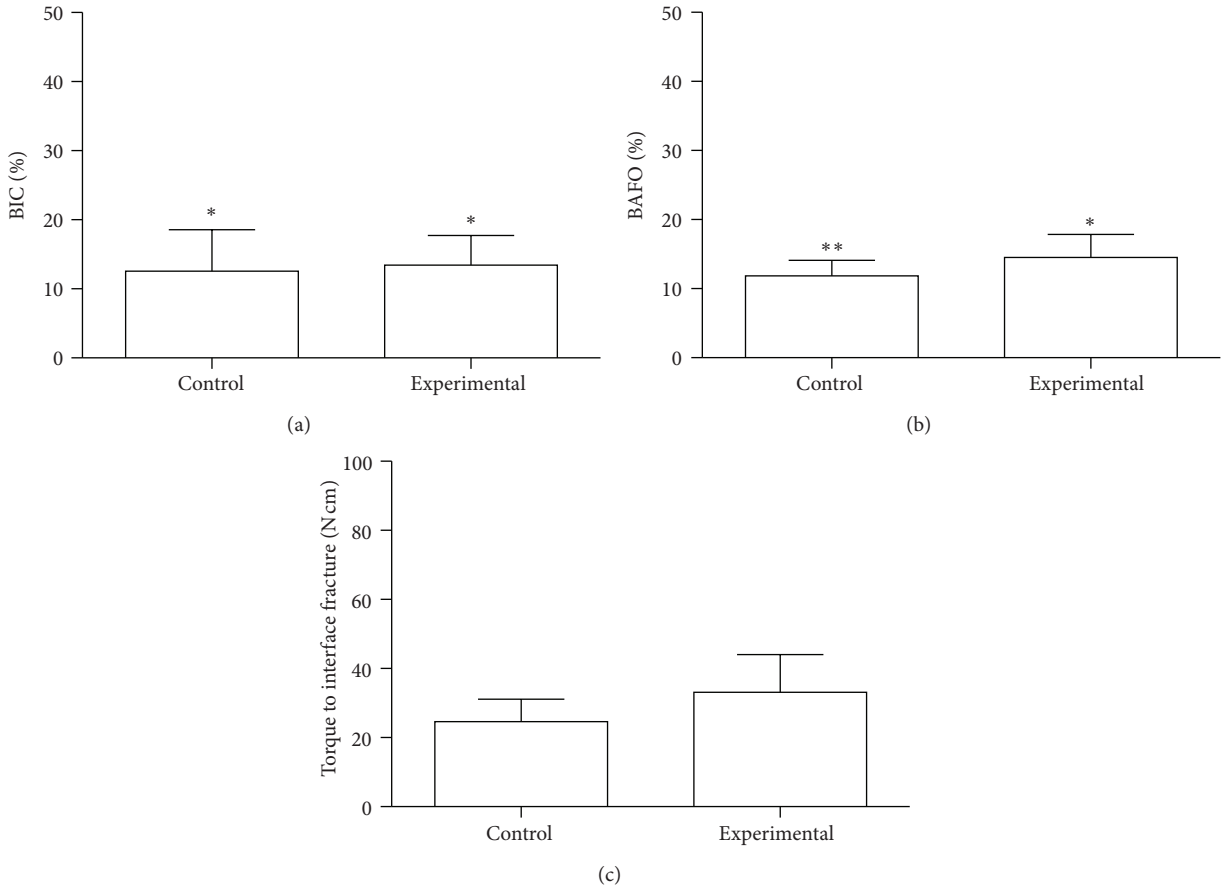

Figure 2: (a) Bone-to-implant contact (BIC), (b) bone area fraction occupancy (BAFO) percentages, and (c) raw torque data (mean ± 95% CI) for the control and experimental groups in the experimental period. The number of asterisks depicts statistically homogeneous groups.

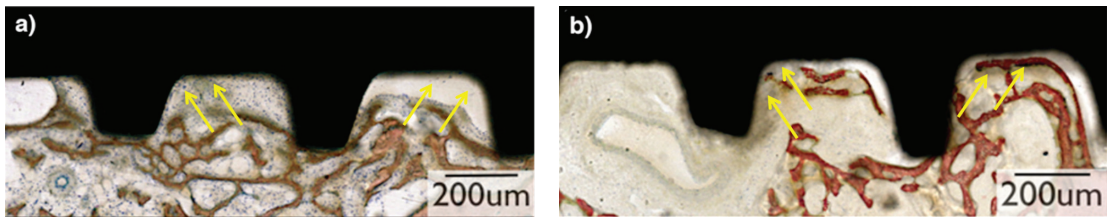

Figure 3: Representative overview of the histological micrographs of the plateaus at 2-week experimental period. (a) The histologic sections of the NWRBM group although presented layers of early connective tissue (stroma) filling the region between plateaus (arrows), there are some areas that the stroma collapsed (arrows). (b) The histologic sections of the Plasma 30 days group showed initial signs of bone formation adjacent to the implant surface (arrows) and the presence of layers of early connective tissue (stroma) filling the region between plateaus without detachment of the surface (arrows).

distant from the implant inner diameter and the osteogenic connective tissue was not in as intimate contact with the implant surface as the experimental group (Figure 3).

4. Discussion

Previous SEM and optical interferometry assessment showed that the roughness of the utilized in the present study was similar to that of several other commercially available products [1, 34]. From a surface chemistry standpoint, the nonwashed resorbable blasting media treatment resulted in Ca and P comprising close to 10% of the surface elemental chemistry.

The surface energy assessment after Ar-based nonthermal plasma (NTP) application showed a substantial increase in surface energy (in both polar and disperse components) for the implants immediately after plasma treatment and that such increase was slightly lost 30 days after treatment. The disperse component of the surface energy characterizes the interaction between the surface and the dispensed liquid in

terms of the nonpolar interactions between molecules. The roughness, unevenness, and the branching level of the surface determine this component. The polar component of the surface energy characterizes the polar interaction between the surface of the material and the working fluid. This component is determined by the presence of polar groups, electric charges, and free radicals on the surface [35].

The XPS results showed that surface elemental chemistry was modified by the Ar-based NTP treatment and that this change resulted in a higher degree of exposure of the surface chemical elements mainly at the expense of the removal of adsorbed C species immediately after plasma treatment [34]. Such surface exposure also slightly decreased as a function of time after plasma treatment as the 30-day plasma-treated group (experimental) presented elemental chemistry and showed evidence of adsorbed carbon species on the surface relative to implants evaluated immediately after plasma treatment. Nonetheless, relative to the control group a higher amount of surface exposure was still detected and was likely related to the removal of the adsorbed C species from the surface. Overall, both surface energy and XPS results supported that the plasma treatment presented potential of changing bone healing kinetics after placement 30 days after argon plasma treatment as surface energy and chemistry were still altered relative to the control group, suggesting that the effect of the plasma treatment was still effective after 30 days of storage.

Unlike our previous studies where the KinPen device was utilized immediately prior to implant placement, the present study considered that the device may not be readily available to all clinicians but utilized by implant manufacturers several days before the implant is placed. Thus, the present investigation is the first of a series of studies necessary to support the application of plasma on implants surface and prove the maintenance of their chemical properties over short and long periods of storage.

The histologic study suggested that intimate interaction between tissues and implant surface occurred for the experimental group relative to the control. It is probable that more intimate relationship between the collagen fibers in the bone and implant surface resulted in the significantly higher torque and BAFO results detected for the experimental group.

These results obtained in the present study are in agreement with previous work that showed that surface wettability is beneficial in hastening osseointegration at early times *in vivo* [15, 36–39]. It has been demonstrated that increasing the surface energy of a grit-blasted implant surface by means of proprietary cleaning and storage in isotonic solution hastened osseointegration of dental implants at early implantation times relative to controls presenting the same surface roughness profile but lower surface energy levels [15].

In contrast to NTP treatment, where any given implant surface may be treated immediately prior to placement, the implant is stored in isotonic solution, so that the gain in surface energy is maintained. In contrast to this scenario, NTPs applied immediately prior to implantation has shown to be effective in altering the surface energy and chemistry resulting in a hastened host-to-implant response; however, concerns related to NTPs potential shelf life has been raised [3, 37, 40].

The present study partially answers the question as to whether NTPs present adequate shelf life for potential manufacturing based surface treatment, and further studies concerning longer periods of time are warranted. It is acknowledged that the main limitation of the present study is the absence of implants treated with plasma immediately prior to implantation, and such limitation impaired the evaluation of relative changes in bone response to NTP treated implants stored for 30 days in comparison to its treated and immediately placed counterpart.

5. Conclusion

Our results demonstrated that the surface elemental chemistry was modified by the plasma and lasted for 30 days after treatment, resulting in improved biomechanical fixation and bone formation at shortly after implantation compared to the control group.

Acknowledgment

The present study was partially supported by Adin Dental Implants and Fapemig.

References

[1] P. G. Coelho, J. M. Granjeiro, G. E. Romanos et al., "Basic research methods and current trends of dental implant surfaces," *Journal of Biomedical Materials Research B*, vol. 88, no. 2, pp. 579–596, 2009.

[2] R. Jimbo, T. Sawase, Y. Shibata et al., "Enhanced osseointegration by the chemotactic activity of plasma fibronectin for cellular fibronectin positive cells," *Biomaterials*, vol. 28, no. 24, pp. 3469–3477, 2007.

[3] P. G. Coelho, G. Giro, H. S. Teixeira et al., "Argon-based atmospheric pressure plasma enhances early bone response to rough titanium surfaces," *Journal of Biomedical Materials Research A*, vol. 100, pp. 1901–1906, 2012.

[4] T. Albrektsson and A. Wennerberg, "Oral implant surfaces: part 1-review focusing on topographic and chemical properties of different surfaces and in vivo responses to them," *International Journal of Prosthodontics*, vol. 17, no. 5, pp. 536–543, 2004.

[5] T. Albrektsson and A. Wennerberg, "Oral implant surfaces: part 2-review focusing on clinical knowledge of different surfaces," *International Journal of Prosthodontics*, vol. 17, no. 5, pp. 544–564, 2004.

[6] A. Wennerberg and T. Albrektsson, "On implant surfaces: a review of current knowledge and opinions," *The International Journal of Oral & Maxillofacial Implants*, vol. 25, no. 1, pp. 63–74, 2010.

[7] T. Albrektsson, D. Buser, and L. Sennerby, "on crestal/marginal bone loss around dental implants," *The International Journal of Oral & Maxillofacial Implants*, vol. 27, pp. 736–738, 2012.

[8] T. Albrektsson, D. Buser, and L. Sennerby, "On crestal/marginal bone loss around dental implants," *The International Journal of Prosthodontics*, vol. 25, pp. 320–322, 2012.

[9] A. Göransson, A. Arvidsson, F. Currie et al., "An in vitro comparison of possibly bioactive titanium implant surfaces,"

Journal of Biomedical Materials Research A, vol. 88, no. 4, pp. 1037–1047, 2009.

[10] B. S. Kang, Y. T. Sul, S. J. Oh, H. J. Lee, and T. Albrektsson, "XPS, AES and SEM analysis of recent dental implants," *Acta Biomaterialia*, vol. 5, no. 6, pp. 2222–2229, 2009.

[11] R. Jimbo, J. Sotres, C. Johansson, K. Breding, F. Currie, and A. Wennerberg, "The biological response to three different nanostructures applied on smooth implant surfaces," *Clinical Oral Implants Research*, vol. 23, no. 6, pp. 706–712, 2012.

[12] T. Sawase, R. Jimbo, K. Baba, Y. Shibata, T. Ikeda, and M. Atsuta, "Photo-induced hydrophilicity enhances initial cell behavior and early bone apposition," *Clinical Oral Implants Research*, vol. 19, no. 5, pp. 491–496, 2008.

[13] R. E. Baier, A. E. Meyer, and J. R. Natiella, "Surface properties determine bioadhesive outcomes: methods and results," *Journal of Biomedical Materials Research*, vol. 18, no. 4, pp. 337–355, 1984.

[14] L. V. Carlsson, T. Alberktsson, and C. Berman, "Bone response to plasma-cleaned titanium implants," *The International Journal of Oral & Maxillofacial Implants*, vol. 4, no. 3, pp. 199–204, 1989.

[15] D. Buser, N. Broggini, M. Wieland et al., "Enhanced bone apposition to a chemically modified SLA titanium surface," *Journal of Dental Research*, vol. 83, no. 7, pp. 529–533, 2004.

[16] O. Santos, I. E. Svendsen, L. Lindh, and T. Arnebrant, "Adsorption of HSA, IgG and laminin-1 on model titania surfaces—effects of glow discharge treatment on competitively adsorbed film composition," *Biofouling*, vol. 27, pp. 1003–1015, 2011.

[17] R. Jimbo, M. Ivarsson, A. Koskela, Y.-T Sul, and C. B. Johansson, "Protein adsorption to surface chemistry and crystal structure modification of titanium surfaces," *Journal of Oral & Maxillofacial Research*, vol. 1, no. 3, article e3, 2010.

[18] R. Jimbo, T. Sawase, K. Baba, T. Kurogi, Y. Shibata, and M. Atsuta, "Enhanced initial cell responses to chemically modified anodized titanium," *Clinical Implant Dentistry and Related Research*, vol. 10, no. 1, pp. 55–61, 2008.

[19] M. Hayashi, R. Jimbo, L. Lindh et al., "In vitro characterization and osteoblast responses to nanostructured photocatalytic TiO_2 coated surfaces," *Acta Biomaterialia*, vol. 8, pp. 2411–2416, 2012.

[20] J. Karlsson, R. Jimbo, H. M. Fathali et al., "In vivo biomechanical stability of osseointegrating mesoporous TiO_2 implants," *Acta Biomaterialia*, vol. 8, no. 12, pp. 4438–4446, 2012.

[21] R. Foest, E. Kindel, A. Ohl, M. Stieber, and K. D. Weltmann, "Non-thermal atmospheric pressure discharges for surface modification," *Plasma Physics and Controlled Fusion*, vol. 47, no. 12, pp. B525–B536, 2005.

[22] R. Foest, M. Schmidt, and K. Becker, "Microplasmas, an emerging field of low-temperature plasma science and technology," *International Journal of Mass Spectrometry*, vol. 248, no. 3, pp. 87–102, 2006.

[23] K. Duske, I. Koban, E. Kindel et al., "Atmospheric plasma enhances wettability and cell spreading on dental implant metals," *Journal of Clinical Periodontology*, vol. 39, pp. 400–407, 2012.

[24] T. Albrektsson, "Hydroxyapatite-coated implants: a case against their use," *Journal of Oral and Maxillofacial Surgery*, vol. 56, no. 11, pp. 1312–1326, 1998.

[25] A. Quaranta, G. Iezzi, A. Scarano et al., "A histomorphometric study of nanothickness and plasma-sprayed calcium-phosphorous-coated implant surfaces in rabbit bone," *Journal of Periodontology*, vol. 81, no. 4, pp. 556–561, 2010.

[26] M. Laroussi and T. Akan, "Arc-free atmospheric pressure cold plasma jets: a review," *Plasma Processes and Polymers*, vol. 4, no. 9, pp. 777–788, 2007.

[27] B. Eliasson and U. Kogelschatz, "Modeling and applications of silent discharge plasmas," *IEEE Transactions on Plasma Science*, vol. 19, no. 2, pp. 309–323, 1991.

[28] T. Sawase, R. Jimbo, A. Wennerberg, N. Suketa, Y. Tanaka, and M. Atsuta, "A novel characteristic of porous titanium oxide implants," *Clinical Oral Implants Research*, vol. 18, no. 6, pp. 680–685, 2007.

[29] M. J. Stachowski, J. Medige, and R. E. Baier, "Methodology for testing the mechanical properties of the bone/titanium implant interface," in *Environmental Degradation of Engineering Materials*, vol. 3, pp. 493–500, University Park: Pensilvania State University, 1987.

[30] R. J. Good and C. J. van Oss, *Modern Approaches to Wettability: Theory and Applications*, Edited by M. E. Schrader, G.I. Loeb, Plenum Press, New York, NY, USA, 1992.

[31] P. G. Coelho, M. Suzuki, M. V. Guimaraes et al., "Early bone healing around different implant bulk designs and surgical techniques: a study in dogs," *Clinical Implant Dentistry and Related Research*, vol. 12, no. 3, pp. 202–208, 2010.

[32] C. Marin, R. Granato, M. Suzuki et al., "Biomechanical and histomorphometric analysis of etched and non-etched resorbable blasting media processed implant surfaces: an experimental study in dogs," *Journal of the Mechanical Behavior of Biomedical Materials*, vol. 3, no. 5, pp. 382–391, 2010.

[33] G. Leonard, P. Coelho, I. Polyzois, L. Stassen, and N. Claffey, "A study of the bone healing kinetics of plateau versus screw root design titanium dental implants," *Clinical Oral Implants Research*, vol. 20, no. 3, pp. 232–239, 2009.

[34] P. G. Coelho and J. E. Lemons, "Physico/chemical characterization and in vivo evaluation of nanothickness bioceramic depositions on alumina-blasted/acid-etched Ti-6Al-4V implant surfaces," *Journal of Biomedical Materials Research A*, vol. 90, no. 2, pp. 351–361, 2009.

[35] D. Staack, A. Fridman, A. Gutsol, Y. Gogotsi, and G. Friedman, "Nanoscale corona discharge in liquids, enabling nanosecond optical emission spectroscopy," *Angewandte Chemie*, vol. 47, no. 42, pp. 8020–8024, 2008.

[36] P. G. Coelho, C. Marin, R. Granato, G. Giro, M. Suzuki, and E. A. Bonfante, "Biomechanical and histologic evaluation of non-washed resorbable blasting media and alumina-blasted/acid-etched surfaces," *Clinical Oral Implants Research*, vol. 23, pp. 132–135, 2012.

[37] G. Giro, N. Tovar, L. Witek et al., "Osseointegration assessment of chairside argon-based nonthermal plasma-treated Ca-P coated dental implants," *Journal of Biomedical Materials Research A*, vol. 101, no. 1, pp. 98–103, 2013.

[38] Y. Hirakawa, R. Jimbo, Y. Shibata, I. Watanabe, A. Wennerberg, and T. Sawase, "Accelerated bone formation onphoto-induced hydrophilic titanium implants: an experimental study in the dog mandible," *Clinical Oral Implants Research*. In press.

[39] R. Jimbo, D. Ono, Y. Hirakawa, T. Odatsu, T. Tanaka, and T. Sawase, "Accelerated photo-induced hydrophilicity promotes osseointegration: an animal study," *Clinical Implant Dentistry and Related Research*, vol. 13, pp. 79–85, 2011.

[40] H. S. Teixeira, C. Marin, L. Witek et al., "Assessment of a chairside argon-based non-thermal plasma treatment on the surface characteristics and integration of dental implants with textured surfaces," *Journal of the Mechanical Behavior of Biomedical Materials*, vol. 9, pp. 45–49, 2012.

Hindawi Publishing Corporation
International Journal of Biomaterials
Volume 2012, Article ID 305638, 9 pages
doi:10.1155/2012/305638

Research Article

The Effect of Laminin-1-Doped Nanoroughened Implant Surfaces: Gene Expression and Morphological Evaluation

Humberto Osvaldo Schwartz-Filho,[1,2] Kostas Bougas,[1] Paulo G. Coelho,[3] Ying Xue,[4] Mariko Hayashi,[1] Rafael Silveira Faeda,[2] Rosemary Adriana Chiérici Marcantonio,[2] Daisuke Ono,[5] Fumio Kobayashi,[6] Kamal Mustafa,[4] Ann Wennerberg,[1] and Ryo Jimbo[1]

[1] *Department of Prosthodontics, Faculty of Odontology, Malmö University, 205 06 Malmö, Sweden*
[2] *Division of Periodontology, Department of Oral Diagnosis and Surgery, School of Dentistry, UNESP, São Paulo State University, 01049-010 Araraquara, SP, Brazil*
[3] *Department of Biomaterials and Biomimetics, New York University, New York, NY 10010, USA*
[4] *Department of Clinical Dentistry, Center for Clinical Dental Research, University of Bergen, 5020 Bergen, Norway*
[5] *Division of Applied Prosthodontics, Nagasaki University Graduate School of Biomedical Sciences, Nagasaki 852-8102, Japan*
[6] *Private Practice, Kobe 658-0012, Japan*

Correspondence should be addressed to Paulo G. Coelho, paulogcoelho@me.com

Received 17 August 2012; Accepted 13 October 2012

Academic Editor: Carlos Nelson Elias

Aim. This study aimed to observe the morphological and molecular effect of laminin-1 doping to nanostructured implant surfaces in a rabbit model. *Materials and Methods*. Nanostructured implants were coated with laminin-1 (test; dilution, 100 μg/mL) and inserted into the rabbit tibiae. Noncoated implants were used as controls. After 2 weeks of healing, the implants were removed and subjected to morphological analysis using scanning electron microscopy (SEM) and gene expression analysis using the real-time reverse transcriptase-polymerase chain reaction (RT-PCR). *Results*. SEM revealed bony tissue attachment for both control and test implants. Real-time RT-PCR analysis showed that the expression of osteoblast markers RUNX-2, osteocalcin, alkaline phosphatase, and collagen I was higher (1.62-fold, 1.53-fold, 1.97-fold, and 1.04-fold, resp.) for the implants modified by laminin-1 relative to the control. All osteoclast markers investigated in the study presented higher expression on the test implants than controls as follows: tartrate-resistant acid phosphatase (1.67-fold), calcitonin receptor (1.35-fold), and ATPase (1.25-fold). The test implants demonstrated higher expression of inflammatory markers interleukin-10 (1.53-fold) and tumour necrosis factor-α (1.61-fold) relative to controls. *Conclusion*. The protein-doped surface showed higher gene expression of typical genes involved in the osseointegration cascade than the control surface.

1. Introduction

The osseointegration cascade begins immediately after the implant is placed in the bone, where the blood contiguously interacts with the implant surface. Irrespective of the biomaterial, surface topography, or wettability status of the surface, the initial contact with blood will rapidly attract proteins [1], which in turn will initiate the process of bone formation [2, 3]. In fact, protein adsorption to the implant surface has been suggested to be important for the osteoconduction stage of osseointegration [4–6]. Studies have also investigated the significance of the protein-implant interaction phenomenon [7–9], in which some proteins significantly enhance migration, attachment, proliferation, and differentiation at the implant surface [8]. Protein adsorption to biomaterials is intriguing since one specific protein never remains in a single niche for extended periods of time and constantly undergoes alterations depending on its molecular weight [10]. The so-called "Vroman effect" is an indication that proteins play different roles in biological reactions. For example, the effect of plasma fibronectin has been thoroughly studied along with bone biomechanical properties, and it has been

reported to play an important role in the migration and attachment of mesenchymal cells and to be a regulator of bone density [11, 12]. Another example is collagen type I, which is the major constituent protein of the bone matrix, assembles in the presence of fibronectin [13], and is thereby considered indispensible protein for osteogenesis [14]. Hence, intentionally doping implant surfaces with proteins that have direct relationship with osteogenic events such as bone matrix formation may improve both the quality and the quantity of osseointegration [8, 15–18].

When protein doping implant surfaces that are typically textured (rough), further topographical alterations may occur and might therefore affect cell adhesion and differentiation by potentially enhancing the effects of adsorbed protein layers [19]. In addition, it has been suggested that substrate surfaces possessing nanostructures show a high affinity for protein adsorption [20–22]. As reported by Puckett et al., intentionally applied nanogrooved surfaces presented higher fibronectin attachment compared to the control surfaces (no grooves) [21]. Such surface topography may be suitable for sustaining higher volumes of target proteins and thus may facilitate implant adherence for a longer duration [8], supposedly owing to the augmented surface area rendered by such length scale texturization. It has been reported that cell morphology, cytoskeleton and adhesion formation, and then subsequent cell growth and differentiation are altered by nanotopographies, thereby stimulating the osteoprogenitor cell differentiation towards an osteoblastic phenotype [23]. These findings are confirmed by another study conducted in human embryonic palatal mesenchymal cells. Apart from alterations in cell morphology, it was demonstrated that an increased gene expression of the osteoblastic markers, Runx-2, and osteocalcin was evident when the cells were cultured on rough and grooved implant surfaces as compared to tissue culture plastic [24].

In the present study, we have focused on a potential osteogenesis-enhancing protein, namely, laminin-1, which is a heterotrimeric glycoprotein that contains an arginine-glycine-aspartic acid (RGD) sequence [25]. RGD is an integrin receptor binder, which is commonly found within the extracellular matrix proteins, and is the most widely occurring cell adhesive motif recognised by about 50% of all known integrins such as $\alpha_2\beta_1$, $\alpha_3\beta_1$, $\alpha_5\beta_1$, $\alpha_V\beta_1$, $\alpha_V\beta_3$, $\alpha_V\beta_5$, and $\alpha_6\beta_4$ [26]. It has been reported that when applied to implant surfaces, the RGD sequence-impregnated modification significantly hastens osseointegration [27, 28] and upregulates the osteoblast focal adhesion through integrin-mediated mechanisms [29]. Besides the well-known bone forming ability of the RGD sequence, another interesting feature of laminin-1 is that it has the ability to selectively recruit osteoprogenitor cells [30].

Another reported feature of the laminin-1 is that it may possibly act as a nucleation center for the precipitation of calcium phosphates (CaP) [31]. It was shown that in a model using the simulated body fluid (SBF), the titanium surface presented more CaP precipitation when laminin-1 was added to the SBF than SBF alone. Thus, it can be hypothesised that this unique protein may have an impact on the initial responses of implant-bone interactions.

The aim of the present study was to dope an implant surface presenting nanostructures with laminin-1 and observe the biological response at the implant interface. We hypothesised that the addition of laminin-1 would enhance osteogenic markers in the early stages of osseointegration. To test our hypothesis, implants were placed in rabbit tibiae for two weeks; bone morphology and total mRNA were extracted to evaluate the expression of genes involved in the inflammation and bone remodelling processes.

2. Materials and Methods

2.1. Surface Characterization. Scanning electron microscopy (SEM) (LEO 440-Zeiss, Oberkochen, Germany) was used for the assessment of surface morphology.

The topography of the control implants was characterized using an interferometer (MicroXam; ADE Phase Shift Technology Inc., Tucson, AZ, USA). The parametric calculation was performed after form errors and waviness were removed with a $50\,\mu m \times 50\,\mu m$ Gaussian filter. The following three-dimensional parameters were selected: S_a (μm), the arithmetic average height deviation from a mean plane; S_{ds} (μm^{-2}), the density of summits, and S_{dr} (%), the developed surface ratio. Three implants were randomly selected for the analysis.

2.2. Implants and Laminin Coating. Commercially pure titanium (Grade 4) implants (Neodent, Curitiba, Parana, Brazil, length, 2 mm; diameter, 1.5 mm) were used. The surface was nanotextured by treating it with a solution consisting of equal volumes of concentrated H_2SO_4 and 30% aqueous H_2O_2 for 2 h at room temperature under sterile conditions [32].

Laminin-1 (L2020, Sigma-Aldrich, Stockholm, Sweden) was diluted to a concentration of 100 μg/mL in Dulbecco's phosphate-buffered saline (DPBS) without $CaCl_2$ or $MgCl_2$ (14190-094; GIBCO, Invitrogen Corporation, Grand Island, NY, USA). The implants were subsequently incubated in 48-well plates (Nunclon Surface, Nunc, Roskilde, Denmark) containing 250 μL of the laminin solution per well for 1 h at room temperature.

To characterize the coated laminin-1, ellipsometry was used in order to estimate the amount of adsorbed laminin-1 on optically smooth titanium surfaces. The descriptive methodology can be found in a study by Linderbäck et al. [33]. In brief, cleaned SiO_2 surfaces were placed in an evaporation chamber with final pressure below 1×10^{-8} Torr. Approximately 200 nm of titanium was physical vapour deposited (PVD) and spontaneously oxidized at room conditions. Thereafter, the prepared surfaces were fixed in the ellipsometric quvette filled with PBS at room temperature. Angles Δ_0 and Ψ_0 were measured in three locations with a Rudolph Research AutoEL III ellipsometer operating in a wavelength of 632.8 nm at a 70° angle of incidence. The quvette was emptied and filled with laminin-1 solution and new angles Δ and Ψ were calculated. The thickness of the adsorbed protein was estimated to be 26 Å by using the MacCrackin algorithm [34].

2.3. Animals and Implant Surgery. Nine lop-eared male rabbits (mean body weight, 4.0 kg) were used for the study. One test (laminin-1-coated) implant and one control (non-coated) implant were inserted into the left and right tibial metaphysis, respectively. The animal study was approved by the Malmö/Lund, Sweden regional animal ethics committee (approval number: M282-09).

Before surgery, the hind legs were shaved and disinfected with 70% ethanol and 70% chlorhexidine. The animals were anaesthetised with intramuscular injections of a mixture of 0.15 mL/kg medetomidine (1 mg/mL Dormitor; Orion Pharma, Sollentuna, Sweden) and 0.35 mL/kg ketamine hydrochloride (50 mg/mL Ketalar; Pfizer AB, Sollentuna, Sweden). Lidocaine hydrochloride (Xylocaine; AstraZeneca AB, Södertälje, Sweden) was administrated as the local anaesthetic at each insertion site at a dose of 1 mL. After the operation, buprenorphine hydrochloride (0.5 mL Temgesic; Reckitt Benckiser, Slough, UK) was administered as an analgesic for 3 days. After 2 weeks, the rabbits were sacrificed with an overdose (60 mg/mL) of pentobarbital natrium (Apoteksbolaget AB, Stockholm, Sweden).

2.4. Observation of the Implant Interface by SEM. Implants from both groups ($n = 3$) were removed from the tibiae, cleaned in 4% neutral-buffered formaldehyde solution for 10 min, dehydrated using an ascending series of ethanol, and dried. The retrieved implant samples were observed using SEM under various magnifications.

2.5. Extraction of RNA and Real-Time RT-PCR. For gene expression analysis, both control and test groups from all 9 rabbits were removed and the retrieved samples were placed in RNA later solution (QIAGEN GmbH, Hilden, Germany) until analysis. In order to obtain detectable RNA, each of the 9 samples in the control and test groups were pooled for RNA isolation. Total RNA was isolated from the surrounding tissue using Trizol reagent (Gibco BRL, Carlsbad, CA, USA) and EZNA tissue RNA isolation kit (Omega Bio-Tek, Norcross, GA, USA). Total RNA was quantified using a nanodrop spectrophotometer (Thermo Scientific NanoDrop Technologies, Wilmington, DE).

The reverse transcription reaction test was performed according to the manufacturer's instructions, using the high capacity cDNA archive kit (Applied Biosystems, Foster City, USA). 600 ng total RNA was mixed with 100 uL reaction volume of reverse transcriptase (RT) buffer, primers, nuclease-free water, and MultiScribe RT.

Real-time quantitative PCR was conducted under standard enzyme and cycling conditions on a StepOne system, using custom-designed real-time assays and SYBR green detection (PrimerDesign Ltd., Southampton, UK) (Table 1). cDNA corresponding to 6 ng of mRNA was used in each PCR reaction, and mixtures were prepared according to the manufacturer's instructions in 10 μL triplicates for each target cDNA. Amplification was carried out in 96-well thermal cycle plates on a StepOne system (Applied Biosystems). The data were analysed using a comparative Ct method by StepOne. Gene expression levels were normalized with the housekeeping gene β-actin. Glyceraldehyde-3-phosphate dehydrogenase (GAPDH) served as an endogenous control.

3. Results

3.1. Implant Characterization. The SEM image for the surface of the nanostructures is presented in Figures 1(a)–1(c), which depicted homogeneous nanostructures covering the entire implant surface. Nanostructures below 50 nm were identified at higher magnification images (Figure 1(c)).

The mean $S_a \pm$ (SD) was $0.28 \pm (0.07)\,\mu$m; $S_{ds} \pm$ (SD) was 195,203 (7,871); $S_{dr} \pm$ (SD) was 8.15 (0.53)%. Figure 1(d) shows three-dimensional optical interferometry image of the surface.

3.2. Scanning Electron Microscopic Observation of the Retrieved Implants. Out of the 3 samples of each group, Figures 2(a)–2(d) present representative electron micrographs for the samples that remained for 2 weeks *in vivo*. In both control and test implants, remnants of some bony tissue were visible. No remarkable morphologic and quantitative differences were observed between the 2 groups.

3.3. Gene Expression. The results of real-time RT-PCR are presented in Figure 3. In general, the osteoblast markers that presented higher expression in the case of the test implants were RUNX-2 (1.62-fold), osteoclcin (1.53-fold), alkaline phosphatase (ALP) (1.97-fold), and collagen I (1.04-fold). On the other hand, the expression of IGF-1 was low (0.84-fold). In the case of the test implants, all osteoclast markers investigated in the present study showed higher expression for the experimental group relative to control, namely, tartrate-resistant acid phosphatase (TRAP) (1.67-fold), calcitonin receptor (1.35-fold), and ATPase (1.25-fold). The inflammatory markers that showed higher expression for the test implants than the control implants were IL-10 (1.53-fold) and TNF-α (1.61-fold), whereas IL-6 showed lower expression (0.59-fold).

4. Discussion

Protein doping is considered one of the promising methods of surface modifications for hastening the early stages of osseointegration both qualitatively and quantitatively [8, 27, 35, 36]. In most studies concerning protein doping of implant surfaces, the beneficial enhancements were primarily restricted to the initial stages of healing and have been shown to have smaller effects when longer periods of experimental time were observed. Such early effect may be related to competitive protein adsorption, and thereby given the protein adsorption desorption dynamics at the implant surface region, protein doping of implant surfaces is indeed expected to be effective in the initial stages of osseointegration. Such an improvement and upregulation of the early bone response is of great clinical importance since it is in both practitioners' and patients' interest that implants osseointegrate faster for shortening the treatment period.

Table 1: Primers used and specific parameters of the real-time PCR.

Gene	Primer sequence	Tm	Amplicon size (bp)	Primer source
ALP	S TGGACCTCGTGGACATCTG A CAGGAGTTCAGTGCGGTTC	75	80	Oryctolagus cuniculus
ATPase	S CCTGGCTATTGGCTGTTACG A GCTGGTAGAAGGACACTCTTG	77.7	98	Oryctolagus cuniculus
Calcitonin receptor	S CGTTCACTCCTGAAAACTACA A GCAACCAAGACTAATGAAACA	72.6	128	Oryctolagus cuniculus
Collagen I	S GGAAACGATGGTGCTACTGG A CCGACAGCTCCAGGGAAG	80.4	83	Oryctolagus cuniculus
IGF-1	S CCGACATGCCCAAGACTCA A TACTTCCTTTCCTTCTCCTCTGA	70.3	81	Oryctolagus cuniculus
IL-6	S GAGGAAAGAGATGTGTGACCAT A AGCATCCGTCTTCTTCTATCAG	73.5	104	Oryctolagus cuniculus
IL-10	S CCGACTGAGGCTTCCATTCC A CAGAGGGTAAGAGGGAGCT	73.3	75	Oryctolagus cuniculus
Osteocalcin	S GCTCAHCCTTCGTGTCCAAG A CCGTCGATCAGTTGGCGC	77.8	70	Oryctolagus cuniculus
Runx2	S GCAGTTCCCAAGCATTTCATC A GTGTAAGTAAAGGTGGCTGGATA	72.8	81	Oryctolagus cuniculus
TNF-α	S CTCACTACTCCCAGGTTCTCT A TTGATGGCAGAGAGGAGGTT	78.2	122	Oryctolagus cuniculus
TRAP	S GCTACCTCCGCTTCCACTA A GCAGCCTGGTCTTGAAGAG	78.5	129	Oryctolagus cuniculus
β-actin	S CACCCTGATGCTCAAGTACC A CGCAGCTCGTTGTAGAAGG	76.4	96	Oryctolagus cuniculus

The results obtained by RT-PCR showed distinct differences between the nanostructured surface with/without laminin-1-coating. Evaluation of the selected osteoblastogenesis-related markers revealed that most of the markers showed higher expression around laminin-1-coated implants relative to the control implant group. It is of great interest that the expression levels of ALP, RUNX-2, and collagen I were higher in the case of the laminin-1-coated implant since these markers are indicators of higher osteoprogenitor and osteoblast precursor activity [37]. In addition, the higher expression of osteocalcin, the specific marker for bone formation, indicates that the differentiation activity of cells into osteoblasts was upregulated around laminin-1-coated implants [38]. On the other hand, lower amounts of IGF-1 expression (reported to promote osteoblast activity [39] and osteoblast proliferation [40]) were detected around laminin-1-coated implants, indicating that the proliferation activity at the interface was suppressed. While our results are contradictory concerning the early osteogenic events, osteoblast proliferation and differentiation activity have been previously reported to be contradictory [41, 42]. Thus, the doped laminin may have suppressed proliferation while upregulating differentiation.

Osteoclast-mediated bone resorption around dental implants plays an important role in bone remodelling and thereby osseointegration establishment and maintenance [43, 44]. In the present study, all osteoclastic markers tested presented higher expression for the laminin-1-coated implant. It has been reported that osteoblastogenesis and osteoclastogenesis transact and regulate each other through the receptor activator of nuclear factor-kappa B ligand (RANKL)/RANK/osteoprotegerin (OPG) system pathway [45, 46]. Thus, we speculate that the higher level of osteoblastic gene expression may have induced higher osteoclastic gene expression. In the present study, the osteoclastic activity may have been highly active due to mutual interactions after surface doping with laminin. It is well recognized that integrin $\alpha_V\beta_3$, which is highly produced by osteoclasts, presents high affinity for the RGD-motif, which is included in many of the extracellular matrix proteins. Although this might be a non-laminin specific mechanism, another integrin molecule, that is, $\alpha_2\beta_1$, is also expressed by mammalian osteoclasts and is highly specific for laminin and collagen. Thus, the increase in osteoclast proliferation denoted by higher levels of TRAP and calcitonin receptor may be laminin specific directly by means of laminin/$\alpha_2\beta_1$ interaction [47].

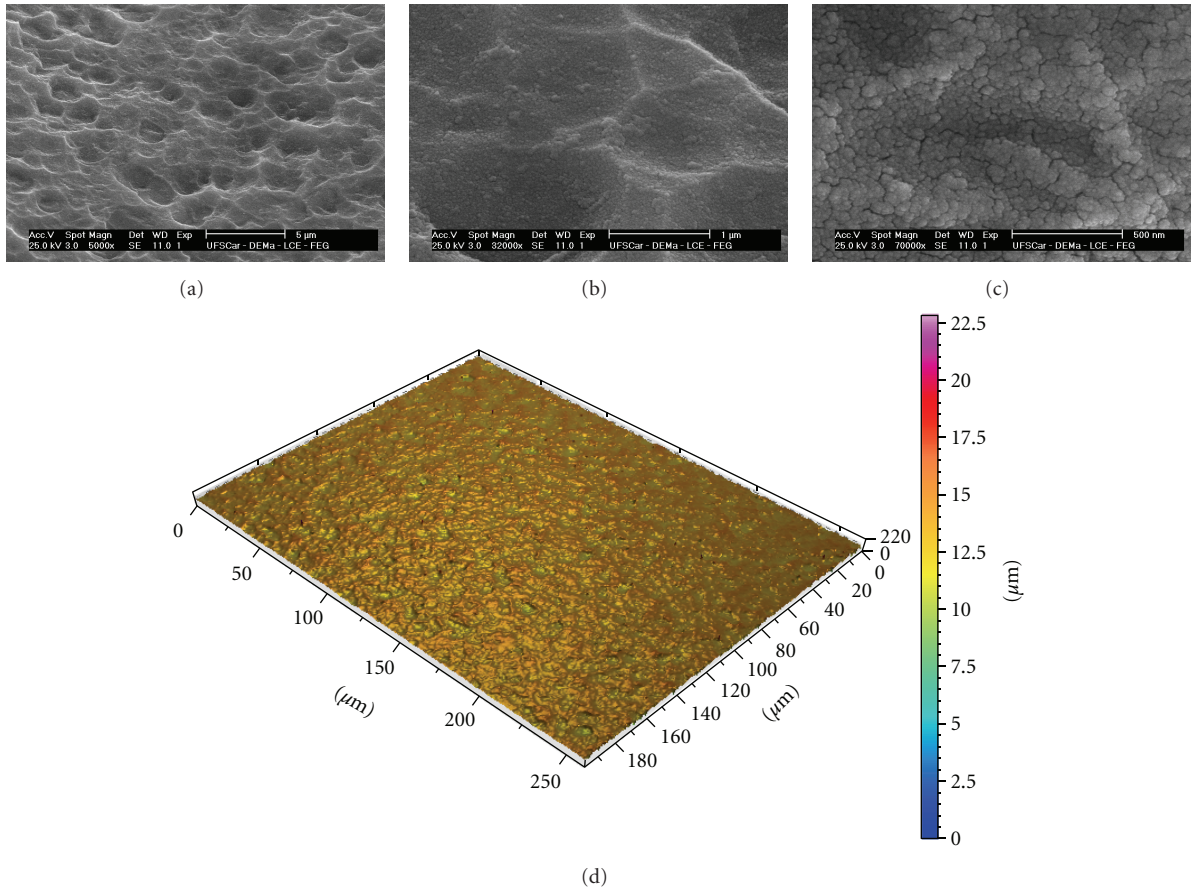

Figure 1: SEM micrographs of nanoroughened implant surface before protein coating (magnification (a) ×5,000, (b) ×32,000, and (c) ×70,000). (d) Interferometer image of nanoroughened implant surface before protein coating (measurement area: 260 mm × 200 mm).

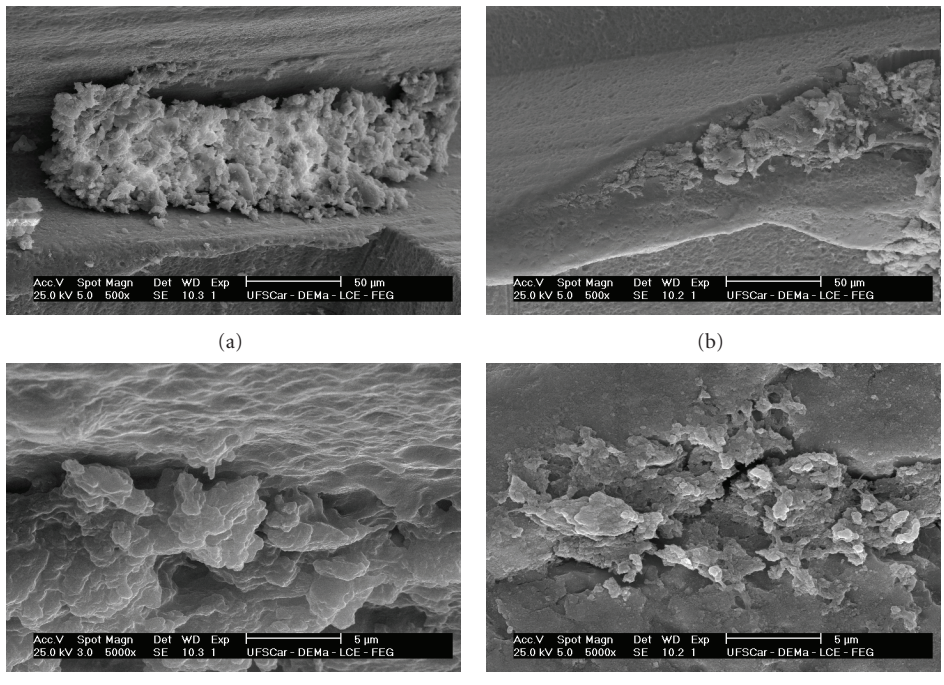

Figure 2: Scanning electron micrographs of retrieved implants for (a) nanoroughened implant surface (control), (b) nanoroughened implant surface + laminin-1 (test) (magnification ×500), (c) higher magnification of the nanoroughened implant surface (control) (×5000), and (d) higher magnification of the nanoroughened implant surface + laminin-1 (test) (×5000).

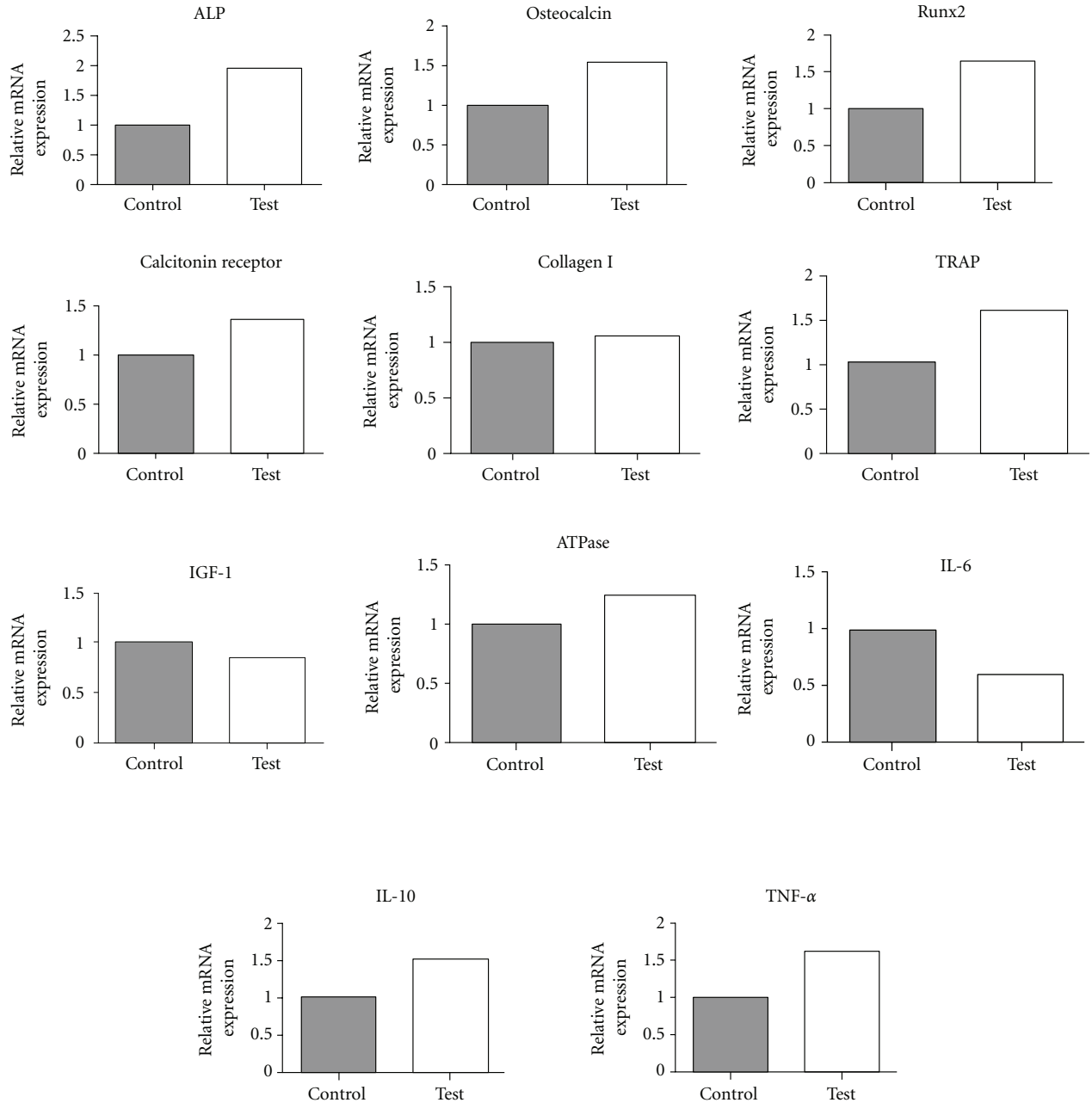

Figure 3: Gene expressions of bone formation markers by real-time RT-PCR for the non-laminin-1-coated (control) and -coated (test) groups. After 2 weeks, the surrounding tissues of implants were collected and total RNA of pooled samples was isolated. The osteogenic markers (ALP, osteocalcin, Runx2, calcitonin receptor, collagen I, TRAP, IGF-1, and ATPase) and inflammation markers (IL-6, IL-10, and TNF-α) were evaluated and higher values were detected for the experimental group. The relative expressions of target genes were normalized with housekeeping gene β-actin.

The RT-PCR results also demonstrated that most of the inflammatory factors were upregulated for the laminin-1-doped group. Haapasalmi et al. have reported that laminin-1 localises where inflammation exists, as seen in chronic periodontal inflammatory responses [48]. Since inflammatory reactions are part of the healing process [49], the induced inflammatory gene expression further supports higher degrees of osteogenesis at the laminin-1-coated implant interface. For example, TNF-α has been proven to be necessary for intramembranous ossification [50] and to increase matrix mineralization and the levels of bone morphogenic protein-2 and alkaline phosphatase *in vitro* [51]. These findings are in agreement with the observed increase of osteoclcin and alkaline phosphatase in our study.

A study in knockout IL-10 mice has demonstrated decreased gene expression of alkaline phosphatase and osteocalcin in the absence of the IL-10 gene [52]. Thus, the elevated levels of IL-10 in our study are well correlated to the

increased gene expression of those osteoblast markers. Additionally, IL-6 has been reported to stimulate osteoclastic bone resorption [53] hence explaining the enhanced expression of osteoclastic markers.

The SEM investigation depicted similar bone formation on both surfaces. It is speculated that because of the early time point, the mechanical attachment strength of the bone tissue to the implant surface may be low, and the mineralisation is still in progress. This statement is further supported by the high gene expression of ALP, which indicates that bone is still under maturation. For this reason, it is potentially like that large segment of immature bony tissues may have detached from the implant interface, rather than development of a fracture within the bone.

Although the results of this study are preliminary, the information motivates further investigation of the novel protein we utilized in the current study as an implant coating. Further, evaluation of gene expression may help capture detailed differences, which may be difficult to detect with the conventional imaging and biomechanical evaluation techniques.

5. Conclusion

We hypothesised that the addition of laminin-1 would enhance osteogenic markers in the early stages of osseointegration. Compared to the noncoated nanostructured implant surface, the protein-doped nanostructured implant surface presented higher gene expression of typical genes involved in the osseointegration cascade, and therefore the hypothesis of the study was accepted.

Authors' Contributions

H. O. Schwartz-Filho and K. Bougas contributed equally to the work.

Acknowledgments

This study was supported by the Swedish Knowledge Foundation, the Swedish Research Council, the Hjalmar Svensson Research Foundation, and the Swedish National Graduate School in Odontological Science. The authors would like to thank Neodent for the kind support. There were no conflict of interests.

References

[1] P. Turbill, T. Beugeling, and A. A. Poot, "Proteins involved in the Vroman effect during exposure of human blood plasma to glass and polyethylene," *Biomaterials*, vol. 17, no. 13, pp. 1279–1287, 1996.

[2] F. Rupp, L. Scheideler, D. Rehbein, D. Axmann, and J. Geis-Gerstorfer, "Roughness induced dynamic changes of wettability of acid etched titanium implant modifications," *Biomaterials*, vol. 25, no. 7-8, pp. 1429–1438, 2004.

[3] R. Jimbo, D. Ono, Y. Hirakawa, T. Odatsu, T. Tanaka, and T. Sawase, "Accelerated photo-induced hydrophilicity promotes osseointegration: an animal study," *Clinical Implant Dentistry and Related Research*, vol. 13, no. 1, pp. 79–85, 2011.

[4] Y. Akagawa, T. Kubo, K. Koretake et al., "Initial bone regeneration around fenestrated implants in Beagle dogs using basic fibroblast growth factor-gelatin hydrogel complex with varying biodegradation rates," *Journal of Prosthodontic Research*, vol. 53, no. 1, pp. 41–47, 2009.

[5] J. Y. Park and J. E. Davies, "Red blood cell and platelet interactions with titanium implant surfaces," *Clinical Oral Implants Research*, vol. 11, no. 6, pp. 530–539, 2000.

[6] A. H. Reddi, "Implant-stimulated interface reactions during collagenous bone matrix-induced bone formation," *Journal of Biomedical Materials Research*, vol. 19, no. 3, pp. 233–239, 1985.

[7] R. Jimbo, M. Ivarsson, A. Koskela, Y. T. Sul, and C. B. Johansson, "Protein adsorption to surface chemistry and crystal structure modification of titanium surfaces," *Journal of Oral & Maxillofacial Research*, vol. 1, no. 3, article e3, 2010.

[8] R. Jimbo, T. Sawase, Y. Shibata et al., "Enhanced osseointegration by the chemotactic activity of plasma fibronectin for cellular fibronectin positive cells," *Biomaterials*, vol. 28, no. 24, pp. 3469–3477, 2007.

[9] G. Schneider and K. Burridge, "Formation of focal adhesions by osteoblasts adhering to different substrata," *Experimental Cell Research*, vol. 214, no. 1, pp. 264–269, 1994.

[10] L. Vroman and A. L. Adams, "Identification of rapid changes at plasma-solid interfaces," *Journal of Biomedical Materials Research*, vol. 3, no. 1, pp. 43–67, 1969.

[11] A. Bentmann, N. Kawelke, D. Moss et al., "Circulating fibronectin affects bone matrix, whereas osteoblast fibronectin modulates osteoblast function," *Journal of Bone and Mineral Research*, vol. 25, no. 4, pp. 706–715, 2010.

[12] S. Miyamoto, B. Z. Katz, R. M. Lafrenie, and K. M. Yamada, "Fibronectin and integrins in cell adhesion, signaling, and morphogenesis," *Annals of the New York Academy of Sciences*, vol. 857, pp. 119–129, 1998.

[13] D. Guarnieri, S. Battista, A. Borzacchiello et al., "Effects of fibronectin and laminin on structural, mechanical and transport properties of 3D collageneous network," *Journal of Materials Science: Materials in Medicine*, vol. 18, no. 2, pp. 245–253, 2007.

[14] V. Sollazzo, A. Palmieri, A. Girardi, F. Farinella, and F. Carcini, "Early effects of P-15 on human bone marrow stem cells," *Journal of Oral & Maxillofacial Research*, vol. 1, article 1, 2010.

[15] R. Jimbo, Y. Xue, M. Hayashi, H. O. Schwartz-Filho, M. Andersson, K. Mustafa et al., "Genetic responses to nanostructured calcium-phosphate-coated implants," *Journal of Dental Research*, vol. 90, no. 12, pp. 1422–1427, 2011.

[16] S. Rammelt, T. Illert, S. Bierbaum, D. Scharnweber, H. Zwipp, and W. Schneiders, "Coating of titanium implants with collagen, RGD peptide and chondroitin sulfate," *Biomaterials*, vol. 27, no. 32, pp. 5561–5571, 2006.

[17] M. Nagai, T. Hayakawa, A. Fukatsu et al., "In vitro study of collagen coating of titanium implants for initial cell attachment," *Dental Materials Journal*, vol. 21, no. 3, pp. 250–260, 2002.

[18] H. Hilbig, M. Kirsten, R. Rupietta et al., "Implant surface coatings with bone sialoprotein, collagen, and fibronectin and their effects on cells derived from human maxillar bone," *European Journal of Medical Research*, vol. 12, no. 1, pp. 6–12, 2007.

[19] M. L. Cairns, B. J. Meenan, G. A. Burke, and A. R. Boyd, "Influence of surface topography on osteoblast response to

fibronectin coated calcium phosphate thin films," *Colloids and Surfaces B*, vol. 78, no. 2, pp. 283–290, 2010.

[20] R. Jimbo, P. G. Coelho, S. Vandeweghe, H. O. Schwartz-Filho, M. Hayashi, D. Ono et al., "Histological and three-dimensional evaluation of osseointegration to nanostructured calcium phosphate-coated implants," *Acta Biomaterialia*, vol. 7, no. 12, pp. 4229–4234, 2011.

[21] S. D. Puckett, E. Taylor, T. Raimondo, and T. J. Webster, "The relationship between the nanostructure of titanium surfaces and bacterial attachment," *Biomaterials*, vol. 31, no. 4, pp. 706–713, 2010.

[22] R. Jimbo, J. Sotres, C. Johansson, K. Breding, F. Currie, and A. Wennerberg, "The biological response to three different nanostructures applied on smooth implant surfaces," *Clinical Oral Implants Research*, vol. 23, no. 6, pp. 706–712, 2012.

[23] M. J. Dalby, D. McCloy, M. Robertson et al., "Osteoprogenitor response to semi-ordered and random nanotopographies," *Biomaterials*, vol. 27, no. 15, pp. 2980–2987, 2006.

[24] G. B. Schneider, R. Zaharias, D. Seabold, J. Keller, and C. Stanford, "Differentiation of preosteoblasts is affected by implant surface microtopographies," *Journal of Biomedical Materials Research*, vol. 69, no. 3, pp. 462–468, 2004.

[25] K. I. Tashiro, G. C. Sephel, D. Greatorex et al., "The RGD containing site of the mouse laminin A chain is active for cell attachment, spreading, migration and neurite outgrowth," *Journal of Cellular Physiology*, vol. 146, no. 3, pp. 451–459, 1991.

[26] Z. Wang, D. Telci, and M. Griffin, "Importance of syndecan-4 and syndecan -2 in osteoblast cell adhesion and survival mediated by a tissue transglutaminase-fibronectin complex," *Experimental Cell Research*, vol. 317, no. 3, pp. 367–381, 2011.

[27] P. Valderrama, R. E. Jung, D. S. Thoma, A. A. Jones, and D. L. Cochran, "Evaluation of parathyroid hormone bound to a synthetic matrix for guided bone regeneration around dental implants: a histomorphometric study in dogs," *Journal of Periodontology*, vol. 81, no. 5, pp. 737–747, 2010.

[28] H. C. Kroese-Deutman, J. Van Den Dolder, P. H. M. Spauwen, and J. A. Jansen, "Influence of RGD-loaded titanium implants on bone formation in vivo," *Tissue Engineering*, vol. 11, no. 11-12, pp. 1867–1875, 2005.

[29] K. L. Kilpadi, P. L. Chang, and S. L. Bellis, "Hydroxylapatite binds more serum proteins, purified integrins, and osteoblast precursor cells than titanium or steel," *Journal of Biomedical Materials Research*, vol. 57, no. 2, pp. 258–267, 2001.

[30] P. Roche, H. A. Goldberg, P. D. Delmas, and L. Malaval, "Selective attachment of osteoprogenitors to laminin," *Bone*, vol. 24, no. 4, pp. 329–336, 1999.

[31] K. Bougas, V. Franke Stenport, P. Tengvall, F. Currie, and A. Wennerberg, "Laminin coating promotes calcium phosphate precipitation on titanium discs in vitro," *Journal of Oral and Maxillofacial Research*, vol. 2, no. 4, article e5, 2011.

[32] A. Nanci, J. D. Wuest, L. Peru et al., "Chemical modification of titanium surfaces for covalent attachment of biological molecules," *Journal of Biomedical Materials Research*, vol. 40, no. 2, pp. 324–335, 1998.

[33] P. Linderbäck, N. Harmankaya, A. Askendal, S. Areva, J. Lausmaa, and P. Tengvall, "The effect of heat- or ultra violet ozone-treatment of titanium on complement deposition from human blood plasma," *Biomaterials*, vol. 31, no. 18, pp. 4795–4801, 2010.

[34] A. McCrackin, *FORTRAN Program for the Analysis of Ellipsometer Measurements*, NBS Technical Note, Washington, DC, USA, 1969.

[35] T. Ishibe, T. Goto, T. Kodama, T. Miyazaki, S. Kobayashi, and T. Takahashi, "Bone formation on apatite-coated titanium with incorporated BMP-2/heparin in vivo," *Oral Surgery, Oral Medicine, Oral Pathology, Oral Radiology and Endodontology*, vol. 108, no. 6, pp. 867–875, 2009.

[36] B. Wildemann, A. Sander, P. Schwabe et al., "Short term in vivo biocompatibility testing of biodegradable poly(D,L-lactide)—growth factor coating for orthopaedic implants," *Biomaterials*, vol. 26, no. 18, pp. 4035–4040, 2005.

[37] J. J. Pinzone, B. M. Hall, N. K. Thudi et al., "The role of Dickkopf-1 in bone development, homeostasis, and disease," *Blood*, vol. 113, no. 3, pp. 517–525, 2009.

[38] P. Ducy, R. Zhang, V. Geoffroy, A. L. Ridall, and G. Karsenty, "Osf2/Cbfa1: a transcriptional activator of osteoblast differentiation," *Cell*, vol. 89, no. 5, pp. 747–754, 1997.

[39] T. Taniguchi, T. Matsumoto, and H. Shindo, "Changes of serum levels of osteocalcin, alkaline phosphatase, IGF-I and IGF-binding protein-3 during fracture healing," *Injury*, vol. 34, no. 7, pp. 477–479, 2003.

[40] E. Canalis, "Effect of insulinlike growth factor I on DNA and protein synthesis in cultured rat calvaria," *Journal of Clinical Investigation*, vol. 66, no. 4, pp. 709–719, 1980.

[41] G. M. Boland, G. Perkins, D. J. Hall, and R. S. Tuan, "Wnt 3a promotes proliferation and suppresses osteogenic differentiation of adult human mesenchymal stem cells," *Journal of Cellular Biochemistry*, vol. 93, no. 6, pp. 1210–1230, 2004.

[42] S. Walsh, G. R. Jordan, C. Jefferiss, K. Stewart, and J. N. Beresford, "High concentrations of dexamethasone suppress the proliferation but not the differentiation or further maturation of human osteoblast precursors in vitro: relevance to glucocorticoid-induced osteoporosis," *Rheumatology*, vol. 40, no. 1, pp. 74–83, 2001.

[43] C. Minkin and V. C. Marinho, "Role of the osteoclast at the bone-implant interface," *Advances in Dental Research*, vol. 13, pp. 49–56, 1999.

[44] M. Monjo, S. F. Lamolle, S. P. Lyngstadaas, H. J. Rønold, and J. E. Ellingsen, "In vivo expression of osteogenic markers and bone mineral density at the surface of fluoride-modified titanium implants," *Biomaterials*, vol. 29, no. 28, pp. 3771–3780, 2008.

[45] B. F. Boyce and L. Xing, "Biology of RANK, RANKL, and osteoprotegerin," *Arthritis Research and Therapy*, vol. 9, supplement 1, article S1, 2007.

[46] G. D. Roodman, "Bone-breaking cancer treatment," *Nature Medicine*, vol. 13, no. 1, pp. 25–26, 2007.

[47] S. B. Rodan and G. A. Rodan, "Integrin function in osteoclasts," *Journal of Endocrinology*, vol. 154, pp. S47–S56, 1997.

[48] K. Haapasalmi, M. Makela, O. Oksala et al., "Expression of epithelial adhesion proteins and integrins in chronic inflammation," *American Journal of Pathology*, vol. 147, no. 1, pp. 193–206, 1995.

[49] M. G. Araujo and J. Lindhe, "Dimensional ridge alterations following tooth extraction. An experimental study in the dog," *Journal of Clinical Periodontology*, vol. 32, no. 2, pp. 212–218, 2005.

[50] L. C. Gerstenfeld, T. J. Cho, T. Kon et al., "Impaired intramembranous bone formation during bone repair in the absence of tumor necrosis factor-alpha signaling," *Cells Tissues Organs*, vol. 169, no. 3, pp. 285–294, 2001.

[51] K. Hess, A. Ushmorov, J. Fiedler, R. E. Brenner, and T. Wirth, "TNFα promotes osteogenic differentiation of human mesenchymal stem cells by triggering the NF-κB signaling pathway," *Bone*, vol. 45, no. 2, pp. 367–376, 2009.

[52] M. Claudino, T. P. Garlet, C. R. B. Cardoso et al., "Down-regulation of expression of osteoblast and osteocyte markers in periodontal tissues associated with the spontaneous alveolar bone loss of interleukin-10 knockout mice," *European Journal of Oral Sciences*, vol. 118, no. 1, pp. 19–28, 2010.

[53] B. S. Moonga, O. A. Adebanjo, H. J. Wang et al., "Differential effects of interleukin-6 receptor activation on intracellular signaling and bone resorption by isolated rat osteoclasts," *Journal of Endocrinology*, vol. 173, no. 3, pp. 395–405, 2002.

Hindawi Publishing Corporation
International Journal of Biomaterials
Volume 2012, Article ID 279167, 7 pages
doi:10.1155/2012/279167

Research Article

Bone Morphometric Evaluation around Immediately Placed Implants Covered with Porcine-Derived Pericardium Membrane: An Experimental Study in Dogs

Ryo Jimbo,[1] Charles Marin,[2] Lukasz Witek,[3] Marcelo Suzuki,[4] Nick Tovar,[5] Ioana Chesnoiu-Matei,[5] Irina Florentina Dragan,[6] and Paulo G. Coelho[5]

[1] *Department of Prosthodontics, Faculty of Odontology, Malmö University, 205 06 Malmö, Sweden*
[2] *Department of Dentistry, UNIGRANRIO, Brazil*
[3] *Department of Chemical Engineering, Oklahoma State University, Stillwater, OK 74078, USA*
[4] *Department of Prosthodontics, Tufts University School of Dental Medicine, Boston, MA 0211, USA*
[5] *Departments of Biomaterials & Biomimetics and Periodontology & Implant Dentistry, New York University College of Dentistry, New York, NY 10010, USA*
[6] *Department of Periodontology, Tufts University School of Dental Medicine, Boston, MA 0211, USA*

Correspondence should be addressed to Ryo Jimbo, ryo.jimbo@mah.se

Received 24 June 2012; Accepted 24 October 2012

Academic Editor: Carlos Nelson Elias

Objective. To investigate whether porcine-derived bioresorbable pericardium membrane coverage enhances the osseointegration around implants placed in fresh extraction sockets. *Study Design*. Twenty-four commercially available endosseous implants were placed in the fresh extraction sockets of the mandibular first molar of mature beagles ($n = 6$). On one side, implants and osteotomy sites were covered with porcine-derived bioresorbable pericardium membranes, whereas on the other side, no membranes were used. After 6 weeks, samples were retrieved and were histologically processed for histomorphometric analysis. *Results*. The histological observation showed that bone loss and soft tissue migration in the coronal region of the implant were evident for the control group, whereas bone fill was evident up to the neck of the implant for the membrane-covered group. Bone-to-implant contact was significantly higher for the membrane-covered group compared to the control group, 75% and 45% ($P < 0.02$), respectively. *Conclusion*. The experimental membranes proved to regenerate bone around implants placed in fresh extraction sockets without soft tissue intrusion.

1. Introduction

The regeneration and healing of bone is a gradual process, and are constantly prone to soft tissue infiltration, particularly in large defects. In order to enhance the healing process, and at the same time, to prevent the migration of unwanted cells, it has been suggested that segregation of the defects via a membrane barrier is effective [1, 2]. Membranes also sustain blood clots in place and allow time for bone forming cells to reconstruct bone unobstructed, which is beneficial for applications such as implant placement in fresh extraction sockets.

The surgical and restorative advantages of placing dental implants in fresh extraction sockets have been discussed clinically by various authors [3–7] with a sufficient number of in vivo studies supporting that successful osseointegration can be achieved in these situations [8–12]. The so-called immediate implant placement is less invasive and potentially more efficient than the classic approach, where multiple surgeries may be needed if using a graft material for the initial bone healing process. However, one of the surgical limitations of an immediate implant placement procedure is that often a socket presents dimensions that may be greater than the diameter of a conventional implant, which at many times results in the presence of a substantial gap between the implant and the socket wall [13] and resorption of the buccal bone wall [14]. It has been proposed that minimizing the gap itself by the use of a conical or a wide diameter implant may

be one of the solutions to overcome this problem [15, 16]. However, it has been suggested that full regeneration of the bone is a difficult task, since it seems that alveolar bone resorption to a certain extent is unavoidable regardless of the type of the implant placed [17]. Therefore, the use of a membrane material to create a contained atmosphere could prevent alveolar bone alteration, and simultaneously promote osseointegration.

Today, a wide variety of membrane materials are commercially available from nonresorbable synthetic to naturally derived membranes. Nonresorbable synthetic membranes, such as polytetrafluoroethylene (PTFE), require removal after 3-4 weeks in order to prevent an immunogenic response. For longer periods, there will be a potential risk of gingival dehiscence, resulting in membrane exposure, moreover infection [18]. On the other hand, naturally derived membranes on the market are mainly manufactured from animal-derived collagen, more specifically, porcine-derived, which are suggested to be biocompatible and biodegradable [19, 20]. This degradation minimizes an immunologic response, possibly reduces patient follow-up visits, and prevents further gingival tissue damage, which has been suggested to be beneficial as compared to the nonresorbable membranes. Studies using the nonresorbable membranes have indeed shown successful bone regeneration due to their excellent space-making and growth factor sustaining properties [21]. However, a recent study showed that even with the resorbable naturally derived membranes, similar biologic outcomes may be expected [22]. These materials are typically fabricated from porcine dermis/peritoneum, or pericardium. Membranes, derived from the porcine peritoneum, are mechanically weaker than their pericardium counterpart [23]. Moreover, since peritoneum-derived membrane barriers naturally present a smooth side and a rough side, the membrane should be oriented in a specific, unidirectional fashion to ensure clinical success. When compared to dermis and other dual-layer membranes, the structure of fibrous pericardium is unique; it has a basement membrane on both sides, resulting not only in a smooth yet porous surface for cellular attachment and proliferation, but also in sufficient density for soft tissue exclusion.

In this study, the bone morphometry and/or morphology around implants placed in fresh extraction sockets and covered with pericardium derived collagen membrane was evaluated and compared to a group without a membrane, to investigate whether the unique feature of the membrane could provide enhanced bone regeneration.

2. Materials and Methods

2.1. Surgical Procedures. This study used a commercially available pericardium membrane (Vitala, Osteogenics, Lubbock, TX, USA) and 24 commercially available endosseous implants of 3.3 × 13 mm (DT Implants- Ossean Surface, Intra-Lock International, Boca Raton, FL, USA). Following approval of the bioethics committee for animal experimentation (ENVA, France), six beagle dogs with closed growth plates (~1.5 years of age) in good health were acquired for the study and allowed to acclimate for two weeks before surgery. All surgical procedures were performed under general anesthesia. The preanesthetic procedure comprised of an intramuscular administration of atropine sulfate (0.044 mg/kg) and xylazine chlorate (8 mg/kg). General anesthesia was then obtained following an intramuscular injection of ketamine chlorate (15 mg/kg). Bilateral extractions of first mandibular molars were performed (Figure 1(a)). The procedure involved a full thickness mucoperiosteal flap; teeth were sectioned in the buccolingual direction so that individual roots could easily be extracted by root elevators and forceps without any damage to the alveolar bone wall. Following extraction, implants were placed lingually (to replicate the clinical situation) in the mesial and distal sockets, at the buccal bone crest level (Figure 1(b)). Upon measuring with a periodontal probe, it was made sure that a gap of at least 3 mm (range 3.2 to 4.5 mm) was present between the implant body and the buccal side of the alveolar bone.

On the right side of the mandible, the implants were covered with Vitala (Figure 1(c)); the implants on the contralateral side were used as controls. All implants were placed following the manufacturer's surgical protocol, and primary closure was achieved with resorbable sutures (3-0 Vicryl, Ethicon; Figure 1(d)). Postsurgical medication included antibiotics (penicillin, 20.000 UI/kg) and analgesics (ketoprofen, 1 mL/5 kg) for a period of 48 hours postoperatively. The animals were euthanized 6 weeks after the implant surgery. The euthanasia was performed by anesthesia overdose.

2.2. Histological Processing and Quantitative Analysis. Bone block explants consisting of the test and control groups were harvested and processed. The bone blocks were kept in 10% buffered formalin solution for 24 hours, washed in running water for 24 hours, and gradually dehydrated in a series of ethanol solutions ranging from 70% to 100%. Following dehydration, the samples were embedded in a methacrylate-based resin (Technovit 9100; Heraeus Kulzer, Wehrheim, Germany) according to the manufacturer's instructions. The blocks were then cut into slices (300 μm thickness) aiming at the center of the implant along its long axis with a precision diamond saw (Isomet 2000; Buehler, Lake Bluff, IL), glued to acrylic plates with an acrylate-based cement, and a 24-hour setting time was allowed before grinding and polishing. The sections were then reduced to a final thickness of ~30 μm by means of a series of SiC abrasive papers (400, 600, 800, 1200, and 2400; Buehler) in a grinding/polishing machine (Metaserv 3000, Buehler) under water irrigation. The sections were then toluidine blue stained and referred for optical microscopy evaluation. The histologic features were qualitatively evaluated at 50x to 200x magnifications (Leica DM2500M; Leica Microsystems, Wetzlar, Germany). The amount of bone-to-implant contact (BIC) and buccal bone loss (BBL) were calculated by means of a computer software (Leica Application Suite, Leica Microsystems GmbH, Wetzlar, Germany). The regions of bone-to-implant contact along the implant perimeter were subtracted from the total implant perimeter, and calculations were performed to determine the BIC. Wilcoxon matched-pairs test at 95% was utilized for statistical evaluation.

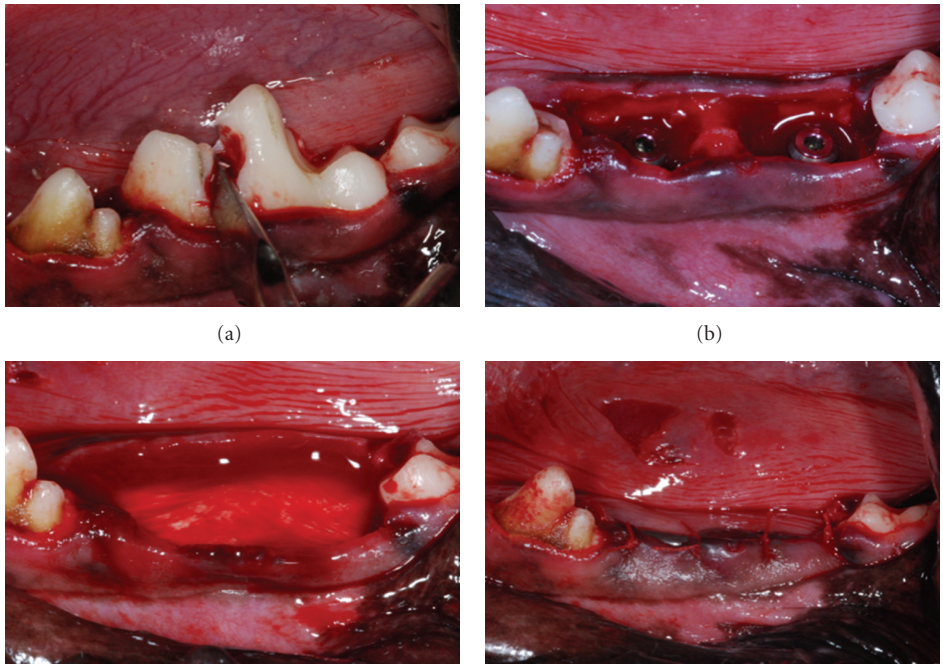

(a) (b)

(c) (d)

Figure 1: (a) Following sectioning, the teeth were extracted and (b) two 3.3 mm × 13 mm implants were placed in each of the sockets. (c) In one of the sides, a collagen-based membrane was placed and (d) extraction sockets with implants in place were closed with standard suture techniques.

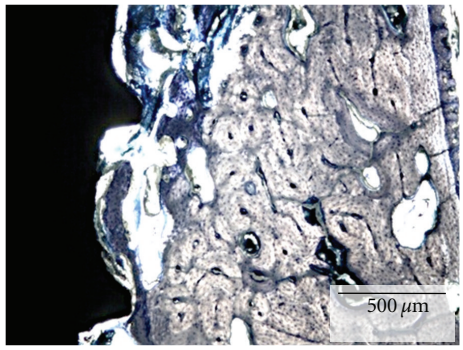

Figure 2: Optical micrograph depicting the new bone filling the gap between the extraction socket wall and implant surface, a common finding for both experimental and control groups.

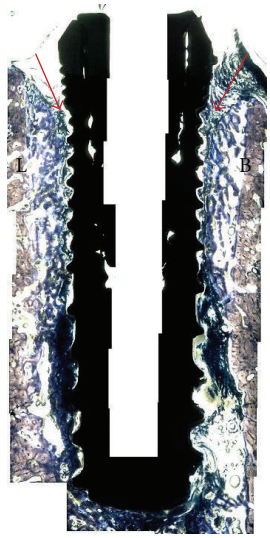

Figure 3: Merged optical micrograph depicting the control group, where the immediate implant placed at the mesial molar socket was not covered with a resorbable membrane prior to suturing. For this group, apical migration (arrows) occurred at both buccal (B) and lingual (L) aspects resulting in lower bone insertion levels along the length of the implant.

3. Results

3.1. Histological and Histomorphometrical Evaluation. The surgical procedures and followup demonstrated no complications or other immediate clinical concerns. There were no signs of infection or inflammation at the surgical sites or surrounding tissues throughout the duration of the study.

At 6 weeks, the qualitative analysis of the histologic sections showed for both groups, regions of direct bone-to-implant contact and new woven bone bridging the gap between implant and the old bone of the socket walls (Figure 2). Apical migration of soft tissue resulting in lower cervical to apical bone to implant first contact was observed for the implants in the control group (Figure 3). In the experimental group, where the implants were covered by the membrane at the time of placement, an intimate contact between implant and bone was observed throughout the implant level (Figure 4). Higher magnification optical

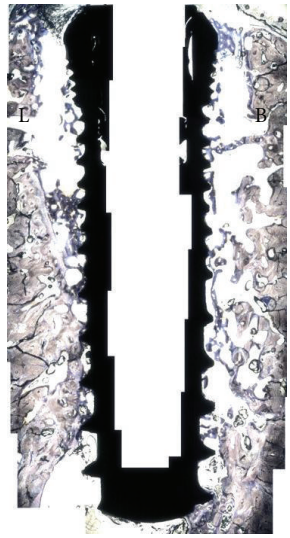

Figure 4: Merged optical micrograph depicting the experimental group, where the immediate implant placed at the mesial molar socket was covered with a resorbable membrane prior to suturing. For this group, extensive apical migration (arrows) did not occur at both buccal (B) and lingual (L) aspects resulting in osseointegration at higher levels relative to the control side. The red and blue boxes are described in detail in Figure 5.

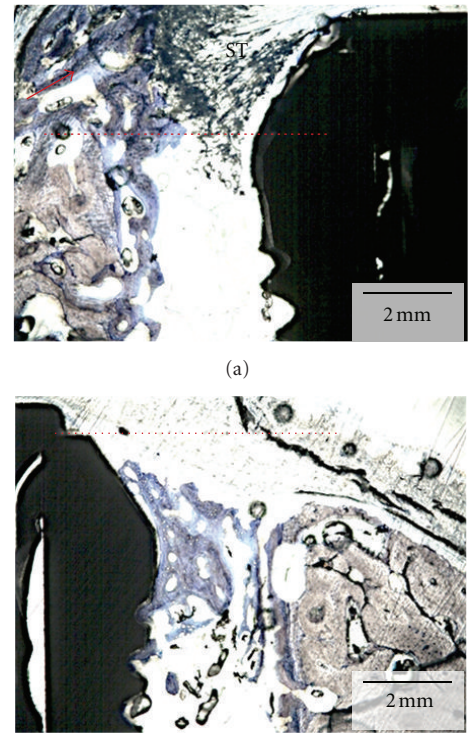

Figure 5: (a) Optical micrograph depicting the lingual aspect of the section presented in the red box in Figure 3. The dashed red line represents the implant cervical level (immediately below the implant cover screw). New bone formation through the course of six weeks resulted in higher levels than at the time of placement (red arrow). The soft tissue (ST) limited migration likely occurred due to membrane movement during suture where it partially bent in the apical direction allowing tissue migration. (b) Optical micrograph depicting the buccal aspect of the section presented in the blue box in Figure 4. The dashed red line represents the implant cervical level (immediately below the implant cover screw). New bone formation through the course of six weeks resulted in bone height maintenance and closure of the gap between implant surface and socket wall. For this section, no soft tissue apical migration occurred.

micrographs of an experimental group section are presented in Figure 5.

Quantitative analysis of the test group rendered a significantly higher BIC in comparison to the BIC observed for the control group, 75% versus 45% ($P < 0.02$), respectively. The sites that were covered with the membrane presented a 0.7 mm buccal bone loss which was significantly lower than the control group that showed a 2.5 mm loss in buccal plate ($P < 0.02$, Figure 6). The implantation site within arch (mesial or distal) did not influence BIC or BBL in either control or test groups ($P > 0.80$).

4. Discussion

Immediate implant therapy has been proven to be a successful clinical treatment, since it is less invasive and is beneficial in shortening the treatment period [24, 25]. The survival rate of immediately placed and loaded implants over a 7–10 year followup varies between 85 and 91%, depending on location of the implant [26]. Following tooth extraction, a discrepancy between the diameter of the extraction socket and an immediate implant renders a gap that can influence the osseointegration of the implant by allowing apical soft tissue migration. In this study, the implants placed in the fresh extraction sockets of dogs showed appropriate osseointegration with direct bone-implant-contact when an occlusive collagen pericardial membrane barrier was used.

Previous studies have shown that the gap width was one of the decisive factors in order to achieve implant osseointegration [27]; for instance, a gap ranging 0.35–1 mm was shown to result in incomplete bone healing around the implants [28, 29]. Knox et al. evaluated the coronal positioning of the bone-to-implant contact in dogs, in gaps up to 2 mm without the placement of a membrane [30]. Their results showed that the level of coronal bone position along the implant surface was dependent on the initial gap between alveolar bone and implant. These conclusions are supported by the results obtained from the current study where, by eliminating apical soft tissue migration over the implant by means of a membrane barrier, higher levels of BIC, lower buccal bone loss, and a more coronal direct bone apposition was observed compared to controls.

Although implant surface and implant design play an important role in the osseointegration and survival of implants in fully healed bone [31], the data may not be fully applicable in sites such as implant placement in extraction sockets or in immediate loading conditions [25]. Under progressive and dynamic ridge alteration, the effect of the state

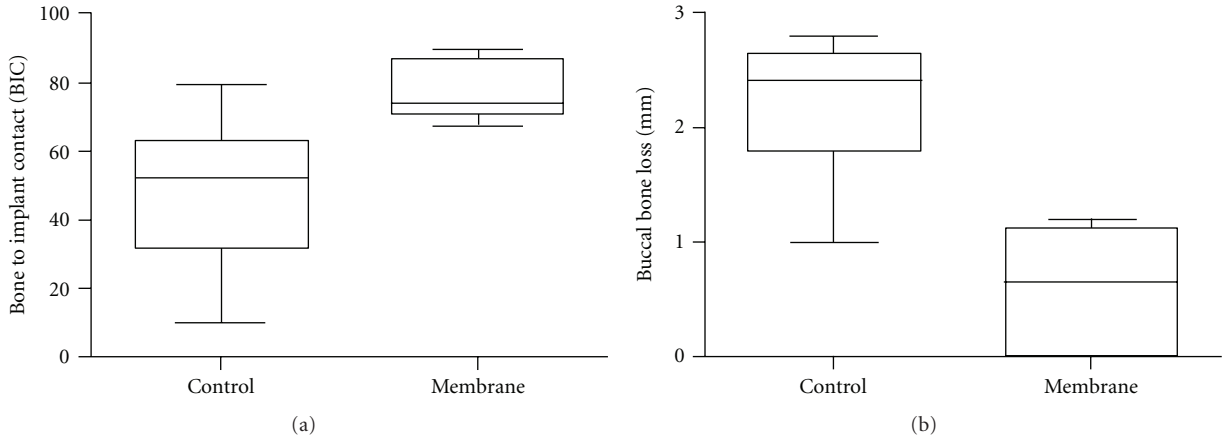

Figure 6: Wilcoxon matched paired test revealed (a) significant higher BIC to the experimental group ($P < 0.02$), and (b) significantly lower buccal bone loss for the membrane group compared to the control group ($P < 0.02$).

of the art surface architecture may be less effective, and the biological reassembly takes initiative in the configuration procedure [14]. Thus, in order to successfully obtain bone fill and osseointegration in a gap created during implant placement in fresh extraction sockets, additional regenerative procedures such as the guided soft tissue/bone regeneration (GTR/GBR) with the use of occlusive membranes may be necessary to maintain space for blood clot infiltration and maturation, further to exclude soft tissue invasion [32].

The appropriate bone regenerative outcomes around the implants placed in fresh extraction sockets of the current study has indicated that the use of membrane to cover the gap is an effective procedure. This is in agreement with other studies using a commercially available bioresorbable membrane, which presented that the use of such membrane contributed to the preservation of the buccal outline of the alveolar process [33, 34]. Moreover, the structural characteristics of the pericardium-derived porcine membrane may have been responsible for further bone enhancing effects since our histologic sections did not show extensive membrane collapsing into the gap between the socket wall and implant bulk. Mechanical property wise, it has been reported that these membranes possess a better tensile strength and ball burst than other collagen membranes derived from small intestine submucosa (peritoneum) or acellular dermal matrix [35]. With regards to the structure of the membrane, the noncross linked matrix derived from the porcine pericardium has a bionic feature [36], which has been suggested to be a key factor for cell migration and morphogenesis [37].

To conclude, the findings of the present study showed that using a bioresorbable, pericardium membrane resulted in significantly higher BIC and a closer fit between the bone margin and the abutment-fixture margin as compared to sites without membrane coverage. Although it has not been compared to other membrane materials in the present study, the outcomes of this study strongly suggests the bioeffectiveness of the biologically inspired design membrane in challenging cases such as implant placement in the fresh extraction sockets. Another aspect to further clarify the effect of the membrane is to identify the time course changes in relation to the anatomical landmarks as presented in numerous studies conducted by Araújo et al. [38–40]. In order to bring in clinical benefits, further investigations comparing the pericardium membrane to other membrane materials which are clinically used are necessary.

Conflict of Interests

The authors declare no conflict of interests.

References

[1] C. Dahlin, A. Linde, J. Gottlow, and S. Nyman, "Healing of bone defects by guided tissue regeneration," *Plastic and Reconstructive Surgery*, vol. 81, no. 5, pp. 672–676, 1988.

[2] M. Simion, A. Scarano, L. Gionso, and A. Piattelli, "Guided bone regeneration using resorbable and nonresorbable membranes: a comparative histologic study in humans," *International Journal of Oral and Maxillofacial Implants*, vol. 11, no. 6, pp. 735–742, 1996.

[3] B. E. Becker, W. Becker, A. Ricci, and N. Geurs, "A prospective clinical trial of endosseous screw-shaped implants placed at the time of tooth extraction without augmentation," *Journal of Periodontology*, vol. 69, no. 8, pp. 920–926, 1998.

[4] D. A. Gelb, "Immediate implant surgery: three-year retrospective evaluation of 50 consecutive cases," *The International Journal of Oral & Maxillofacial Implants*, vol. 8, no. 4, pp. 388–399, 1993.

[5] R. J. Lazzara, "Immediate implant placement into extraction sites: surgical and restorative advantages," *The International Journal of Periodontics & Restorative Dentistry*, vol. 9, no. 5, pp. 332–343, 1989.

[6] S. Nyman, N. P. Lang, D. Buser, and U. Bragger, "Bone regeneration adjacent to titanium dental implants using guided tissue regeneration: a report of two cases," *The International Journal of Oral & Maxillofacial Implants*, vol. 5, no. 1, pp. 9–14, 1990.

[7] D. Schwartz-Arad and G. Chaushu, "Placement of implants into fresh extraction sites: 4 to 7 years retrospective evaluation of 95 immediate implants," *Journal of Periodontology*, vol. 68, no. 11, pp. 1110–1116, 1997.

[8] W. Becker, B. E. Becker, M. Handelsman, C. Ochsenbein, and T. Albrektsson, "Guided tissue regeneration for implants placed into extraction sockets: a study in dogs," *Journal of Periodontology*, vol. 62, no. 11, pp. 703–709, 1991.

[9] K. Gotfredsen, L. Nimb, D. Buser, and E. Hjorting-Hansen, "Evaluation of guided bone generation around implants placed into fresh extraction sockets: an experimental study in dogs," *Journal of Oral and Maxillofacial Surgery*, vol. 51, no. 8, pp. 879–884, 1993.

[10] R. J. Kohal, M. B. Hürzeler, L. F. Mota, G. Klaus, R. G. Caffesse, and J. R. Strub, "Custom-made root analogue titanium implants placed into extraction sockets: an experimental study in monkeys," *Clinical Oral Implants Research*, vol. 8, no. 5, pp. 386–392, 1997.

[11] C. Karabuda, P. Sandalli, S. Yalcin, D. E. Steflik, and G. R. Parr, "Histologic and histomorphometric comparison of immediately placed hydroxyapatite-coated and titanium plasma-sprayed implants: a pilot study in dogs," *International Journal of Oral and Maxillofacial Implants*, vol. 14, no. 4, pp. 510–515, 1999.

[12] M. G. Araújo, F. Sukekava, J. L. Wennström, and J. Lindhe, "Tissue modeling following implant placement in fresh extraction sockets," *Clinical Oral Implants Research*, vol. 17, no. 6, pp. 615–624, 2006.

[13] D. Botticelli, T. Berglundh, D. Buser, and J. Lindhe, "The jumping distance revisited: an experimental study in the dog," *Clinical Oral Implants Research*, vol. 14, no. 1, pp. 35–42, 2003.

[14] M. G. Araújo, F. Sukekava, J. L. Wennström, and J. Lindhe, "Ridge alterations following implant placement in fresh extraction sockets: an experimental study in the dog," *Journal of Clinical Periodontology*, vol. 32, no. 6, pp. 645–652, 2005.

[15] L. Carlsson, T. Rostlund, B. Albrektsson, and T. Albrektsson, "Implant fixation improved by close fit. Cylindrical implant-bone interface studied in rabbits," *Acta Orthopaedica Scandinavica*, vol. 59, no. 3, pp. 272–275, 1988.

[16] G. E. Romanos, "Bone quality and the immediate loading of implants-critical aspects based on literature, research, and clinical experience," *Implant Dentistry*, vol. 18, no. 3, pp. 203–209, 2009.

[17] M. Sanz, D. Cecchinato, J. Ferrus, E. B. Pjetursson, N. P. Lang, and J. Lindhe, "A prospective, randomized-controlled clinical trial to evaluate bone preservation using implants with different geometry placed into extraction sockets in the maxilla," *Clinical Oral Implants Research*, vol. 21, no. 1, pp. 13–21, 2010.

[18] M. Chiapasco, S. Abati, E. Romeo, and G. Vogel, "Clinical outcome of autogenous bone blocks or guided bone regeneration with e-PTFE membranes for the reconstruction of narrow edentulous ridges," *Clinical Oral Implants Research*, vol. 10, no. 4, pp. 278–288, 1999.

[19] F. Schwarz, M. Sager, D. Rothamel, M. Herten, A. Sculean, and J. Becker, "Use of native and cross-linked collagen membranes for guided tissue and bone regeneration," *Schweizer Monatsschrift für Zahnmedizin*, vol. 116, no. 11, pp. 1112–1123, 2006.

[20] P. Gentile, V. Chiono, C. Tonda-Turo, A. M. Ferreira, and G. Ciardelli, "Polymeric membranes for guided bone regeneration," *Biotechnology Journal*, vol. 6, no. 10, pp. 1187–1197, 2011.

[21] C. Dahlin, M. Simion, U. Nanmark, and L. Sennerby, "Histological morphology of the e-PTFE/tissue interface in humans subjected to guided bone regeneration in conjunction with oral implant treatment," *Clinical Oral Implants Research*, vol. 9, no. 2, pp. 100–106, 1998.

[22] R. E. Jung, N. Fenner, C. H. F. Hämmerle, and N. U. Zitzmann, "Long-term outcome of implants placed with guided bone regeneration (GBR) using resorbable and non-resorbable membranes after 12–14 years," *Clinical Oral Implants Research*. In press.

[23] J. Zhang, G. Y. Wang, Y. P. Xiao, L. Y. Fan, and Q. Wang, "The biomechanical behavior and host response to porcine-derived small intestine submucosa, pericardium and dermal matrix acellular grafts in a rat abdominal defect model," *Biomaterials*, vol. 32, no. 29, pp. 7086–7095, 2011.

[24] H. de Bruyn, F. Raes, L. F. Cooper et al., "Three-years clinical outcome of immediate provisionalization of single osseospeed implants in extraction sockets and healed ridges," *Clinical Oral Implants Research*. In press.

[25] H. Browaeys, S. Vandeweghe, C. B. Johansson, R. Jimbo, E. Deschepper, and H. De Bruyn, "The histological evaluation of osseointegration of surface enhanced microimplants immediately loaded in conjunction with sinuslifting in humans," *Clinical Oral Implants Research*. In press.

[26] G. Romanos, S. Froum, C. Hery, S. C. Cho, and D. Tarnow, "Survival rate of immediately versus delayed loaded implants: analysis of the current literature," *The Journal of Oral Implantology*, vol. 36, no. 4, pp. 315–324, 2010.

[27] W. H. Harris, R. E. White Jr., J. C. McCarthy, P. S. Walker, and E. H. Weinberg, "Bony ingrowth fixation of the acetabular component in canine hip joint arthroplasty," *Clinical Orthopaedics and Related Research*, vol. 176, pp. 7–11, 1983.

[28] L. Carlsson, T. Rostlund, B. Albrektsson, and T. Albrektsson, "Implant fixation improved by close fit. Cylindrical implant-bone interface studied in rabbits," *Acta Orthopaedica Scandinavica*, vol. 59, no. 3, pp. 272–275, 1988.

[29] R. F. Caudill and R. M. Meffert, "Histologic analysis of the osseointegration of endosseous implants in simulated extraction sockets with and without e-PTFE barriers. 1. Preliminary findings," *The International Journal of Periodontics & Restorative Dentistry*, vol. 11, no. 3, pp. 207–215, 1991.

[30] R. Knox, R. Caudill, and R. Meffert, "Histologic evaluation of dental endosseous implants placed in surgically created extraction defects," *The International Journal of Periodontics & Restorative Dentistry*, vol. 11, no. 5, pp. 364–375, 1991.

[31] P. G. Coelho, J. M. Granjeiro, G. E. Romanos et al., "Basic research methods and current trends of dental implant surfaces," *Journal of Biomedical Materials Research*, vol. 88, no. 2, pp. 579–596, 2009.

[32] J. Campbell, C. Bassett, J. Girado, R. Seymour, and J. Rossi, "Application of monomolecular filter tubes in bridging gaps in peripheral nerves and for prevention of neuroma formation; a preliminary report," *Journal of Neurosurgery*, vol. 13, no. 6, pp. 635–637, 1956.

[33] M. Caneva, D. Botticelli, L. A. Salata, S. L. Scombatti Souza, L. Carvalho Cardoso, and N. P. Lang, "Collagen membranes at immediate implants: a histomorphometric study in dogs," *Clinical Oral Implants Research*, vol. 21, no. 9, pp. 891–897, 2010.

[34] V. Lekovic, P. M. Camargo, P. R. Klokkevold et al., "Preservation of alveolar bone in extraction sockets using bioabsorbable membranes," *Journal of Periodontology*, vol. 69, no. 9, pp. 1044–1049, 1998.

[35] J. Zhang, G. Y. Wang, Y. P. Xiao, L. Y. Fan, and Q. Wang, "The biomechanical behavior and host response to porcine-derived small intestine submucosa, pericardium and dermal matrix acellular grafts in a rat abdominal defect model," *Biomaterials*, vol. 32, no. 29, pp. 7086–7095, 2011.

[36] M. Schlee, S. Ghanaati, I. Willershausen, M. Stimmlmayr, A. Sculean, and R. A. Sader, "Bovine pericardium based non-cross linked collagen matrix for successful root coverage,

a clinical study in human," *Head and Face Medicine*, vol. 8, article 6, 2012.

[37] V. Quaranta, "Cell migration through extracellular matrix: membrane-type metalloproteinases make the way," *Journal of Cell Biology*, vol. 149, no. 6, pp. 1167–1170, 2000.

[38] M. G. Araújo, F. Sukekava, J. L. Wennström, and J. Lindhe, "Ridge alterations following implant placement in fresh extraction sockets: an experimental study in the dog," *Journal of Clinical Periodontology*, vol. 32, no. 6, pp. 645–652, 2005.

[39] M. G. Araújo and J. Lindhe, "Dimensional ridge alterations following tooth extraction. An experimental study in the dog," *Journal of Clinical Periodontology*, vol. 32, no. 2, pp. 212–218, 2005.

[40] M. G. Araújo, F. Sukekava, J. L. Wennström, and J. Lindhe, "Tissue modeling following implant placement in fresh extraction sockets," *Clinical Oral Implants Research*, vol. 17, no. 6, pp. 615–624, 2006.

Hindawi Publishing Corporation
International Journal of Biomaterials
Volume 2012, Article ID 290179, 7 pages
doi:10.1155/2012/290179

Research Article

Preparation of Bioactive Titanium Surfaces via Fluoride and Fibronectin Retention

Carlos Nelson Elias,[1] Patricia Abdo Gravina,[1] Costa e Silva Filho,[2] and Pedro Augusto de Paula Nascente[3]

[1] *Biomaterials Laboratory, Instituto Militar de Engenharia, Pr Gen Tibúrcio 80, 22290-270 Rio de Janeiro, RJ, Brazil*
[2] *Avenue Carlos Chagas Filho, 373, Cidade Universitária-21941-902 Rio de janeiro, RJ, Brazil*
[3] *Rodovia Washington Luís km 235, 13565-905 São Carlos, SP, Brazil*

Correspondence should be addressed to Carlos Nelson Elias, elias@ime.eb.br

Received 4 August 2012; Accepted 26 September 2012

Academic Editor: Paulo Guilherme Coelho

Statement of Problem. The chemical or topographic modification of the dental implant surface can affect bone healing, promote accelerated osteogenesis, and increase bone-implant contact and bonding strength. *Objective*. In this work, the effects of dental implant surface treatment and fibronectin adsorption on the adhesion of osteoblasts were analyzed. *Materials and Methods*. Two titanium dental implants (Porous-acid etching and PorousNano-acid etching followed by fluoride ion modification) were characterized by high-resolution scanning electron microscopy, atomic force microscopy, and X-ray diffraction before and after the incorporation of human plasma fibronectin (FN). The objective was to investigate the biofunctionalization of these surfaces and examine their effects on the interaction with osteoblastic cells. *Results*. The evaluation techniques used showed that the Porous and PorousNano implants have similar microstructural characteristics. Spectrophotometry demonstrated similar levels of fibronectin adsorption on both surfaces (80%). The association indexes of osteoblastic cells in FN-treated samples were significantly higher than those in samples without FN. The radioactivity values associated with the same samples, expressed as counts per minute (cpm), suggested that FN incorporation is an important determinant of the *in vitro* cytocompatibility of the surfaces. *Conclusion*. The preparation of bioactive titanium surfaces via fluoride and FN retention proved to be a useful treatment to optimize and to accelerate the osseointegration process for dental implants.

1. Introduction

The phenomenon of endosseous implant osseointegration, conceptualized by Branemark as the "direct, structural and functional link between the living and orderly bone and the surface of an implant subjected to functional loads" [1], is fundamental to the success of dental implant applications. Commercially pure titanium (cp Ti) is the main material used for this purpose because it has good biocompatibility and adequate mechanical strength. Ti exposed to oxidizing agents spontaneously forms a 10-100 Å thick titanium oxide layer. This layer is stable in most media, especially under physiological conditions, and, surgically, it shows no change in thickness or corrosion. This ensures implant-bone tissue interaction and osseointegration [2]. The reactions of the tissue host with the biomaterial are determined by the surface properties of the biomaterial. The dental implant surface treatment should induce the differentiation of the desired cells [3]. Surface treatments of available implants promote changes in the mechanical, microstructural, and physical properties, as well as the wettability, energy, chemical composition, and density of chemical groups or molecules on the surface [2, 4].

This paper shows that the bone-implant interface strength is greater in dental implants with rough surfaces than in those with smooth surfaces [5, 6]. Treatments to increase the surface area for fibrin adhesion encourages implant adhesion. The presence of these surfaces also

increases platelet activation, which produces large gradients of cytokines and growth factors through which leukocytes and osteogenic cells can penetrate the healing site [7]. Titanium surfaces coated with proteins can influence host reactions and thus enhance tissue integration [4]. Fibronectin is a major adhesion protein in the extracellular membrane, and it is important for cell adhesion, migration, proliferation, differentiation, and survival because it facilitates focal contacts with the receptors.

Appropriate changes in dental implant surface roughness can produce better anchoring strength and mechanical locking in the early stages of osseointegration [2, 6]. Moreover, surfaces with different microtopographies provide a larger area for fibrin adhesion, potentiate platelet activation, and favorably affect local angiogenesis and cellular functions including migration, alignment, orientation, attachment, and differentiation [5, 6].

Johansson et al. [8] observed that surfaces treated with fluoride are smoother than sandblasted surfaces but that fluoride-treated surfaces showed higher calcium-phosphorus binding capacity, which could indicate an increased ability of the surface to react with calcified tissues and promote integration between bone and implant. According to Ellingsen and Lyngstadaas [9], *in vitro* tests have shown that titanium fluoride treatments have a greater capacity for the nucleation of phosphate crystals than sandblasted Ti implants. *In vivo* fluoride ion-modified implants have generally proven superior to sandblasted surfaces in terms of osseointegration, ultimately increasing the removal torques.

Fibronectin is a major extracellular matrix protein that is known to promote cell attachment and spreading, differentiation, and phagocytosis. It is a dimeric glycoprotein found in all vertebrates in two basic forms: soluble (plasma and other fluids) and insoluble (extracellular matrix of various tissues). It has a molecular weight between 440 and 500 kDa. Disulfide bridges link one subunit to another via sites near the carboxy termini of each subunit. The fibronectin protein has folds that lead to structural remodeling and various conformations according to the medium [10–12].

Fibronectin (FN) functions in cell adhesion, migration, survival, proliferation, and differentiation as well as tissue organization. The FN molecule can interact with other biomolecules, such as collagen, proteoglycan, heparin, hyaluronic acid, fibrin/fibrinogen, plasmin, gangliosides, complement components, and also integral proteins of cell plasma membrane-integrins, as well as with itself [13].

Menezes [10] conducted a study to assess the interaction of human osteoblasts with films of human plasma fibronectin prepared under different pH conditions. The results showed no quantitative differences in the interaction of human osteoblastic cells (HOB) to different coatings, but qualitative differences were observed; osteoblasts adhered to each of the substrates in very different ways. The largest areas of cells adhesion were observed for substrates preincubated at 4.5 pH.

Petrie et al. [14] conducted a clinical study to evaluate the effects of specific bioactive coatings on the healing of bone tissue and the osseointegration of titanium dental implants. The author showed that surfaces containing a FN fragment for the integrin $\alpha 5\beta 1$ ($FNIII^{7-10}$) increase osteoblastic differentiation and optimize tissue formation and functional integration compared with untreated surfaces or surfaces containing only the RGD sequence.

The purpose of this study was to evaluate the effect of the fluoride treatment of cp titanium samples on the adhesion and proliferation of osteoblastic cells on surfaces with and without fibronectin coating.

2. Materials and Methods

2.1. Samples. Implants and discs of grade 4 machined cp Ti were provided by Conexão Sistemas de Prótese (Arujá, SP, Brazil). Samples were submitted to surface treatment and divided into four groups:

Porous: samples treated in acidic solutions containing HNO_3, H_2SO_4, and HCl (surface treatment similar to Porous implants available from Conexão Sistemas de Prótese);

PorousNano: treatment similar to Group 1 followed by fluoride ion modification by immersion for one hour in a solution containing fluorine ions;

Porous-FN: treatment similar to Group 1 with FN incorporation;

PorousNano-FN: treatment similar to Group 2 with FN incorporation.

After treatments, samples from the Porous and PorousNano groups were washed with distilled water and absolute alcohol, dried in oven at 70°C for two hours, and packed and sterilized by gamma irradiation (25 kGy).

2.2. Surface Characterization. To characterize the surface morphology and identify differences in samples submitted to treatments with acids and/or fluorides, the samples were characterized by a high-resolution scanning electron microscopy (FEG/EDS, Philips XL30FEG). The results were complemented by analysis with an MFP-3D atomic force microscope (Asylum Research, CA, USA) operating in contact at room temperature mode. The cantilevers used were V shaped, NP-S model (Veeco Probes, CA, USA) with an 0.08 N/m spring constant, and calibrated using the thermal noise method. To reduce damage to samples and reduce noise, images were acquired using low-frequency scanning (1.0 Hz) with 256×256 pixel resolution. Image processing was performed in the program IGOR PRO (WaveMetrics, Portland, OR, USA) using a MFP-3D platform developed by Asylum Research.

2.3. Identification of Crystalline Phases. An X-ray diffractometer was used to identify crystalline phases on discs. X-ray diffraction for the analysis of thin films (grazing incidence technique) was conducted at 40 kV and 30 mA. A copper anode was used ($Cu - K\alpha = 1,542$ Å) with an RU 200B model Rigaku generator and 0.02° step/minute.

2.4. Fibronectin Incorporation. Human serum fibronectin (Sigma-Aldrich Co., São Paulo, Brazil)) was diluted to

10 g/mL, pH 4.5 in previously filtered 20 mM sodium acetate (Reagen Laboratory Products, Paraná, Brazil) buffer solution. NaCl was added to the solution to maintain the medium's ionic strength between 0.145 and 0.150 mol·dm^{-3}.

Samples from the Porous and PorousNano groups were coated with fibronectin at room temperature for 2 hours. Substrates with FN were washed with PBS (phosphate [0.01 M] buffered saline [0.15 M], pH 7.2) to remove non-adsorbed molecules. Then, the adsorbed molecules were detached using 0.1% trypsin and PBS. One to two minutes later, the excess was removed, and the resulting solution was collected and analyzed with a Spectrum 22PC spectrophotometer to quantify the adsorbed molecules. Spectrophotometry was also used to determine the FN's absorbance on both surfaces (protein concentration in solutions that absorb radiation). Negative (PBS) and positive (FN suspension 100 μg/mL) controls were performed. The wavelength used was 550 nm (protein reading).

2.5. Culture of Osteoblasts. Cells were maintained in polystyrene bottles containing DMEM (Dulbecco's Modified Eagle Medium) culture medium with low glucose, 10% fetal bovine serum (Soromed Industry, São Paulo, Brazil), and 1% essential amino acids solution (Minimum Essential amino acid solution 100x, Sigma-Aldrich) ascorbic acid (0.15 gL^{-1}, Sigma-Aldrich) buffered with 10 mM HEPES (Sigma-Aldrich) and 14.3 mM $NaHCO_3$ (Reagen). The pH of the medium was adjusted to 7.2. Cultures were incubated at 37°C in 5% CO_2 atmosphere. The enzymatic cell detachment technique was used to transpose cells from the stock culture flask to substrates for the adhesion assay. Confluent cultures were treated with 0.2% trypsin (Difco Microbiology Co., USA) and 0.02% EDTA (Sigma-Aldrich) in saline solution (0.8% NaCl [Reagan], 0.01% KCl [Sigma-Aldrich]; 0.29% $NaHPO_4 \cdot 7H_2O$ [Reagan], and 0.02% KH_2PO_4 [Sigma-Aldrich] in H_2O) for 5 minutes at 37°C. Then, the detached cells were collected, and the proteolytic action of trypsin was inhibited by adding fetal calf serum to the solution. The suspension was then centrifuged at 1500 rpm at 22°C, and the pelleted cells were resuspended in culture medium without fetal calf serum. The cell concentration/density of the suspension was estimated by counting in a hematimetric Neubauer chamber.

2.6. Interaction of Cells with Samples. After the cell concentration of the suspension was measured in a hematimetric chamber, 10^6 cells/mL were taken and allowed to interact with the samples with and without FN coating, which totaled four groups. After an hour of interaction, the supernatants were discarded, and the cells that were attached (adsorbed and adhered) to surfaces were washed with PBS and fixed using glutaraldehyde (2.5% in PBS). Glutaraldehyde was used as fixative to avoid damaging cell integrity (glutaraldehyde contains two functional groups that link two proteins). This procedure was adopted because the use of formaldehyde (which has only one functional group) as a fixative profoundly deformed the cells. After fixation, cells were trypsinized and counted in a hematimetric Neubauer chamber.

2.7. Surface Radioactivity. Human osteoblastic cells (HOBs) were cultivated to evaluate cell adhesion and proliferation by liquid scintillation counting. Cells from confluent HOB cultures were detached with trypsin, washed, and counted in a hematimetric chamber. Then, the culture was resuspended in DMEM containing serum and [^{3}H]-thymidine (1143 cpm). After allowing incorporation for a period of 12 hours, the confluent cells were again detached and washed in DMEM without serum, and a liquid scintillator (Beckman, Rack III) was used to evaluate the radioactivity associated with cells. The resulting values were expressed as counts per minute (cpm). These cells, incorporating [^{3}H]-thymidine, were associated with different surfaces (Porous, Porous-FN, PorousNano, and PorousNano-FN) for a period of 3 hours, and counts were carried out after 1, 2, and 3 hours. This cell behavior evaluation method allows accurate reproduction, favoring the future applicability of FN incorporation onto surfaces of dental implants.

3. Results

3.1. Surface Morphology. Figure 1 shows Porous and PorousNano titanium surfaces before coating with fibronectin. These surfaces exhibited microcavities with different sizes and sharp edges. Immersion into a solution containing fluoride ions (PorousNano) did not change the microcavity morphology, and the sharp edges persisted. A minor modification caused by immersion is shown in Figure 1(c); some white regions are observed when compared with Figure 1(b). At high magnification (Figure 1(d)), the PorousNano group showed evidence of particle clusters at the surface due to immersion in the solution containing fluoride ions. This is the major ultrastructural characteristic of the PorousNano sample.

Figure 2 shows images obtained by atomic force microscopy. In Figure 2(a), the microcavity edges are more flattened but maintain the sharp features that seem to assist or facilitate the adsorption of fibronectin and cells. Figure 2(b) shows the PorousNano sample surface at high magnification, demonstrating that the roughness pattern at the microcavity edges is flattened by immersion treatment in a solution containing fluoride ions.

The surface roughness of the Porous sample (Figure 2(a)) was 1759.7 nm (±204.4 nm), whereas the roughness of the PorousNano surface sample (Figure 2(b)) was 1406.5 nm (±226.9 nm).

3.2. Identification of Crystalline Phases. Figure 3 shows the X-ray diffraction spectra of the Porous and PorousNano surfaces. Both contain only titanium as the crystalline phase.

3.3. Incorporation of Fibronectin. Porous and PorousNano titanium surfaces were treated with crystal violet (1% in PBS), and the stain associated with the surfaces was eluted with methanol. Negative (buffer solution) and positive (FN suspension) controls were assessed by spectrophotometry. The absorbance was proportional to the amount of the cells such that more the cells on the surface corresponded to larger absorbance values. Cells treated with PBS measured at 0.326

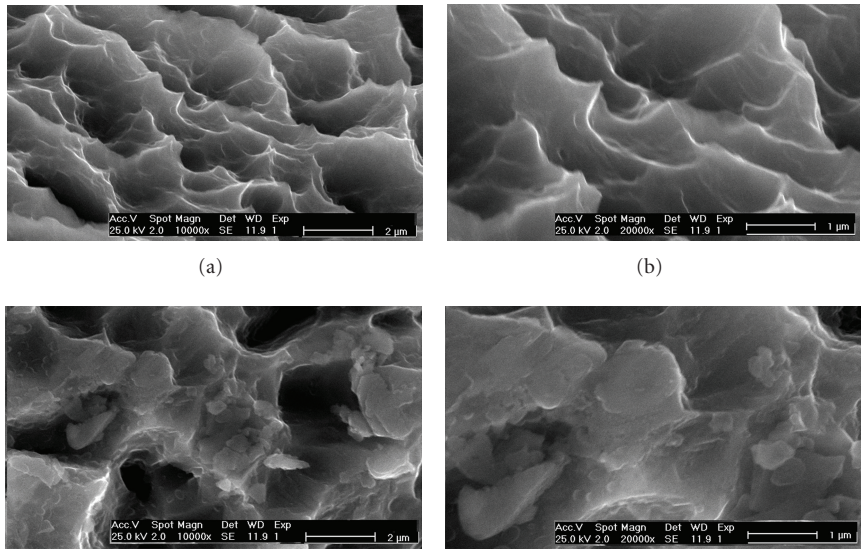

Figure 1: SEM images of the samples before coating with fibronectin. (a) and (b) Porous samples (acid treatment). (c) and (d) PorousNano samples (acid treatment followed by fluoride ion modification).

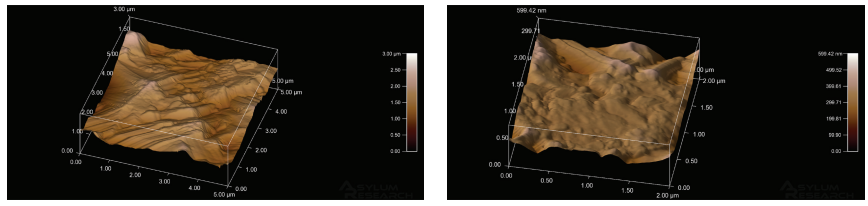

Figure 2: AFM images: (a) Porous and (b) PorousNano.

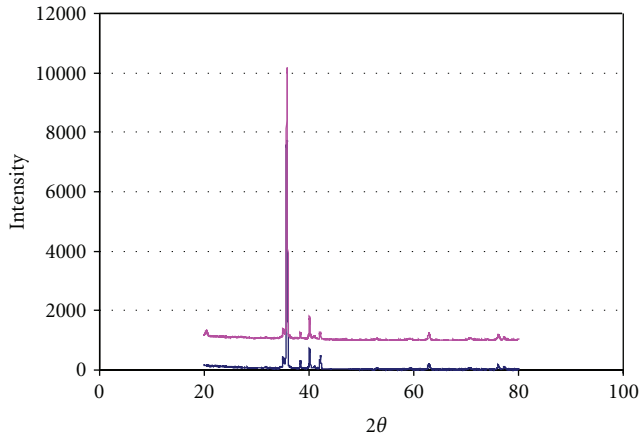

Figure 3: X-ray diffraction spectra of Porous and PorousNano surfaces.

absorbance units (AU) at 550 nm (reading for proteins). The FN suspension (100 μg/mL) measured at 2.992 units. After the FN incorporation in Porous, and PorousNano tablets, both spectrophotometric measurements were 2.473 absorbance units (82.6%) at 550 nm, indicating that the two surfaces exhibit similar behavior with respect to fibronectin incorporation.

3.4. Interaction of Cells with Surfaces. A total of 10^6 human osteoblastic cells/mL were delivered to Porous and PorousNano surfaces, and, after a 1.0 hour interaction, 7.9×10^4 cells/mL and 2.3×10^5 cells/mL were associated with the Porous and PorousNano (no protein coating) surfaces, respectively. The combination of cells to both surfaces, with and without the fibronectin incorporation, resulted in different association indices. For comparison, association index values were considered null for samples without FN. After one hour, the association indices values of cells with samples with FN showed increase of 44.7% (±0.8%) and 57.4% (±0.3%) for Porous-FN and PorousNano-FN surfaces, respectively, compared to the same surfaces without FN.

The cell-surface interaction index of the PorousNano-FN was approximately 28% higher than that of the Porous-FN.

3.5. Surface Radioactivity. After the incorporation of [^{3}H]-thymidine for 12 hours, the radioactivity associated with osteoblast cells was evaluated. Subsequently, 1.8×10^6 cells/mL, corresponding to 1,100 cpm, were delivered

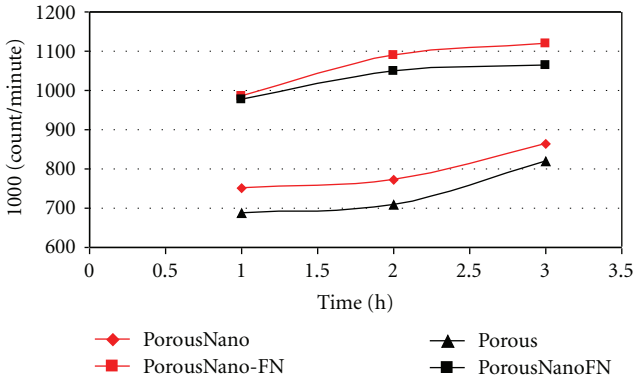

Figure 4: Radioactivity associated with osteoblasts on Porous, Porous-FN, PorousNano, and PorousNano-FN surfaces. The resulting values were expressed as counts per minute (cpm).

to Porous, Porous-FN, PorousNano, and PorousNano-FN surfaces. The results are shown in Figure 4.

After one hour of interaction, 70% of cells (0.751 cpm) were associated with the PorousNano surface. This number is most likely low because some cells died or were not associated with the sample at the beginning of the process. The number of associated cells increased with interaction time, reaching 0.864 cpm after three hours; that is, there was a 15% increase in the amount of associated cells due to proliferation and cell division.

Only 64% of the cells interacting with the Porous surface (0.687 cpm) remained associated after one hour, but this number increased approximately 32% after 3 hours of interaction, reaching 0.905 cpm.

On the Porous-FN surface, 90% of cells (0.976 cpm) were associated after 1 hour of interaction. The number of attached cells increased 9% after three hours, reaching 1.064 cpm. For the PorousNano-FN surface, 92% of cells (0.986 cpm) were associated after one hour of interaction, and this number increased by 11.5% over three hours, reaching 1.100 cpm.

4. Discussion

Figure 1(a) shows the surface morphology of a Porous sample obtained by immersion treatment in acid solution. The acid etching produces a homogeneous surface characterized by microcavities surrounded by tapered summits. This pattern of roughness produces a homogeneous surface without preferential roughness orientation.

Figure 1(c) shows that the immersion of the Porous surface in a solution containing fluoride ions did not change the microcavity morphology, and the sharp edges persisted. At higher magnification, the presence of flatter areas and smaller micropeaks may be noted although these surfaces remain tapered. This change may be associated with the high reactivity of fluorine ions and the chemical susceptibility of titanium oxide to these ions, which may produce a coalescence of peaks. These results are consistent with those of Ellingsen and Lyngstadaas [9] and Johansson et al. [8], which showed that titanium surfaces treated with fluoride present smoother microtopographies and lower R_a values than acid-treated surfaces without fluoride. Figure 1(d) demonstrates the presence of microcavities, summits, and conglomerates on their edges, most likely due to the corrosion process and consequent decrease in surface roughness for the surface subjected to immersion in solution containing fluoride.

Images obtained by atomic force microscopy (Figure 2) show that both the Porous and PorousNano surfaces exhibit microcavities surrounded by summits. Like the high-resolution SEM images, the AFM images indicate that summits and microcavities of the PorousNano sample surface have smoother edges although they remain tapered. These sharp edges seem to assist or facilitate the adsorption of FN and cells.

As measured based on the images obtained through AFM, the roughness of the PorousNano surface sample was lower than that of the Porous surface, demonstrating that treatment with fluoride reduced the summit height, most likely due to the reaction of titanium oxide with fluoride ions. This ultrastructural aspect of the summits contributes to the more homogeneous roughness pattern of the PorousNano surface, in addition to the presence of smoother areas and larger microcavities.

The presence of only one crystalline phase of titanium was revealed by X-ray diffraction of the Porous and PorousNano samples. It is likely that the immersion in a solution containing fluoride ions adds only a small amount of this element to the titanium surface and that this trace amount of fluoride cannot be detected by the XRD technique for the analysis of thin films (grazing incidence technique).

Approximately 80% of the FN allowed to interact with Porous and PorousNano surfaces was adsorbed (2.473 AU). This result demonstrates that the chemical treatment with acids (Porous) and chemical treatment with acids followed by immersion in solution containing fluoride ions (PorousNano) did not affect the incorporation of biomolecule; that is, the presence of the fluoride ion did not influence the protein adsorption. Dos Santos et al. [15] observed that FN adsorption to anodized titanium samples was 68%. It can be concluded that titanium surfaces have an affinity for fibronectin and that differences in the percentage of incorporation in different studies most likely are due to the conditions under which the FN was reacted with the surfaces (pH used, for example) and/or the various treatments performed on them.

Cell counting in a hematimetric chamber is a sensitive and accurate technique for the evaluation of cell adhesion to titanium surfaces. In this study, the PorousNano surface showed a stronger association with osteoblastic cells ($2,3 \times 10^5$ cells/mL) than the Porous surface ($7,9 \times 10^4$ cells/mL) after one hour of interaction. Because 10^6 cells/mL were taken to interact with surfaces, approximately 8% adhered to the Porous sample, while 23% were associated with the PorousNano sample. These indices suggest that the surface subjected to chemical treatment followed by immersion in a solution containing fluoride ions favors the adhesion of most cells during the initial interaction period. As mentioned earlier, the association indices of the Porous and PorousNano

surfaces without fibronectin were considered null for evaluations of the influence of protein on cell behavior. Thus, the number of cells associated with the PorousNano with FN surface increased 57.4% compared with the same surface without the biological variable. For the Porous with FN surface, the increase in cell adhesion was 44.7% compared to the same area without the protein. These indices show that the protein variable is responsible for the significant increase in the number of cells attached to the surfaces, confirming the results of Ku et al. [16], who also reported an increase in the adhesion rate of cells to surfaces treated with recombinant fibronectin. They showed that, for TiO_2, cell adhesion was initiated after 3 hours and had significantly lower cell numbers for all measurement points compared with FN. The present work showed the same results.

The cell-surface interaction index of PorousNano with FN was approximately 28% higher than that of the Porous with FN surface. This study demonstrates that, among the four types of surfaces examined, the PorousNano with fibronectin coating most favors the adsorption and adhesion of osteoblastic cells during the tested interaction period. In addition, the study provides strong evidence that FN incorporation into titanium surfaces is much more relevant for biocompatibility and the consequent acceleration of the osseointegration process than surface treatment with acid and/or immersion in solution containing fluoride ions.

A total of 1.8×10^6 cells/mL (1.100 cpm) were allowed to interact with Porous, Porous-FN, PorousNano, and PorousNano-FN titanium surfaces for three hours. After one hour of interaction, 92% of the cells were associated with the PorousNano-FN surface, and 90% of cells were associated with the Porous-FN surface, while 70% and 64% of cells were associated with the PorousNano and Porous surfaces (without FN), respectively. These results confirm that the protein coating accelerated the adsorption of cells during the initial interaction period (adaptation period). This can be explained by the fact that when fibronectin is allowed to interact with titanium samples under ideal conditions of pH such that its cryptic sites are exposed, the fibronectin signals to osteoblasts to activate the cell cycle and initiate the secretion of ECM proteins.

The Porous-FN and PorousNano-FN surfaces showed similar behavior during the three-hour interaction, both during the initial adherence of cells (approximately 90% for both surfaces) and in their proliferation. The cell number increased by 14% for the sample PorousNano-FN and 12% for Porous-FN in the first 3 hours of interaction (Figure 4). Ku et al. [16] also demonstrated that the biomimetization of titanium surfaces with fibronectin increased the adhesion, proliferation, and differentiation rates of cells.

In samples without FN, this study showed that within one-to-three hours of interaction, the number of cells attached to the PorousNano surface increased by 32%, while the number of cells attached to the Porous surface increased by 15%. This difference shows that the surface that received acid treatment followed by immersion in a solution containing fluoride ions (Nano) showed accelerated cell division and proliferation compared to the Porous surface. Figure 4 shows that the PorousNano surface without fibronectin coating exhibited the greatest increase in cpm as a function of time over 3 hours. Ellingsen and Lyngstadaas [9] and Johansson et al. [8] showed that fluoride-treated surfaces have a greater capacity to react with biological tissues and nuclear phosphate crystals *in vitro*, in addition to offering greater osseointegration resistance *in vivo*. Although previous studies have used different methodologies for fluoride treatment, their results also suggest that the presence of fluoride ions on titanium surfaces facilitates various osseointegration processes. Analysis of the experimental cell adhesion and proliferation data presented in Figure 4 showed that the cell behavior was similar in all samples containing fibronectin. The results of this study show that the FN is critical to the biocompatibility of surfaces of titanium implants, but when this protein is not present, treatment with acids and fluorides seems to favor more tissue integration than treatment with acid only (i.e., no fluoride).

5. Conclusions

Based on the experimental results, it can be concluded that

(a) the surfaces of titanium samples treated with fluoride ions (PorousNano) retained the basic microstructural characteristics of surfaces not treated with fluoride (Porous),

(b) the Porous and PorousNano surfaces incorporated similar levels of FN (approximately 80%) over the time tested (3 hours), demonstrating that the presence of fluoride ions did not influence protein adsorption,

(c) the association indices of HOB cells to the four tested surfaces suggest that FN incorporation is critical for the *in vitro* cytocompatibility of surfaces,

(d) FN-treated samples showed significantly higher percentages of associated cells during the initial period of one hour, confirming that FN (the biological variable) had a greater effect on the adhesion and proliferation of cells than the fluoride treatment of titanium surfaces used in this study.

Acknowledgments

The authors would like to thank the CNPq for financial support under project 306343/2006-1 and FAPERJ project E26/102.714/2008. They also thank Conexão Sistemas e Prótese for supplying the titanium dental implants and disks.

References

[1] P.-I. Branemark, "Introduction to osseointegration," in *Tissue-Integrated Prostheses, Osseointegration in Clinical Dentistry*, pp. 11–76, Quintessence, Chicago, Ill, USA, 5th edition, 1985.

[2] C. N. Elias and L. Meirelles, "Improving osseointegration of dental implants," *Expert Review of Medical Devices*, vol. 7, no. 2, pp. 241–256, 2010.

[3] L. M. Gil, T. C. Ladeira, G. C. Menezes, and F. C. Silva-Filho, "The cell-extracellular matrix-biomaterial interface and the

biocompatibility of titanium implants," *Innovations Implant Journal*, vol. 4, pp. 58–64, 2009.

[4] L. Scheideler, F. Rupp, H. P. Wendel, S. Sathe, and J. Geis-Gerstorfer, "Photocoupling of fibronectin to titanium surfaces influences keratinocyte adhesion, pellicle formation and thrombogenicity," *Dental Materials*, vol. 23, no. 4, pp. 469–478, 2007.

[5] S. A. Cho and K. T. Park, "The removal torque of titanium screw inserted in rabbit tibia treated by dual acid etching," *Biomaterials*, vol. 24, no. 20, pp. 3611–3617, 2003.

[6] A. Wennerberg, T. Albrektsson, and J. Lindhe, "Surface topography of titanium implants," in *Clinical Periodontology and Implant Dentistry*, pp. 821–825, 4th edition, 2003.

[7] J. E. Davies, "Understanding peri-implant endosseous healing," *Journal of Dental Education*, vol. 67, no. 8, pp. 932–949, 2003.

[8] C. B. Johansson, A. Wennerberg, A. Holmen, and J. E. Ellingsen, "Enhanced fixation of bone to fluoride-modified implants," in *Proceedings of the 6th World Biomaterials Congress*, Sydney, Australia, 2000.

[9] J. E. Ellingsen and S. P. Lyngstadaas, "Increasing biocompatibility by chemical modification of titanium surfaces," in *Bio-Implant Interface: Improving Biomaterials and Tissue Reactions*, pp. 323–340, CRC Press, Boca Raton, Fla, USA, 1st edition, 2003.

[10] G. D. Menezes, *A Interação de Osteoblastos Humanos com Filmes de Fibronectina Plasmática Humana Constituídos Sob Diferentes Condições de pH [Dissertação (Mestrado)]*, Universidade Federal do Rio de Janeiro, IBCCF, 2003.

[11] J. M. Park, J. Y. Koak, J. H. Jang, C. H. Han, S. K. Kim, and S. J. Heo, "Osseointegration of anodized titanium implants coated with fibroblast growth factor-fibronectin (FGF-FN) fusion protein," *International Journal of Oral and Maxillofacial Implants*, vol. 21, no. 6, pp. 859–866, 2006.

[12] M. Antia, G. Baneyx, K. E. Kubow, and V. Vogel, "Fibronectin in aging extracellular matrix fibrils is progressively unfolded by cells and elicits an enhanced rigidity response," *Faraday Discussions*, vol. 139, pp. 229–249, 2008.

[13] S. Miyamoto, B. Z. Katz, R. M. Lafrenie, and K. M. Yamada, "Fibronectin and integrins in cell adhesion, signaling, and morphogenesis," *Annals of the New York Academy of Sciences*, vol. 857, pp. 119–129, 1998.

[14] T. A. Petrie, J. E. Raynor, C. D. Reyes, K. L. Burns, D. M. Collard, and A. J. García, "The effect of integrin-specific bioactive coatings on tissue healing and implant osseointegration," *Biomaterials*, vol. 29, no. 19, pp. 2849–2857, 2008.

[15] A. R. Dos Santos, F. Costa E Silva, and G. A. De Soares, "The interaction between human osteoblastic cells and titanium anodized with sulphuric acid coated or not with human plasma fibronectin," *Key Engineering Materials*, vol. 396-398, pp. 389–392, 2009.

[16] Y. Ku, C. P. Chung, and J. H. Jang, "The effect of the surface modification of titanium using a recombinant fragment of fibronectin and vitronectin on cell behavior," *Biomaterials*, vol. 26, no. 25, pp. 5153–5157, 2005.

Hindawi Publishing Corporation
International Journal of Biomaterials
Volume 2012, Article ID 579274, 9 pages
doi:10.1155/2012/579274

Research Article

Novel Implant Coating Agent Promotes Gene Expression of Osteogenic Markers in Rats during Early Osseointegration

Kostas Bougas,[1] Ryo Jimbo,[1] Ying Xue,[2] Kamal Mustafa,[2] and Ann Wennerberg[1]

[1] *Department of Prosthodontics, Faculty of Odontology, Malmö University, 205 06 Malmö, Sweden*
[2] *Department of Clinical Dentistry, Center for Clinical Research, Faculty of Medicine and Dentistry, University of Bergen, Årstadveien 17, 5009 Bergen, Norway*

Correspondence should be addressed to Kostas Bougas, kostas.bougas@mah.se

Received 9 September 2012; Accepted 6 October 2012

Academic Editor: Carlos Nelson Elias

The aim of this study was to evaluate the early bone response around laminin-1-coated titanium implants. Forty-five rats distributed in three equally sized groups were provided with one control (turned) and one test (laminin-1-coated) implant and were sacrificed after 3, 7, and 21 days. Real-time reverse-transcriptase polymerase chain reaction was performed for osteoblast markers (alkaline phosphatase, runt-related transcription factor 2, osteocalcin, type I collagen, and bone morphogenic protein 2), osteoclast markers (cathepsin K and tartrate-resistant acid phosphatase), inflammation markers (tumor necrosis factor α, interleukin 1β and interleukin 10), and integrin β1. Bone implant contact (BIC) and bone area (BA) were assessed and compared to the gene expression. After 3 days, the expression of bone markers was higher for the control group. After 7 days, the expression of integrin β1 and osteogenic markers was enhanced for the test group, while cathepsin K and inflammation markers were down-regulated. No significant differences in BIC or BA were detected between test and control at any time point. As a conclusion, implant coating with laminin-1 altered gene expression in the bone-implant interface. However, traditional evaluation methods, as histomorphometry, were not adequately sensitive to detect such changes due to the short follow-up time.

1. Introduction

Dental implants have been proven to be a reliable long-term therapy against edentulism [1–3]. However, the reported high success figures of implant therapy have been based on implants inserted using two-stage surgical protocol and conventional loading. The increased demand on implant performance and the broadened treatment indications have led to the development of new moderately rough surfaces. Alterations in both the surface chemistry and topography may contribute to chemical influence on bone tissue, a phenomenon defined as bioactivity [4]. Furthermore, other factors such as surface energy, surface wettability, cellular maturation state, nutrition status, and microstresses alter the degree of bioactivity too. Compared to the previously used turned implants, the bioactively modified implants have demonstrated higher success rate in demanding cases, for example, early functional loading [5], one-stage surgery [6], and reconstructive jaw surgery [7].

When moderately rough surfaces remain within bone tissue no differences on microbial colonization are observed as compared to minimally rough surfaces [8]. However, there has been increasing evidence pointing out that as soon moderately rough implants are exposed to the oral milieu the case changes. A series of studies examining clinical, histological, and radiological aspects of experimental peri-implantitis in a dog model has reported that exposure of the implant surfaces to the oral environment leads to spontaneous progression of experimental peri-implantis [9–11]. The same research group has reported that implant surface characteristics affect the possibility to treat experimental peri-implantitis without antimicrobial therapy, thereby influencing the treatment outcome [12]. Additionally, a recent *in vitro* study has proposed that increased implant roughness promotes bacterial

colonization most likely depending on protection of bacteria from shear forces [13]. Even if the referred studies are experimental in nature, the idea of developing an implant that combines the osseoconductive properties of a moderately rough surface with the accessibility for debridement of turned surfaces is intriguing.

In order to enhance bone formation, implants have been coated with bone specific biomolecules [14–17]. Interestingly, even non-bone-specific molecules have reported to induce osteogenicity [18]. One potential non-bone-specific osteogenic molecule is laminin-1. Laminins are heterotrimeric glycoproteins that bind to integrins, especially β1 and β2 isomers [19]. The N-terminal of laminin-1 has been reported to selectively recruit osteoprogenitors through integrin β1-mediated cell attachment [20, 21] and to stimulate production of alkaline phosphatase by osteoblasts [22]. Additionally, recent *in vitro* studies [23, 24] have elucidated the role of laminin as nucleation center and its potential to enhance osteoid formation in a simulated body fluid. Nevertheless, since the *in vivo* environment is more complex in terms of protein interactions [25] and desorption of the coating agent [26], *in vivo* validation has been imperative. In theory, any effects of a protein coating are more pronounced during the early stages of osseointegration.

The purpose of this *in vivo* study is to investigate the detailed molecular mechanisms underlying the possible effects of the coating agent laminin-1 on osseointegration and to compare them to histological evaluation methods.

2. Materials and Methods

2.1. Implants and Laminin-1 Coating. In total, 90 threaded titanium (grade 4) implants with turned surface were used (diameter: 1.5 mm, length: 2.5 mm, internal hexagonal connection, batch 800101579, Neodent, Brazil). Half of the implants ($N = 45$) were coated with laminin-1 in accordance with previous *in vitro* study [24] and served as the test group. In brief, laminin-1 (L2020, Sigma-Aldrich, Stockholm, Sweden) was diluted to a concentration of 100 μg/mL in Dulbecco's phosphate-buffered saline (DPBS) without $CaCl_2$ or $MgCl_2$ (14190-094; GIBCO, Invitrogen Corporation, Grand Island, NY, USA). The implants were subsequently incubated in 48-well plates (Nunclon Surface, Nunc, Roskilde, Denmark) containing 250 μL of the laminin-1 solution per well, for 1 h at room temperature. The protein thickness after incubation was estimated by ellipsometry. Since the implant surface did not reflect the light beam in a measurable manner, the amount of adsorbed laminin was calculated on optically smooth titanium surfaces produced at the laboratory as described by Linderbäck et al. [27]. As previously described by Bougas et al. [24], the optically smooth titanium surfaces were fixed in the ellipsometric quvette filled with PBS at room temperature. The ellipsometric angles Δ_0 and Ψ_0 were measured at three locations with a Rudolph Research AutoEL III ellipsometer operating in a wavelength of 632.8 nm at a 70° angle of incidence. Subsequently, the quvette was emptied and filled with laminin solution and new angles Δ and Ψ calculated. The protein layer thickness was calculated from the ellipsometric angle changes for a protein refractive index of $n = 1.465$. By using the McCrackin algorithm for the calculations [28], it was concluded that the incubation resulted in protein thickness corresponding to 2.6 nm. The remaining 45 uncoated implants served as controls.

2.2. Surface Characterization. The surface topography of the implants was characterized with an optical interferometer (MicroXam, ADE Phase Shift, Tucson, AZ, USA) operating in wavelength of $\lambda = 550$ nm. According to the proposed guidelines for implant surface characterization [29], three implants from each group were randomly selected and each measured in 9 regions (3 thread tops, 3 thread valleys, and 3 flank regions). A B-spline filter was applied to separate roughness from form and waviness. The following three topographical parameters were evaluated: an amplitude parameter, Sa (μm) = the arithmetic average height deviation from the mean plane; a spatial parameter, Sds (μm^{-2}) = the density of summits; and a hybrid parameter, Sdr (%) = the developed surface ratio.

2.3. Animals and Surgical Procedure. The study was approved by the Malmö/Lund, Sweden, Regional Animal Ethical Committee (approval number: M253-10) and included 45 male Wistar Hannover Galas rats with an average weight of 350 g.

Prior to surgery, the animals were sedated by intraperitoneal administration of a mixture of Dormicum 5 mg/mL (Midazolam, Roche), Hypnorm (fentanylcitrate 0.315 mg/mL and fluanisone 10 mg/mL, Janssen Pharmaceutical) and sterile saline 0.9 mg/mL (Braun) in a dose of 1.5–2 mL/kg body weight. The hind legs were disinfected with 70% ethanol and 70% chlorhexidine, and Lidocaine hydrochloride (Xylocaine; AstraZeneca AB) was administrated as the local anaesthetic at each insertion site at a dose of 0.5 mL. One control implant was operated into the right tibia and one test implant into the left of each animal. One animal died after the sedation procedure. After the operation, buprenorphine hydrochloride (0.5 mL Temgesic; Reckitt Benckiser, Slough, UK) was administered as an analgesic for 3 days.

2.4. RNA Extraction and Real-Time Reverse-Transcription Polymerase Chain Reaction

2.4.1. Sample Retrieval. The animals were divided into three groups and were sacrificed after 3 days ($N = 14$), 1 week ($N = 15$) and 3 weeks ($N = 15$) with an overdose of carbon monoxide in a gas chamber. The skin above the implants was incised, and 20 implants (10 pairs control/test) for each of the two first groups (3 days and 1 week) were turned out manually. Since one implant in the 3-week group did not osseointegrate, 18 implants (9 pairs control/test) were turned out manually. The removed implants, along with the interface bone tissue, were placed in RNA*later* solution (QIAGEN GmbH, Hilden, Germany), and frozen at −80°C until analysis.

2.4.2. RNA Extraction from Implant Screws. The samples were processed in the TissueLyser instrument (Qiagen GmbH) together with β-mercaptoethanol RNeasy Lysis-buffer to remove and disrupt the cells attached to the surface of the implant screw. RNA was extracted from the sample mixtures with RNeasy Micro Kit number 74004 (Qiagen GmbH) according to manufacturer's instructions, including carrier to minimize decrease in yield due to small sample quantity. During extraction, all samples were DNase-treated according to manufacturer's instructions with RNase free DNase Set #1023460 (Qiagen GmbH) to reduce gDNA contamination.

2.4.3. Reverse Transcription (RT). All RNA samples were reverse transcribed in single 10 μL reactions according to manufacturer's instructions using TATAA RT Kit number A103b (TATAA Biocenter AB) to generate cDNA. RT-controls were included to monitor the presence of gDNA. The controls were analyzed in pools of five, containing 1.5 μL of each sample (total volume 7.5 μL). Control of RNA concentration was not possible due to the presence of carrier in extraction procedure.

2.4.4. Real Time Reverse-Transcription Polymerase Chain Reaction (Real Time RT-PCR). For each Real Time RT-PCR, 10 μL mixtures were prepared with 1 μL cDNA, according to the manufacturer's recommendations (Applied Biosystem, CA, USA). Amplification was carried out in 96-well thermal cycle plates on a StepOne detection system (Applied Biosystems, USA) according to the manufacturer's recommendations with custom-designed real-time assays and SYBR green detection (PrimerDesign Ltd, Southampton, UK) (Table 1). Normalization and fold-changes were calculated with StepOneTM software with the $\Delta\Delta$Ct method [30].

2.5. Histomorphometry. The remaining implants from each group were retrieved *en bloc* and were immersed in 4% neutral buffered formaldehyde. Since one implant from the 3 week group did not osseointegrate possibly due to an incorrect insertion angle, the final numbers of implants processed for histology were; $n = 8$ for 3 days, $n = 10$ for 1 week, and $n = 8$ for 3 weeks. All the samples were processed for undecalcified ground sectioning [31]. Briefly, after a series of dehydrations and infiltrations in resin, the samples were embedded in light-curing resin (Technovit 7200 VLC; Heraeus Kulzer Wehrheim, Germany). One central ground section was prepared from each implant by using Exakt sawing and grinding equipment (Exakt Apparatebau, Hamburg, Germany). The sections were ground to a final thickness of approximately 10 μm and histologically stained with Toluidine blue mixed with pyronin G.

Histological evaluations were performed using a light microscope (Eclipse ME600; Nikon, Japan), and the histomorphometrical data were analyzed by image analysis software (Image J v. 1.43u; National Institutes of Health, Bethesda, Maryland). The bone-implant contact (BIC) and the bone area (BA) percentage along the whole implant were calculated at $\times 10$ objective magnification as described previously [32, 33].

Table 1: Oligonucleotides used for real time RT-PCR.

Gene	Cat no.	Amplicon Length (bp)
Runx-2	Rn01512298_m1	86
ALP	Rn01516028_m1	68
Osteocalcin	Rn00566386_g1	104
BMP-2	Rn00567818_m1	126
Collagen 1	Rn01463848_m1	115
Integrin β1	Rn01753534_m1	82
IL-10	Rn00563409_m1	70
TNF-α	Rn99999017_m1	108
IL-1β	Rn00580432_m1	74
TRAP	Rn00569608_m1	95
CTSK	Rn00580723_m1	67
β-actin	4352931E	91

Table 2: Mean values (SD) for surface topography parameters for control and test implant, and P-values for pair-wise comparisons. Asterisk denotes statistically significant difference ($P < 0.05$).

Surface topography parameter	Control	Test	P-value
Sa (μm)	0.284 (0.054)	0.280 (0.066)	0.261
Sds (μm^{-2})	247493.49 (63993.65)	291112.17 (105683.8)	0.009*
Sdr (%)	14.38 (6.52)	20.16 (7.90)	0.446

3. Statistics

The statistical calculations were performed with SPSS (version 18 Chicago, Illinois, USA). The statistical comparison for the mean values of the topographic parameters Sa, Sds, and Sdr was assessed by Students t-test. For BIC and BA the nonparametric Wilcoxon signed ranks test was used while for relative gene expression, the Student's paired t-test was employed. The level of statistical significance was set at $P \leq 0.05$.

4. Results

4.1. Surface Characterization. The laminin-1 coating increased the density of summits (Sds) significantly ($P = 0.009$). On the contrary, the protein coating did neither affect the average height deviation from the mean plane (Sa) ($P = 0.261$) nor the developed surface ratio (Sdr) ($P = 0.446$) of the implants significantly (Table 2).

4.2. Real Time RT-PCR. Although the gene expression for the osteoprogenitor marker runt-related transcription factor 2 (Runx2) was lower for the test than for the control after 3 days, it was doubled at 7 days resulting in statistically significantly higher levels as compared to the control. After 21 days, the difference in the expression of the gene for Runx2 between test and control was evened out (Figure 1(a)). The second osteoprogenitor differentiation, marker bone

morphogenic protein-2 (BMP-2), did not differ between test and control at any time point (Figure 1(b)).

The initial gene expression (3 days) of the osteblastic markers osteocalcin (Figure 1(c)), alkaline phosphatase (ALP) (Figure 1(d)) and type I collagen (Figure 1(e)) was higher for the control group. Nevertheless, after 7 days the expression of the osteoblastic markers increased for the test group and declined for the control. This alteration resulted in statistically significantly higher mRNA levels of osteocalcin and type I collagen in favour of the test group. After 21 days no statistically significant differences were detected between test and control in the expression of osteoclacin and ALP. On the contrary, the expression of type I collagen for the control group was enhanced to statistically significantly higher levels as compared to the test group.

The expression of the osteoclastic marker Cathepsin K (Figure 2(a)) demonstrated a descending trend for the control group during the observation time. In contrast to the control group, the expression of Cathepsin K remained stable for the test group throughout the observation period. The expressed levels of Cathepsin K were statistically significantly lower for the test group at all times (3 days, 7 days, and 21 days). The mRNA levels of the osteoclastic marker tartrate-resistant acid phosphatase (TRAP) (Figure 2(b)) declined with time. After 3 days, the levels of TRAP were statistically significantly higher for the control group, whilst no statistically significant differences were detected between test and control at 7 or 21 days.

The gene expression of integrin $\beta 1$ (Figure 3(a)) for the test group peaked at 7 days. At this time point, the mRNA levels for integrin $\beta 1$ were statistically significantly higher for the test group (4.90-fold). Despite the enhanced levels of integrin $\beta 1$ mRNA expression in the control group after 21 days, no statistically significant differences were detected.

The proinflammatory cytokines tumor necrosis factor α (TNF-α) (Figure 3(b)) and interleukin 1β (IL-1β) (Figure 3(c)) peaked at 7 days. The fold of relative mRNA expression was 6.65 for TNF-α and 51.88 for IL-1β in favour of the control group. However, no statistically significant differences were detected at 3 and 21 days. The expression of TNF-α and IL-1β remained stable for the test group at 3, 7, and 21 days. No statistically significant differences were detected between test and control in the expression of the anti-inflammatory cytokine IL-10 (Figure 3(d)).

4.3. Histomorphometry. The values of BIC and BA were enhanced after 7 and 21 days as compared to 3 days. The test group demonstrated higher median BIC and BA at all the evaluated time points (Figures 4 and 5). The differences between the test and control were though not statistically significant ($P > 0.05$) (Table 2).

5. Discussion

In the current study, we have investigated the effects of laminin-1 coating on the early stages of osseointegration. The implants chosen for this purpose are turned with a smooth surface (Sa = 0.28 μm). Implants with turned surface have a long history of clinical documentation [1–3] and hence may be regarded as the "gold standard." The rational for rather using a smooth implant than a moderately rough, is based upon the theorem that moderately rough implants enhance osseointegration [34], thereby possibly concealing any effects of the biochemical coating. Additionally, a turned implant surface was chosen in order to investigate whether a biochemical coating can induce cell responses equivalent to the ones promoted by surface topography modifications [35, 36]. According to the surface analysis, the coating process has significantly increased the density of peaks (Sds). Since the implant surface has a minimally rough profile, the protein coating may be detected by the interferometer as prominences on the implant surface, hence resulting in elevated peak density of the test implant.

Depending on protein-desorption kinetics [26], the biochemical coating is theoretically most active during the first days after the implant installation. For this reason, we have chosen to investigate the early effects of the laminin-1 coating after 3, 7, and 21 days. The early time-points investigated in this study have been previously used in the literature in order to screen the expression of bone-related genes and inflammatory markers in a rat model [35, 37]. Since the degree of diffusion of the coating into the surrounding bone is unknown, we have chosen to collect the interface bone tissue from the removed implant instead of retrieving the implant along with the surrounding bone *en bloc*. The analysis of the interface bone tissue is further justified by a histological study concluding that implant coating material released by the shear forces during implant insertion residues within the peri-implant space [38].

The gene analyses from the interface bone tissue reveal after 7 days significantly higher levels of the transcription factor Runx-2, which is the master gene for osteoblast differentiation and is expressed by the committed osteoprogenitors [39]. At the same time point, integrin $\beta 1$ is significantly upregulated for the test implant. It has been suggested that laminin stimulates osteoprogenitors by attachment to integrin $\beta 1$ *in vitro* [20, 21]. It has also been demonstrated that activation of Runx2 by MAPK is possible by binding of type I collagen to $\alpha 2$ $\beta 1$ integrins [40]. Since collagen type I is also elevated after 7 days, a possible mechanism of action for laminin-1 could be indirect activation of Runx2 by elevating the expression of type I collagen which attaches to integrin $\beta 1$. After 7 days, no significant difference in BMP-2 levels was detected between test and control. This may imply that laminin-1 has an indirect effect on the existing osteoprogenitors in the peri-implant space, without promoting commitment of the surrounding mesenchymal stem cells to osteoprogenitors via BMP-2 [41].

Apart from the molecular mechanisms involved in the effect of laminin-1 on osteoprogenitors, our results suggest an additional effect on differentiated osteoblasts. The gene expression of collagen type I and the marker for mature post-proliferative osteoblasts, osteocalcin [42], are up-regulated after 7 days. Hence, laminin-1 may contribute to the enrichment of the extracellular matrix in the direct proximity of the implant. If we additionally take into account the significantly decreased expression of the osteoclastic proteolytic enzyme cathepsin K [43], the bone remodeling [44] may be further

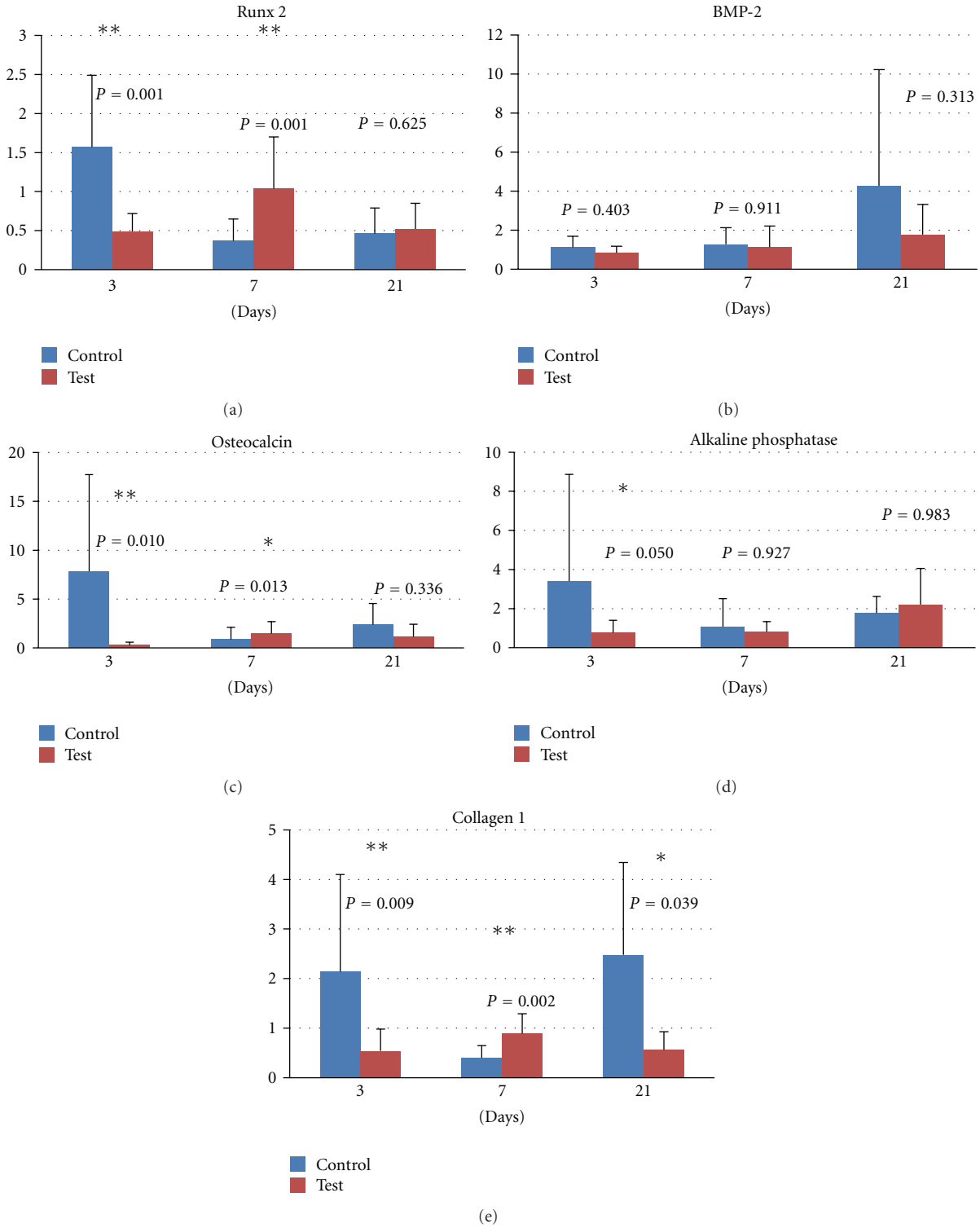

FIGURE 1: Relative gene expression for osteoblast markers at 3, 7, and 21 days: (a) runt-related transcription factor 2, (b) bone morphogenic protein 2, (c) osteocalcin, (d) alkaline phosphatase, and (e) type I collagen.

displaced in favor of osteogenesis. As reported in the literature, low expression of cathepsin K can be correlated to low levels of the proinflammatory cytokines IL-1β and TNF-α, both considered to be expressed on bone sites with pronounced osteoclastic resorption [43]. As it concerns the 3-day time point, the expression of both osteogenic and osteoclastic markers is higher for the control group. Keeping into consideration that the outcome of the bone

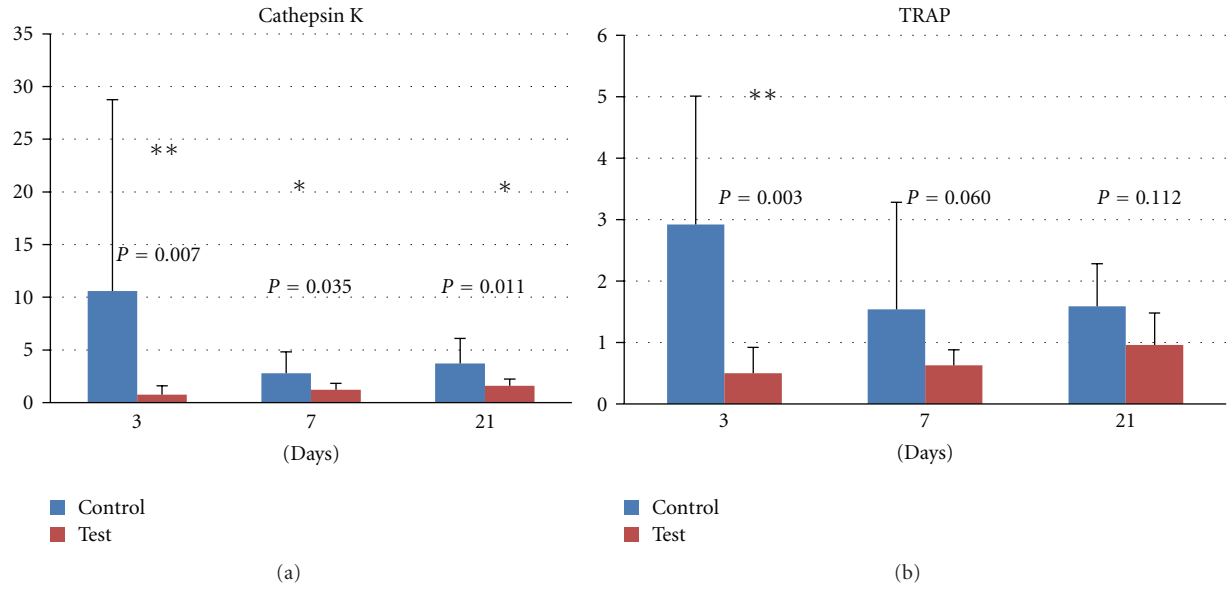

Figure 2: Relative gene expression for osteoclast markers at 3, 7, and 21 days: (a) cathepsin K and (b) tartrate-resistant acid phosphatase.

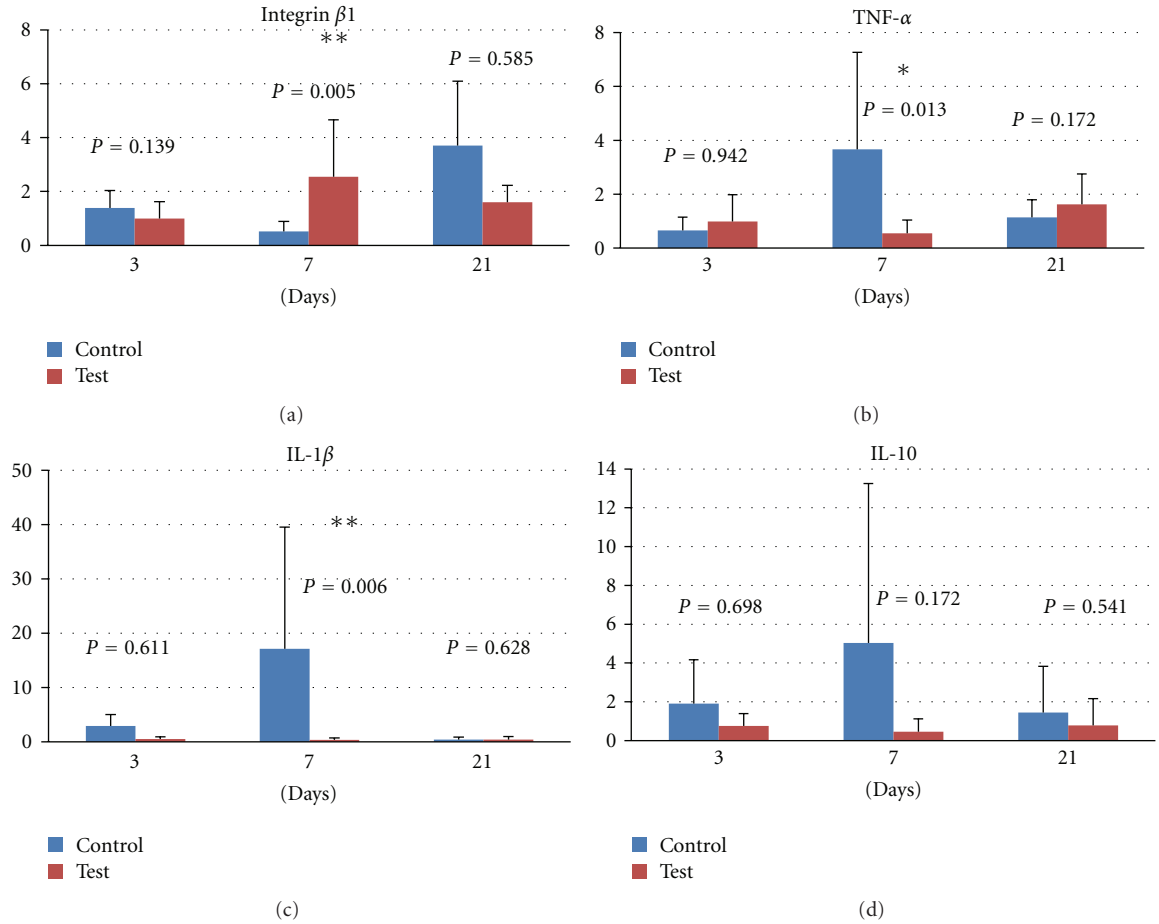

Figure 3: Relative gene expression at 3, 7, and 21 days: (a) integrin $\beta 1$, (b) tumor necrosis factor α, (c) interleukin 1β, and (d) interleukin 10.

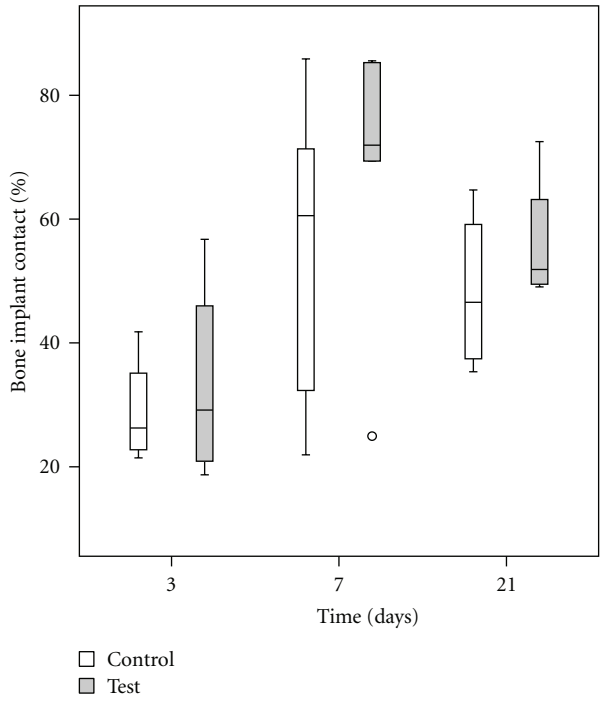

Figure 4: Box plot describing bone implant contact (%) at 3, 7, and 21 days.

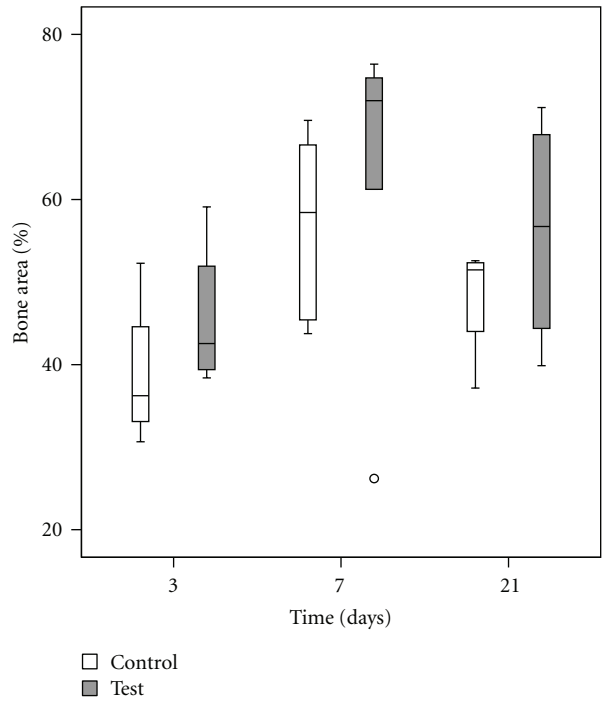

Figure 5: Box-plot describing bone area (%) at 3, 7 and 21 days.

metabolism is decided by a coupled mechanism between bone deposition and bone resorption [44], it is uncertain whether this increased activity will result to more or less new bone.

A comparison of the findings from the gene analyses to the findings from the histomorphometry reveals some discrepancies. Although there are important differences in gene expression, no differences are detected on BIC or BA after 3 and 7 days. This finding is considered reasonable keeping in mind that bone remodeling is a time-demanding process. Discrepancies between the results from traditional evaluation methods and genetic analysis have been reported previously [45]. The fact that no differences were detected on BIC or BA after 21 days is in agreement with the results from the gene expression. This result may be explained by the fact that the coating is expected to be more active during the early stages of osseointegration, since it may be gradually desorbed from the interface as demonstrated *in vitro* [26].

Conclusively, within the limitations of our study, we suggest that it is possible to alter the cell behavior on the implant-bone interface towards the osteogenic direction by coating the implant surface with laminin-1. However, the reported changes are not detected by histomorphometry, most likely depending on the fact that this method is not adequately sensitive at the short times of follow-up applied on the present study.

Acknowledgments

This study was funded by the Swedish National Graduate School in Odontological Science, the Swedish Research Council (K2009-52X-06533-27-3), the Swedish Knowledge Foundation (KK-stiftelsen), Hjalmar Svenson Research Foundation, Wilhelm and Martina Lundgren Science Foundation, Sylvan Foundation and the Council for Research and Development in Södra Älvsborg, Sweden. The implants used in this study were kindly provided by Neodent. The company has no financial interests in this study.

References

[1] T. Jemt and J. Johansson, "Implant treatment in the edentulous maxillae: a 15-year follow-up study on 76 consecutive patients provided with fixed prostheses," *Clinical Implant Dentistry and Related Research*, vol. 8, no. 2, pp. 61–69, 2006.

[2] T. Jemt, "Single implants in the anterior maxilla after 15 years of follow-up: comparison with central implants in the edentulous maxilla," *International Journal of Prosthodontics*, vol. 21, no. 5, pp. 400–408, 2008.

[3] P. Åstrand, J. Ahlqvist, J. Gunne, and H. Nilson, "Implant treatment of patients with edentulous jaws: a 20-year follow-up," *Clinical Implant Dentistry and Related Research*, vol. 10, no. 4, pp. 207–217, 2008.

[4] D. F. Williams, *The Williams Dictionary of Biomaterials*, Liverpool University Press, Liverpool, UK, 1st edition, 1999.

[5] M. Jungner, P. Lundqvist, and S. Lundgren, "Oxidized titanium implants (Nobel Biocare TiUnite) compared with turned titanium implants (Nobel Biocare mark III) with respect to implant failure in a group of consecutive patients treated with early functional loading and two-stage protocol," *Clinical Oral Implants Research*, vol. 16, no. 3, pp. 308–312, 2005.

[6] B. Friberg and T. Jemt, "Rehabilitation of edentulous mandibles by means of five TiUnite implants after one-stage surgery:

a 1-year retrospective study of 90 patients," *Clinical Implant Dentistry and Related Research*, vol. 10, no. 1, pp. 47–54, 2008.

[7] M. Brechter, H. Nilson, and S. Lundgren, "Oxidized titanium implants in reconstructive jaw surgery," *Clinical Implant Dentistry and Related Research*, vol. 7, no. 1, supplement, pp. S83–S87, 2005.

[8] M. Quirynen and N. Van Assche, "RCT comparing minimally with moderately rough implants—part 2: microbial observations," *Clinical Oral Implants Research*, vol. 23, pp. 625–634, 2012.

[9] J. P. Albouy, I. Abrahamsson, L. G. Persson, and T. Berglundh, "Spontaneous progression of peri-implantitis at different types of implants. An experimental study in dogs—I: clinical and radiographic observations," *Clinical Oral Implants Research*, vol. 19, no. 10, pp. 997–1002, 2008.

[10] J. P. Albouy, I. Abrahamsson, L. G. Persson, and T. Berglundh, "Spontaneous progression of ligatured induced peri-implantitis at implants with different surface characteristics. An experimental study in dogs II: histological observations," *Clinical Oral Implants Research*, vol. 20, no. 4, pp. 366–371, 2009.

[11] J. P. Albouy, I. Abrahamsson, and T. Berglundh, "Spontaneous progression of experimental peri-implantitis at implants with different surface characteristics: an experimental study in dogs," *Journal of Clinical Periodontology*, vol. 39, pp. 182–187, 2012.

[12] J. P. Albouy, I. Abrahamsson, L. G. Persson, and T. Berglundh, "Implant surface characteristics influence the outcome of treatment of peri-implantitis: an experimental study in dogs," *Journal of Clinical Periodontology*, vol. 38, no. 1, pp. 58–64, 2011.

[13] V. Fröjd, L. Chávez de Paz, M. Andersson, A. Wennerberg, J. R. Davies, and G. Svensäter, "In situ analysis of multispecies biofilm formation on customized titanium surfaces," *Molecular Oral Microbiology*, vol. 26, no. 4, pp. 241–252, 2011.

[14] U. M. E. Wikesjö, Y. H. Huang, A. V. Xiropaidis et al., "Bone formation at recombinant human bone morphogenetic protein-2-coated titanium implants in the posterior maxilla (Type IV bone) in non-human primates," *Journal of Clinical Periodontology*, vol. 35, no. 11, pp. 992–1000, 2008.

[15] F. Thorey, H. Menzel, C. Lorenz, G. Gross, A. Hoffmann, and H. Windhagen, "Osseointegration by bone morphogenetic protein-2 and transforming growth factor beta2 coated titanium implants in femora of New Zealand white rabbits," *Indian Journal of Orthopaedics*, vol. 45, no. 1, pp. 57–62, 2011.

[16] J. Abtahi, P. Tengvall, and P. Aspenberg, "A bisphosphonate-coating improves the fixation of metal implants in human bone. A randomized trial of dental implants," *Bone*, vol. 50, pp. 1148–1151, 2012.

[17] R. Jimbo, T. Sawase, Y. Shibata et al., "Enhanced osseointegration by the chemotactic activity of plasma fibronectin for cellular fibronectin positive cells," *Biomaterials*, vol. 28, no. 24, pp. 3469–3477, 2007.

[18] M. Nyan, D. Sato, H. Kihara, T. MacHida, K. Ohya, and S. Kasugai, "Effects of the combination with α-tricalcium phosphate and simvastatin on bone regeneration," *Clinical Oral Implants Research*, vol. 20, no. 3, pp. 280–287, 2009.

[19] H. Colognato and P. D. Yurchenco, "Form and function: the laminin family of heterotrimers," *Developmental Dynamics*, vol. 218, pp. 213–234, 2000.

[20] P. Roche, H. A. Goldberg, P. D. Delmas, and L. Malaval, "Selective attachment of osteoprogenitors to laminin," *Bone*, vol. 24, no. 4, pp. 329–336, 1999.

[21] P. Roche, P. Rousselle, J. C. Lissitzky, P. D. Delmas, and L. Malaval, "Isoform-specific attachment of osteoprogenitors to laminins: mapping to the short arms of laminin-1," *Experimental Cell Research*, vol. 250, no. 2, pp. 465–474, 1999.

[22] S. Vukicevic, F. P. Luyten, H. K. Kleinman, and A. H. Reddi, "Differentiation of canalicular cell processes in bone cells by basement membrane matrix components: regulation by discrete domains of laminin," *Cell*, vol. 63, no. 2, pp. 437–445, 1990.

[23] K. Bougas, V. Franke Stenport, F. Currie, and A. Wennerberg, "*In vitro* evaluation of calcium phosphate precipitation on possibly bioactive titanium surfaces in the presence of laminin," *Journal of Oral and Maxillofacial Research*, vol. 2, no. 3, article e3, 2011.

[24] K. Bougas, V. Franke Stenport, P. Tengvall, F. Currie, and A. Wennerberg, "Laminin coating promotes calcium phosphate precipitation on titanium discs in vitro," *Journal of Oral and Maxillofacial Research*, vol. 2, no. 4, e5, 2011.

[25] D. M. Brunette, P. Tengvall, M. Textor, and P. Thomsen, "Proteins at titanium interfaces," in *Titanium in Medicine: Material Science, Surface Science, Engineering, Biological Responses and Medical Applications*, pp. 457–483, Sringer, Berlin, Germany, 2001.

[26] F. Fang, J. Satulovsky, and I. Szleifer, "Kinetics of protein adsorption and desorption on surfaces with grafted polymers," *Biophysical Journal*, vol. 89, no. 3, pp. 1516–1533, 2005.

[27] P. Linderbäck, N. Harmankaya, A. Askendal, S. Areva, J. Lausmaa, and P. Tengvall, "The effect of heat- or ultra violet ozone-treatment of titanium on complement deposition from human blood plasma," *Biomaterials*, vol. 31, no. 18, pp. 4795–4801, 2010.

[28] F. L. McCrackin, "A FORTRAN program for the analysis of ellipsometer measurements," NBS technical note 479, Washington, DC, USA, 1969.

[29] A. Wennerberg and T. Albrektsson, "Suggested guidelines for the topographic evaluation of implant surfaces," *International Journal of Oral and Maxillofacial Implants*, vol. 15, no. 3, pp. 331–344, 2000.

[30] T. D. Schmittgen and K. J. Livak, "Analyzing real-time PCR data by the comparative CT method," *Nature Protocols*, vol. 3, no. 6, pp. 1101–1108, 2008.

[31] K. Donath and G. Breuner, "A method for the study of undecalcified bones and teeth with attached soft tissues. The Sage-Schliff (sawing and grinding) technique," *Journal of Oral Pathology*, vol. 11, no. 4, pp. 318–326, 1982.

[32] C. B. Johansson and T. Albrektsson, "A removal torque and histomorphometric study of commercially pure niobium and titanium implants in rabbit bone," *Clinical Oral Implants Research*, vol. 2, no. 1, pp. 24–29, 1991.

[33] C. B. Johansson, L. Sennerby, and T. Albrektsson, "A removal torque and histomorphometric study of bone tissue reactions to commercially pure titanium and Vitallium implants," *The International Journal of Oral and Maxillofacial Implants*, vol. 6, no. 4, pp. 437–441, 1991.

[34] A. Wennerberg, *On surface roughness and implant incorporation [Doctoral thesis]*, M.S. thesis, , Göteborg, Sweden, 1996.

[35] O. Omar, S. Svensson, N. Zoric et al., "In vivo gene expression in response to anodically oxidized versus machined titanium implants," *Journal of Biomedical Materials Research Part A*, vol. 92, no. 4, pp. 1552–1566, 2010.

[36] O. M. Omar, M. E. Lennerås, F. Suska et al., "The correlation between gene expression of proinflammatory markers and bone formation during osseointegration with titanium implants," *Biomaterials*, vol. 32, no. 2, pp. 374–386, 2011.

[37] O. Omar, F. Suska, M. Lennerås et al., "The influence of bone type on the gene expression in normal bone and at the bone-implant interface: experiments in animal model," *Clinical Implant Dentistry and Related Research*, vol. 13, no. 2, pp. 146–156, 2011.

[38] T. T. Hägi, L. Enggist, D. Michel, S. J. Ferguson, Y. Liu, and E. B. Hunziker, "Mechanical insertion properties of calcium-phosphate implant coatings," *Clinical Oral Implants Research*, vol. 21, no. 11, pp. 1214–1222, 2010.

[39] G. S. Stein, J. B. Lian, A. J. Van Wijnen et al., "Runx2 control of organization, assembly and activity of the regulatory machinery for skeletal gene expression," *Oncogene*, vol. 23, no. 24, pp. 4315–4329, 2004.

[40] R. T. Franceschi, G. Xiao, D. Jiang, R. Gopalakrishnan, S. Yang, and E. Reith, "Multiple signaling pathways converge on the Cbfa1/Runx2 transcription factor to regulate osteoblast differentiation," *Connective Tissue Research*, vol. 44, no. 1, supplement, pp. 109–116, 2003.

[41] M. H. Lee, Y. J. Kim, H. J. Kim et al., "BMP-2-induced Runx2 expression is mediated by Dlx5, and TGF-beta 1 opposes the BMP-2-induced osteoblast differentiation by suppression of Dlx5 expression," *Journal of Biological Chemistry*, vol. 278, no. 36, pp. 34387–34394, 2003.

[42] S. Kuroda, A. S. Virdi, Y. Dai, S. Shott, and D. R. Sumner, "Patterns and localization of gene expression during intramembranous bone regeneration in the rat femoral marrow ablation model," *Calcified Tissue International*, vol. 77, no. 4, pp. 212–225, 2005.

[43] D. Brömme and F. Lecaille, "Cathepsin K inhibitors for osteoporosis and potential off-target effects," *Expert Opinion on Investigational Drugs*, vol. 18, no. 5, pp. 585–600, 2009.

[44] K. I. Nakahama, "Cellular communications in bone homeostasis and repair," *Cellular and Molecular Life Sciences*, vol. 67, no. 23, pp. 4001–4009, 2010.

[45] R. Jimbo, Y. Xue, M. Hayashi et al., "Genetic responses to nanostructured calcium-phosphate-coated implants," *Journal of Dental Research*, vol. 90, pp. 1422–1427, 2011.

Hindawi Publishing Corporation
International Journal of Biomaterials
Volume 2012, Article ID 181024, 14 pages
doi:10.1155/2012/181024

Research Article

In Vitro Osteogenic Properties of Two Dental Implant Surfaces

Marta Monjo,[1,2] Christiane Petzold,[2] Joana Maria Ramis,[1] Staale Petter Lyngstadaas,[2] and Jan Eirik Ellingsen[3]

[1] *Department of Fundamental Biology and Health Sciences, Research Institute on Health Sciences (IUNICS), University of Balearic Islands, E-07122 Palma de Mallorca, Spain*
[2] *Department of Biomaterials, University of Oslo, 0317 Oslo, Norway*
[3] *Oral Research Laboratory, Institute for Clinical Dentistry, University of Oslo, 0317 Oslo, Norway*

Correspondence should be addressed to Marta Monjo, marta.monjo@uib.es

Received 9 May 2012; Revised 12 September 2012; Accepted 15 September 2012

Academic Editor: Paulo Guilherme Coelho

Current dental implant research aims at understanding the biological basis for successful implant therapy. The aim of the study was to perform a full characterization of the effect of two commercial titanium (Ti) surfaces, OsseoSpeed and TiOblast, on the behaviour of mouse preosteoblast MC3T3-E1 cells. The effect of these Ti surfaces was compared with tissue culture plastic (TCP). In vitro experiments were performed to evaluate cytotoxicity, cell morphology and proliferation, alkaline phosphatase activity, gene expression, and release of a wide array of osteoblast markers. No differences were observed on cell viability and cell proliferation. However, changes were observed in cell shape after 2 days, with a more branched morphology on OsseoSpeed compared to TiOblast. Moreover, OsseoSpeed surface increased BMP-2 secretion after 2 days, and this was followed by increased IGF-I, BSP, and osterix gene expression and mineralization compared to TiOblast after 14 days. As compared to the gold standard TCP, both Ti surfaces induced higher osteocalcin and OPG release than TCP and differential temporal gene expression of osteogenic markers. The results demonstrate that the gain of using OsseoSpeed surface is an improved osteoblast differentiation and mineralization, without additional effects on cell viability or proliferation.

1. Introduction

Current dental implant research aims at developing of innovative surfaces able to promote a more favourable biological response to the implant material at the bone-implant interface and to accelerate osseointegration [1]. It has largely been demonstrated that rough surfaces present an increased bone fixation and bone-to-implant contact compared to smooth surfaces [2–4]. In addition to surface topography, the chemical properties of implant surfaces also play an important role in promoting osseointegration [5]. Modification of titanium implants using hydrogen fluoride at low concentrations results in the formation of nanostructures along the titanium surface as well as the incorporation of small amounts of fluoride into the crystal structure of the superficial layer of the implant [1, 6], thereby, modifying both, surface topography and surface chemistry.

In vitro experiments have shown that fluoride-modified titanium implants stimulate osteoblast differentiation in different cell models [7–10], enhance cell osteoblastic adhesion and expression of bone-specific mRNA [8, 11], increase cell viability [11], improve the initial cell response to the implant [12], and augment the thrombogenic properties of titanium, promoting fibrinogen activation and rapid coagulation [13]. In vivo, fluoride-modified titanium implants enhance interfacial bone formation [8], create a firmer bone anchorage [14], augment the amount of new bone formation in the voids and bone-to-implant contact [15], improve biomechanical properties due to a more mature and mineralized interfacial bone matrix [16], and increase implant osseointegration in osteoporotic bone [17].

The aim of the present study was to examine the in vitro bone response of mouse preosteoblast MC3T3-E1 cells to

two commercial Ti surfaces, OsseoSpeed and TiOblast, and to validate the claimed higher bone response of the new generation surface (OsseoSpeed) compared to its respective predecessor (TiOblast). The osteoblast response to these Ti surfaces was also compared with tissue culture plastic (TCP), which is normally considered the gold standard for tissue culture. OsseoSpeed is a further development of the moderately roughened (grit blasted with titanium dioxide particles) titanium surface TiOblast. OsseoSpeed has been reported to gain its additional surface characteristics via a chemical (fluoride) treatment and a slight topographic modification of the TiOblast surface [6, 14].

2. Materials and Methods

2.1. Implants and Treatments. Test implants used were all made of grade 2 titanium, with a diameter of 6.25 mm and a height of 1.95 mm. The test surface was blasted with titanium dioxide (TiO_2) particles (TiOblast) to create a microrough surface. According to the manufacturer, fluoride modified implants (OsseoSpeed) went through an additional cleaning process including diluted HF. The blasted-only implants served as control. Implants were premounted on the carriers, inserted individually in sealed containers, and sterilized by β-irradiation (AstraTech AB, Mölndal, Sweden).

2.2. Roughness Analysis. After surface treatments, the surface roughness of one sample per group was measured with a blue light profilometer (PLμ 2300, Sensofar, Terassa, Spain). Three areas were imaged per surface at 50x magnification ($254 \times 191\,\mu m^2$), and surface parameters were calculated after levelling the images by rotation with the program SensoMap Plus 4.1 (SARL Digital Surf, Besançon, France) and application of a Gaussian filter ($50 \times 50\,\mu m$) to remove underlying waviness. Topographical changes were as follows: average height deviation from the mean plan (S_a), surface skewness (S_{sk}), surface kurtosis (S_{ku}), and core fluid retention index (S_{ci}) were recorded to quantify surface differences among the TiOblast and the OsseoSpeed groups.

2.3. Cell Culture. The murine osteoblast cell line MC3T3-E1 (DSMZ, Braunschweig, Germany) was used as in vitro model. Cells were routinely cultured at 37°C in a humidified atmosphere of 5% CO_2 and maintained in alpha-MEM (PAA Laboratories GmbH, Austria) supplemented with 10% fetal calf serum (PAA Laboratories GmbH, Austria) and 50 IU penicillin/mL and 50 μg streptomycin/mL (Sigma, St. Louis, MO, USA). Cells were subcultured 1 : 4 before reaching confluence using PBS (PAA Laboratories GmbH, Austria) and trypsin/EDTA (Sigma, St. Louis, MO, USA). To test the different surface modification of titanium implants (TiOblast and OsseoSpeed), coins were placed in a 96-well plate (with a diameter size per well of 6.5 mm), and 10^4 cells were seeded on each coin. The same number of cells was cultured in parallel in plastic (TCP) in all the experiments.

2.4. Cell Viability. LDH activity was used as an index of cytotoxicity in the culture media. After 48 h, 7, and 14 days, the culture media was collected, centrifuged at 500 ×g for 5 min at 4°C, and the supernatant was stored at 4°C. LDH activity was determined spectrophotometrically according to the manufacturer's kit instructions (Cytotoxicity Detection kit, Roche Diagnostics, Mannheim, Germany) and presented relative to the LDH activity in the medium of cells cultured on TCP for 2 days, which was set as 100%.

2.5. DAPI Staining and Cell Counting. MC3T3-E1 cells were seeded on the coins modified according to the protocol described above. The MC3T3-E1-cell layers were washed twice with PBS after the respective culture time and fixed in a 4% formaldehyde solution in PBS for 30 min. Subsequently, the samples were washed again with PBS and mounted with a DAPI-containing mounting medium (ProLong Gold antifade reagent with DAPI, Invitrogen Ltd, Paisley, UK) according to their protocol. The samples were stored in dark at −20°C until analysis by fluorescence microscopy (Leica DM RBE, Leica Microsystems, Wetzlar, Germany) with connected digital camera (Olympus DM50, Olympus Europe, Hamburg, Germany). Afterwards, nuclei were counted with the ImageJ software (http://rsbweb.nih.gov/ij/). Four implants were used per treatment and time point, and in each implant three different fields were analysed, giving the number of cells per μm^2.

2.6. SEM Analysis. SEM analyses were performed to study the morphology of MC3T3-E1 cells grown on the surface of both Ti surfaces. For this purpose, cells were first fixed in a formaldehyde solution at 4% in PBS for 30 min. Cell layers were dried in increasing concentrations of ethanol followed by critical point drying (E3000, Quorum Tech, Ashford, UK) and sputter coated with a thin layer of carbon (Cressington Carbon Coater 108/carbon A, Cressington Scientific Intruments Ltd., Watford, UK). SEM scans were taken (Philips XL 30 ESEM, FEI Electron Optics, Eindhoven, The Netherlands) to image the morphology of the cells attaching to the different surfaces. Pictures at 400x of magnification were taken after 2, 7, and 14 days and also at 2000x of magnification after 2 days.

2.7. Release of BMP-2 into the Cell Culture Media. Cell culture supernatants were analysed for BMP-2 release, secreted to the culture medium after 2 days of cell culture, using an enzyme-linked immunosorbent assay (ELISA). Aliquots from the culture media were centrifuged at 1800 rpm for 5 minutes at 4°C, and supernatants were used for BMP-2 determination following instructions described by the manufacturer (Quantikine Immunoassay, R&D Systems, Minneapolis, MN, USA).

2.8. Isolation of Total RNA. Total RNA was isolated using a monophasic solution of phenol and guanidine isothiocyanate (Trizol, Invitrogen Life Technologies, Carlsbad, CA, USA), following the instructions of the manufacturer. RNA was quantified at 260 nm using a Nanodrop spectrophotometer (NanoDrop Technologies, Wilmington, DE, USA).

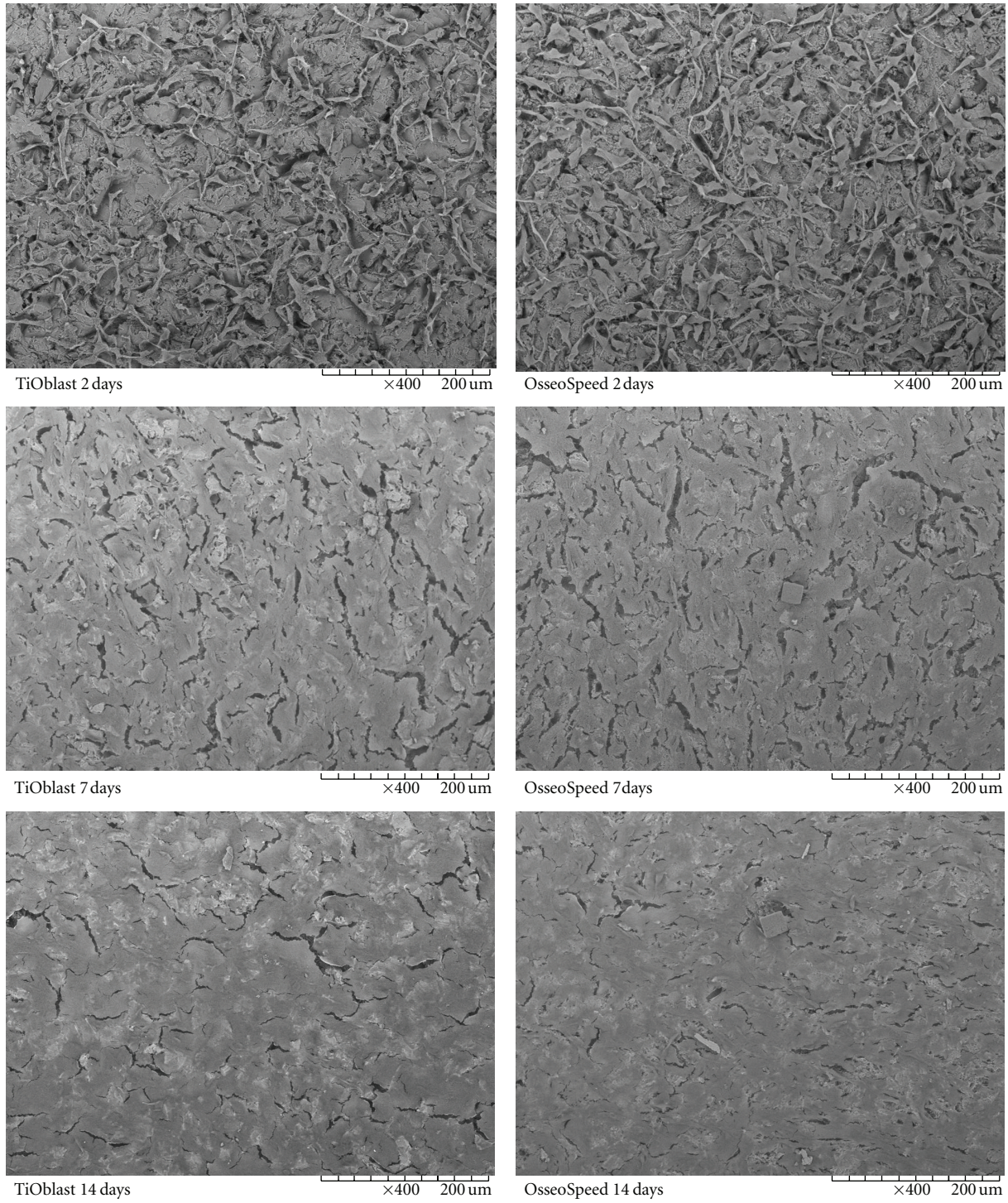

Figure 1: Scanning electron microscope images of MC3T3-E1 cells attached to each coin after 2, 7, and 14 days of cell culture. 400x magnification images are shown.

2.9. Real-Time RT-PCR. The same amount of total RNA (2 μg) from each sample was reverse transcribed to cDNA at 42°C for 60 min in a final volume of 40 μL, using iScript cDNA Synthesis kit (BioRad) that contains both oligo(dT) and random hexamers. Each cDNA was diluted 1/5, and aliquots were frozen (−20°C) until the PCR reactions were carried out. Real-time PCR was performed for two housekeeping genes: 18S ribosomal RNA (18S rRNA), glyceraldehyde-3-phosphate dehydrogenase (GAPDH), and thirteen target genes: alkaline phosphatase (ALP), bone sialoprotein (BSP), CD44, collagen type I (coll-I), distal-less homeobox 2 (Dlx2), hairy and enhancer of split 1

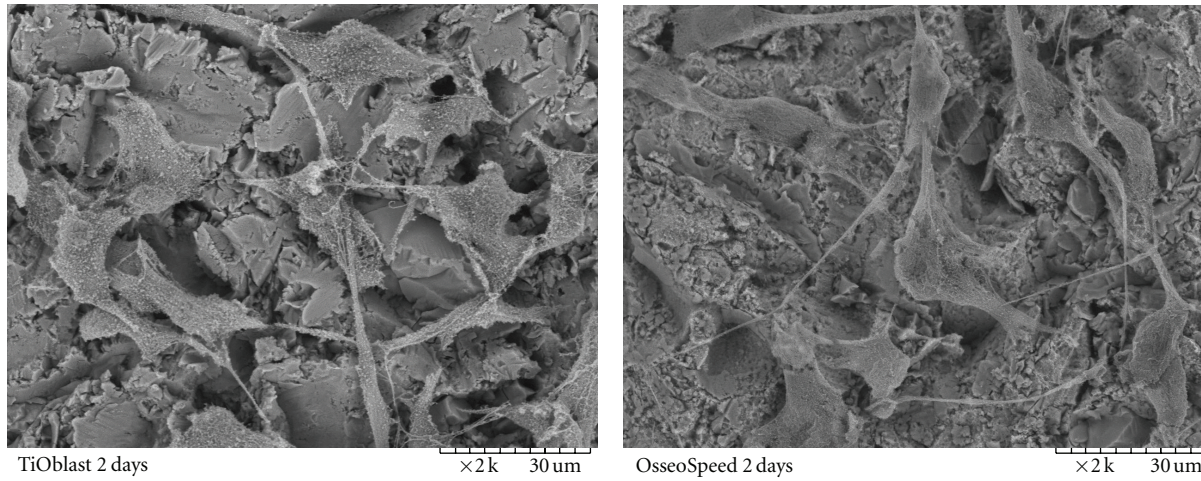

Figure 2: Detail of surface morphology and cell monolayer of MC3T3-E1 cells after 2 days by scanning electron microscope. 2000x magnification images are shown.

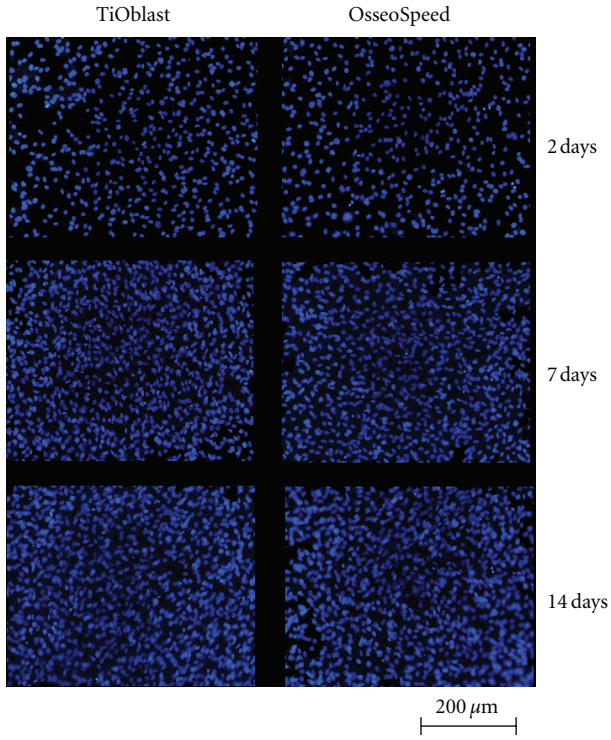

Figure 3: DAPI staining of the nuclei (20x) of the cell monolayer attached to each coin after 2, 7, and 14 days of cell culture.

(Hes1), insulin growth factor-I (IGF-I), interleukin-6 (IL-6), osteoprotegerin (OPG), osterix (Osx), receptor activator of NFkappaB ligand (RANKL), Smad1, and Smad5. Oligonucleotide primer sequences used for the real-time RT-PCR, the length of the resulting amplicons and the GeneBank accession number, are shown in Table 1.

Real-time PCR was performed in the iCycler (BioRad) using SYBR green detection. Each reaction contained 5 μL of cDNA, 500 nM of the sense and antisense specific primers (for all, except for collagen-I which was 300 nM), and 12.5 μL of 2X iQ SYBR Green Supermix in a final volume of 25 μL. The amplification program consisted of a preincubation step for denaturation of the template cDNA (3 min 95°C), followed by 40 cycles consisting of a denaturation step (15 s 95°C), an annealing step (15 s 60°C; for all, except for ALP which was 65°C), and an extension step (30 s 72°C). After each cycle, fluorescence was measured at 72°C. A negative control without cDNA template was run in each assay. Samples were run in duplicate.

Real-time efficiencies were calculated from the given slopes in the iCycler software using serial dilutions, showing all the investigated transcripts high real-time PCR efficiency rates, and high linearity ($r > 0.99$) when different concentrations were used. PCR products were subjected to a melting curve analysis on the iCycler and subsequently 2% agarose/TAE gel electrophoresis to confirm amplification specificity.

2.10. Alkaline Phosphatase Activity. An aliquot of 25 μL of culture media was assayed in duplicate for alkaline phosphatase activity by measuring the cleavage of p-Nitrophenyl Phosphate (pNPP) (Sigma, St. Louis, MO, USA) in a soluble yellow end product which absorbs at 405 nm. A volume of 100 μL of this substrate was used. The reaction was stopped after 30 min in dark with the addition of 50 μL of 3 M sodium hydroxide. The absorbance of the stopped reaction was read at 405 nm. In parallel to the samples, a standard curve with calf intestinal alkaline phosphatase (CIAP, 1 U/μL) (Promega, Madison, WI, USA) was constructed, by mixing 1 μL from the stock CIAP with 5 mL of alkaline phosphatase buffer (1 : 5000 dilution) and then making 1 : 5 serial dilutions.

2.11. Luminex Analysis. Cell culture supernatants were analysed for OPG, osteocalcin, IL-6, TNF-α, and RANKL

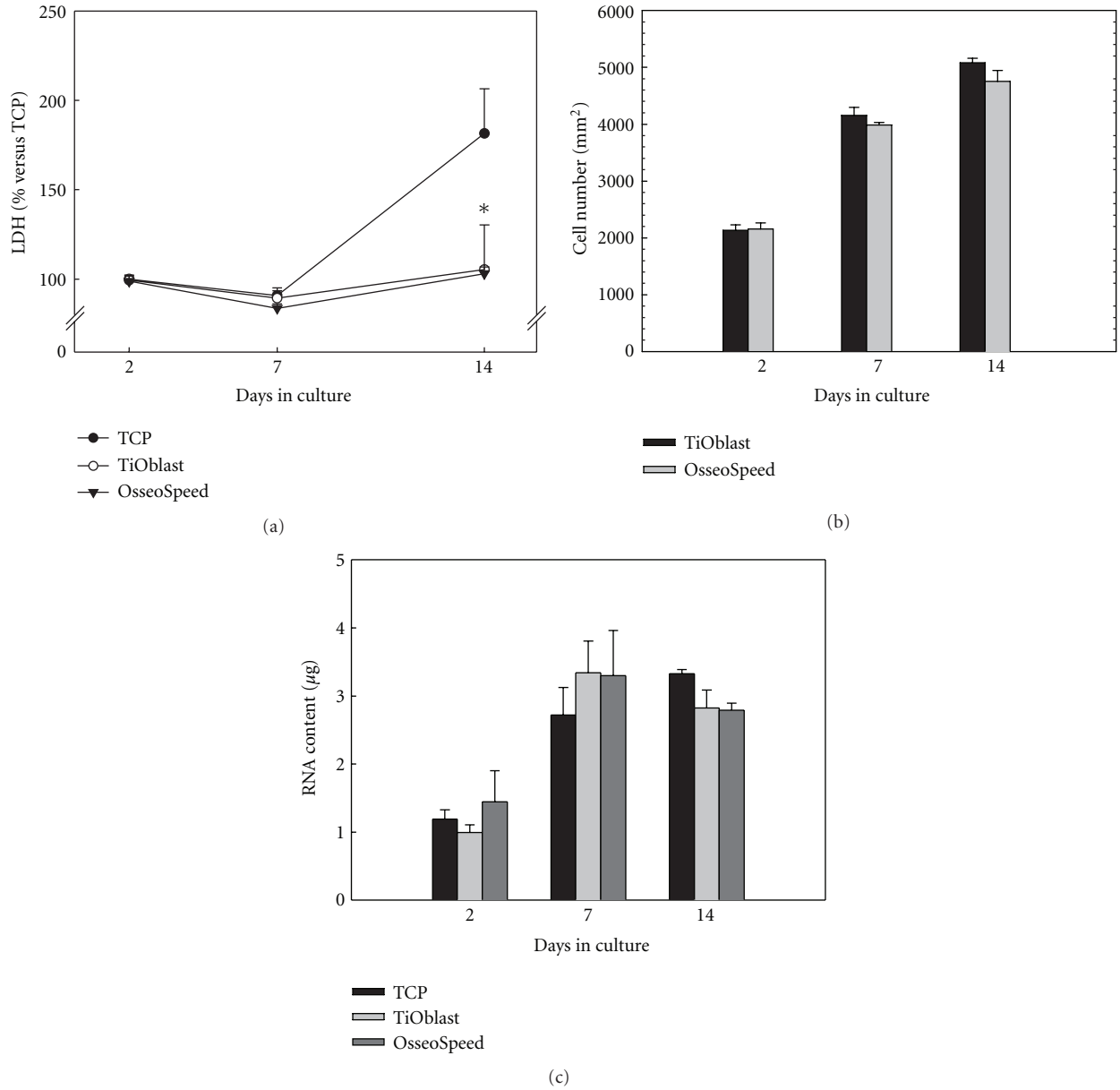

Figure 4: Cell viability, proliferation and RNA content of MC3T3-E1 cells (a) LDH activity measured from culture media collected after 2, 7 and 14 days of culture. Data expressed as a relative to the mean value of the TCP group at day 2, which was set as 100%. (b) Number of nuclei were counted with the ImageJ software and referred to the number of cells/mm^2. (c) RNA content of cells attached after 2, 7 and 14 days of culture. Values represent the mean ± SEM. Student's t-test: $^*P \leq 0.05$ versus TCP; $^\#P \leq 0.05$ versus TiOblast.

using the solid phase sandwich multiplex bead immunoassays (Mouse Bone Panel 1B LINCOplex kit and Mouse RANKL single-plex kit, Cat#MBN1B-41K and Cat#MBN-41K-1RANKL, Linco Research, St. Charles, MO, USA) according to the manufacturer's protocol. Multianalyte profiling was performed on the Luminex-100 analyser (Luminex Corporation, Austin, TX, USA).

2.12. Calcium Crystal Deposition Quantification. After 14 days of cell culture, the entire surface of TiOblast and OsseoSpeed titanium coins ($n = 2$) were examined for calcium deposition with a tabletop scanning electron microscope (SEM) (TM-1000, Hitachi, Tokyo, Japan). Cell layers were dried in increasing concentrations of ethanol followed by critical point drying (E3000, Quorum Tech, Ashford, UK) and sputter coated with a thin layer of carbon (Cressington Carbon Coater 108/carbon A, Cressington Scientific Intruments Ltd, Watford, UK). A 250x magnification was used to examine the shape, size, and number of calcium crystals. The composition of the crystals was analysed by energy dispersive X-ray spectroscopy (EDS unit, TM-1000, Hitachi, Tokyo, Japan).

2.13. Statistical Analysis. All data are presented as mean values ± SEM. Differences between groups were assessed by Student's t-test, using the program SPSS for Windows,

Table 1: Sense (S) and antisense (A) sequences of the primers used in the real-time PCR of target and housekeeping genes.

Gene		Primer sequence (5′ to 3′)	GeneBank accession number	Amplicon size (base pairs)
ALP	S	AACCCAGACACAAGCATTCC	X13409	151
	A	GAGAGCGAAGGGTCAGTCAG		
BSP	S	GAAAATGGAGACGGCGATAG	L20232	141
	A	ACCCGAGAGTGTGGAAAGTG		
CD44	S	CTTCCATCTTGACCCGTTGT	XM_283773	175
	A	ACAGTGCTCCTGTCCCTGAT		
Coll-I	S	AGAGCATGACCGATGGATTC	NM_007742	177
	A	CCTTCTTGAGGTTGCCAGTC		
Dlx2	S	AGTTCGTCTCCGGTCAACAA	NM_010054.1	125
	A	GCCGCCAGCTGGAAACTGGA		
Hes1	S	CTGCAGCGGGCGCAGATGAC	NM_008235.2	114
	A	ACACGTGGACAGGAAGCGGG		
IGF-I	S	GCTCTTCAGTTCGTGTGTGG	U75390	142
	A	ACATCTCCAGCCTCCTCAGA		
IL-6	S	CCGGGAGCAGTGTGAGCTTA	NM_031168	171
	A	TAGATGCGTTTGTAGGCGGTC		
OPG	S	AGACCATGAGGTTCCTGCAC	U94331	131
	A	AAACAGCCCAGTGACCATTC		
Osx	S	ACTGGCTAGGTGGTGGTCAG	NM_007419	135
	A	GGTAGGGAGCTGGGTTAAGG		
RANKL	S	GGCCACAGCGCTTCTCAG	AF019048	141
	A	TGACTTTATGGGAACCCGAT		
Smad1	S	ATGCCAGCTGACACACCCCC	NM_008539.3	112
	A	TTTCAGCGGGCAGTGGAGGC		
Smad5	S	GGAGTTTGCTCAGCTTCTGG	NM_008541.2	134
	A	TGGTGACGTCCTGTCGGTGGT		
18S rRNA	S	GTAACCCGTTGAACCCCATT	X00686	151
	A	CCATCCAATCGGTAGTAGCG		
GAPDH	S	ACCCAGAAGACTGTGGATGG	XM_132897	171
	A	CACATTGGGGGTAGGAACAC		

version 17.0. Results were considered statistically significant at the $P \leq 0.05$ level.

3. Results

3.1. Surface Topographic Characterization. Topographical analyses by blue-light profilometry (Table 2) revealed a significant increase of S_a for the OsseoSpeed surfaces compared to TiOblast. Surface skewness was negative for both groups, and they can be imagined as bearing surfaces with holes. The skewness was significantly increased for OsseoSpeed. Surface kurtosis was significantly higher for TiOblast, indicating a more rounded appearance of the TiOblast surfaces. The core fluid retention index was significantly higher for OsseoSpeed, in accordance with the S_a values and pointing to a better fluid retention for OsseoSpeed surfaces.

3.2. Cell Adhesion and Morphology. Observation of the cell monolayer by SEM microscopy (Figures 1 and 2) and by fluorescence microscopy (Figure 3) confirmed that MC3T3-E1 cells attached well to both Ti surfaces, resulting in similar cell proliferation at the different time points investigated. Cell shape was examined in detail after 2 days. On OsseoSpeed surface, cells exhibited a more branched shape morphology compared to TiOblast.

3.3. Cell Viability, Proliferation, and RNA Content. In order to determine the effect of the different Ti surfaces and TCP

Table 2: Topographical parameters analysed by blue light profilometry of the titanium surfaces used in the studies.

	TiOblast	OsseoSpeed	P
S_a/μm	0.77 ± 0.06	1.35 ± 0.04	$8.3E-08$
S_{sk}	−0.38 ± 0.05	−0.2 ± 0.08	0.003
S_{ku}	3.92 ± 0.05	3.46 ± 0.11	0.00002
S_{ci}	1.41 ± 0.02	1.47 ± 0.02	0.002

Mean values and standard deviation are presented ($n = 5$, 3 combined measurements per sample); Student's t-test being performed between "TiOblast" and "OsseoSpeed". Legends: S_a: average height deviation from the mean plan, S_{sk}: surface skewness, S_{ku}: surface kurtosis, and S_{ci}: core fluid retention index.

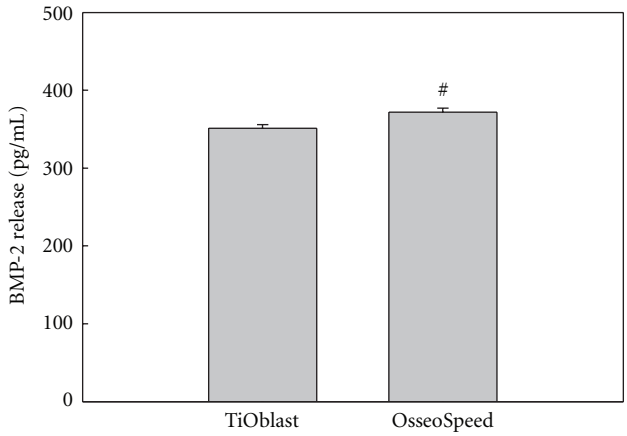

Figure 5: BMP-2 released to culture media after 2 days of culture. Values represent the mean ± SEM. Student's t-test: $^{\#}P \leq 0.05$.

on the cell viability after short- and long-term cell culture on the titanium implants, the LDH activity in the culture media was measured after 2, 7, and 14 days (Figure 4(a)). No differences were found between the OsseoSpeed and TiOblast in the LDH activity at any of the days analysed. However, after 14 days of culture, cells cultured onto TCP showed significantly higher levels of LDH activity compared to cells cultured onto Ti implants. Counting of cells at the different time points using DAPI staining (Figure 4(b)), revealed no differences in cell proliferation between the two Ti surfaces. RNA content was quantified from cell monolayer after 2, 7, and 14 days of culture (Figure 4(c)). No differences were observed among the different groups, although RNA content increased from 2 to 7 days of cell culture.

3.4. BMP-2 Release. The potential to initiate osteogenic differentiation after 2 days of culture was investigated by measuring the BMP-2 release to the culture media using a BMP-2 immunoassay (Figure 5). OsseoSpeed titanium implants induced a significant higher release of BMP-2 compared to TiOblast.

3.5. Gene Expression of Osteogenic Markers. The differentiation of MC3T3-E1 cells cultured on the different implant surfaces and onto plastic was examined by analysing the gene expression after 2, 7, and 14 days of cell culture. As seen in Figures 6, 7, and 8, gene expression levels of fifteen different genes related to osteogenic differentiation like transcriptional factors and regulators, extracellular matrix molecules, cytokines, growth factors, and functional markers were analysed.

Regarding the osteogenic markers (Figure 6), coll-I mRNA expression was significantly higher in cells cultured onto both titanium surfaces compared to those cultured in plastic after 14 days. BSP mRNA expression was upregulated in cells cultured on plastic compared to those cultured on both titanium surfaces. Statistical differences were seen after 2 and 7 days of culture. After 14 days of culture, the OsseoSpeed group displayed higher BSP mRNA levels compared to the TiOblast one. ALP mRNA levels were significantly higher in cells cultured onto plastic compared to those cultured on both titanium surfaces after 2 and 7 days of culture, while after 14 days, ALP levels of cells cultured on both titanium surfaces were higher than those cultured on plastic, although just the OsseoSpeed group reached statistical significance. CD44 mRNA levels were significantly higher in cells cultured on plastic compared to those cultured on both titanium surfaces (day 7) and compared to the TiOblast group (day 2). After 14 days of culture, no differences were observed between groups.

As regards transcriptional factors and regulators (Figure 7), no significant differences were found for Dlx2 and Hes1 among the groups at the different time points, although their gene expression decreased likewise over the time period studied. osterix mRNA levels were higher in cells cultured on both titanium surfaces compared to those cultured on plastic after 2 days of culture. After 14 days of culture, OsseoSpeed implants induced an upregulation osterix mRNA compared to TiOblast. After 14 days of culture, the OsseoSpeed group displayed higher Smad1 mRNA levels compared to TCP. Smad5 mRNA expression was significantly up-regulated in the TCP group compared to the TiOblast one after 2 days of culture, and no differences were observed afterwards.

Regarding cytokines and growth factors (Figure 8), IGF-I mRNA expression was significantly higher in cells cultured on plastic compared to those cultured on both titanium surfaces after 2 and 7 days of culture. However, after 14 days, IGF-I levels of cells cultured on the OsseoSpeed group were significantly higher than for the other groups. No significant differences were found for IL-6 or OPG mRNA levels among the groups at the different time points and their expression decreased likewise over the time period studied. RANKL mRNA levels (day 7) were significantly higher in the

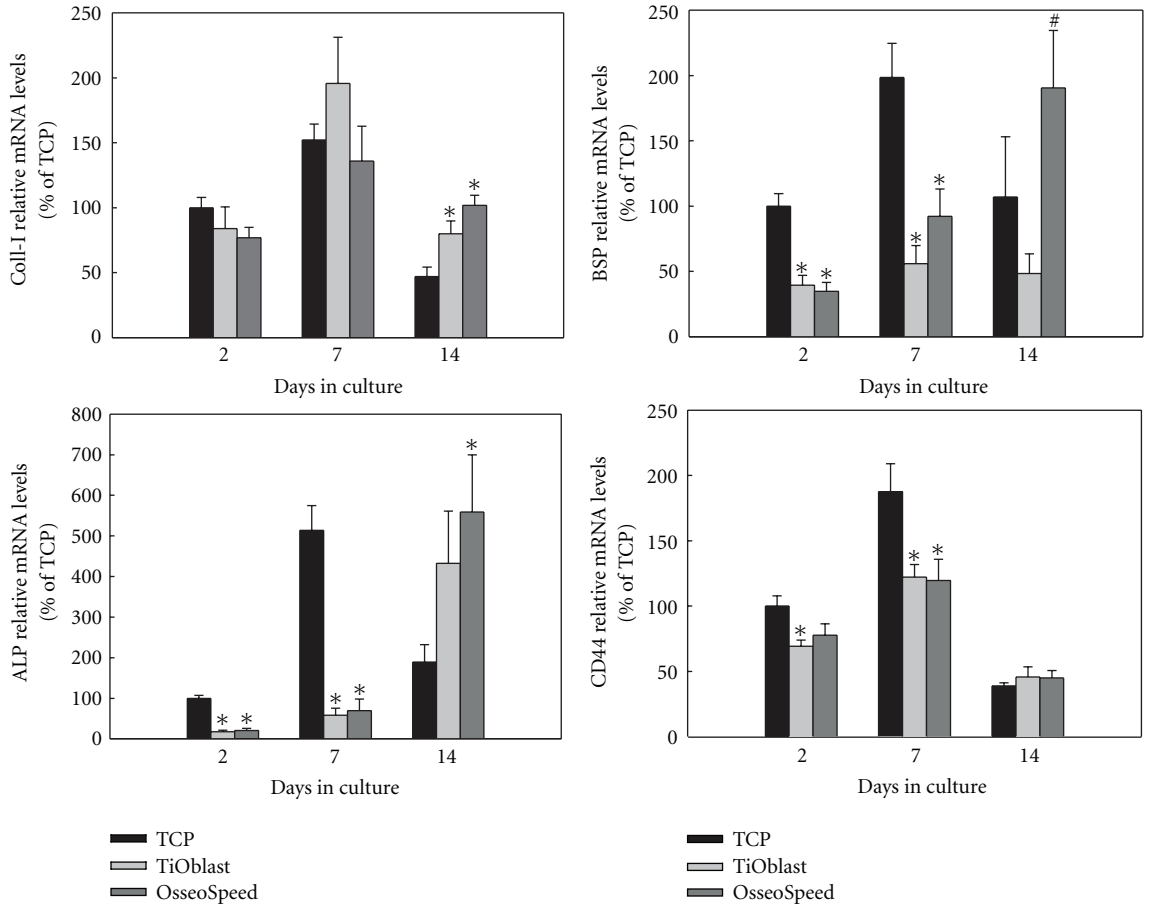

Figure 6: Relative mRNA levels of osteogenic markers (Coll-I, BSP, ALP, CD44) after 2, 7, and 14 days of culture. Ratios of target genes relative to housekeeping genes (GAPDH, B-actin) were expressed relative to the mean value of the TCP group at day 2, which was set as 100%. Values represent the mean ± SEM. Differences between groups ($n = 6$) were assessed by Student's t-test. $^{\#}P \leq 0.05$ versus TiOblast; $^{*}P \leq 0.05$ versus TCP.

OsseoSpeed group compared to the TCP one. No differences were seen for the other groups or time points for this gene.

3.6. Osteocalcin, Osteoprotegerin, and IL-6 Release. Osteocalcin, OPG, and IL-6 release to the culture media was determined by a Luminex bioassay after 2, 7, and 14 days of culture in the TiOblast, the OsseoSpeed and TCP groups (Figure 9). TNF-α and RANKL levels were under detection levels in all cell culture supernatants and are thus, not presented. Osteocalcin and OPG release was higher in both implant groups compared to TCP after 7 and 14 days of culture. After 2 days, cells cultured on TiOblast surfaces released higher amounts of OPG than those cultured on OsseoSpeed surfaces. IL-6 release was higher in the TiOblast group than in the TCP one after 7 days of culture.

3.7. ALP Activity and Crystal Deposition. No statistical differences were found for ALP activity in the culture medium after 2, 7, and 14 days of cell culture (Figure 10). However, ALP activity in the OsseoSpeed group tended to be higher than in the TiOblast one.

After 14 days of culture, cells cultured on OsseoSpeed titanium surfaces displayed a higher number of calcium crystals compared to those cultured on TiOblast surfaces (16.5 ± 1.5 versus 9.5 ± 0.5, respectively; $P = 0.047$).

4. Discussion

The present study provides a wide characterization of the in vitro osteogenic properties of two commercial surfaces, TiOblast and OsseoSpeed. TiOblast was the first moderately roughened implant surface with 10 years followup reported in the literature and the precursor of the OsseoSpeed surface [18–20]. The OsseoSpeed surface is a further development introduced in 2004 that incorporates small amounts of fluoride ions in the oxide layer, a slight increase on the micrometer scale in surface roughness, and the appearance of a nanoscale topography. In the present work, we showed the topographical differences between the two surfaces, mainly an increase in the S_a value in the OsseoSpeed surface, but also changes in surface skewness, kurtosis, and the core fluid retention index. The obtained results confirm

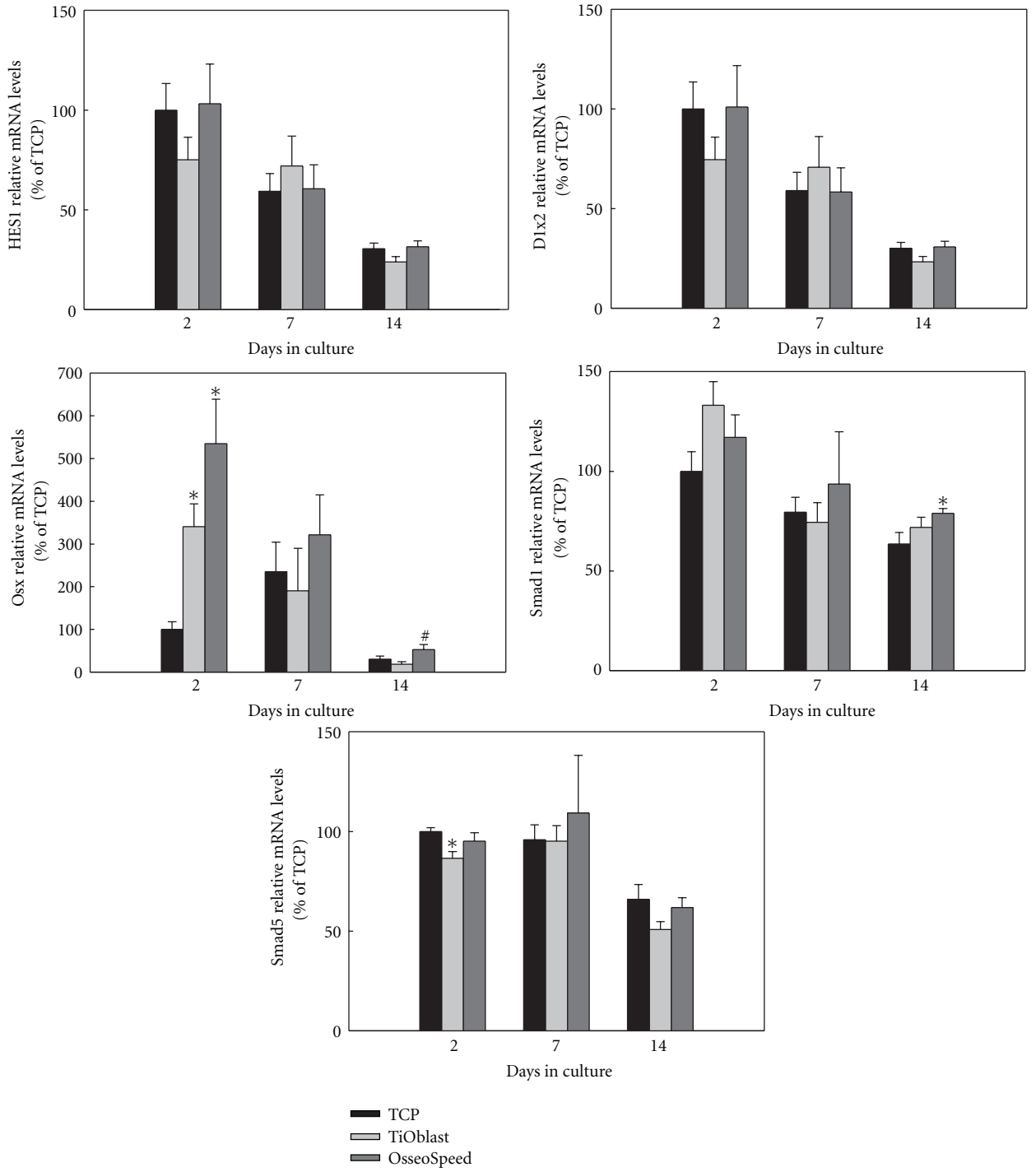

Figure 7: Relative mRNA levels of transcriptional factors and regulators (Hes1, Dlx2, Osx, Smad1, Smad5) after 2, 7 and 14 days of culture. Ratios of target genes relative to housekeeping genes (GAPDH, B-Actin) were expressed relative to the mean value of the TCP group at day 2, which was set as 100%. Values represent the mean ± SEM. Differences between groups ($n = 6$) were assessed by Student's t-test. $^{\#}P \leq 0.05$ versus TiOblast; $^{*}P \leq 0.05$ versus TCP.

that OsseoSpeed surface show an increased micrometer-scale surface roughness, together with the formation of nanostructures, as reported in earlier studies [11]. The presence of micro- and nanoscale topography in OsseoSpeed compared to TiOblast surface and the addition of fluoride, did not change the biocompatibility of the implants and the initial attachment and proliferation of the MC3T3-E1 cells. However, it was observed that OsseoSpeed surfaces induced a more branched cell morphology. It has been reported that this cell shape may increase the contractility

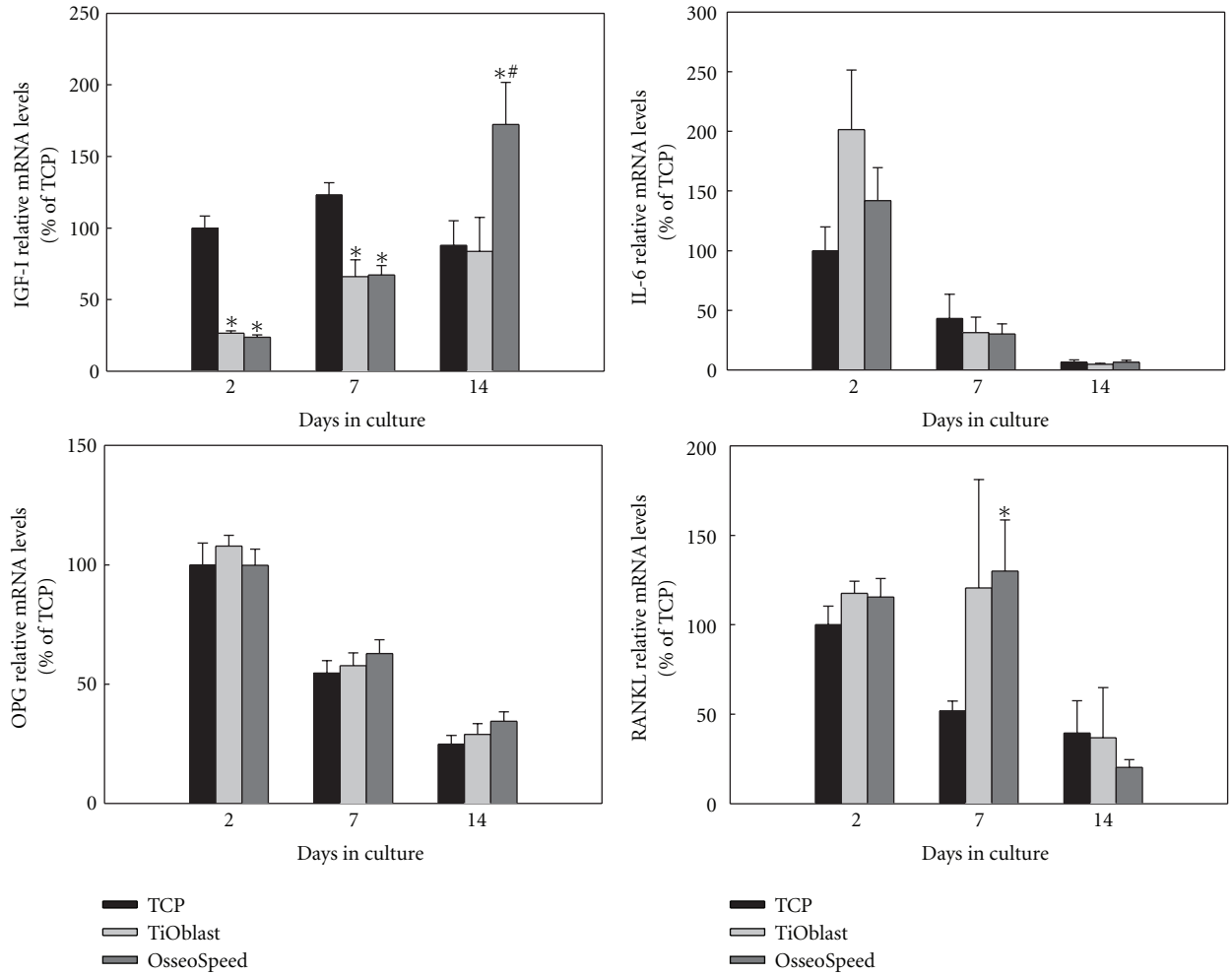

Figure 8: Relative mRNA levels of cytokines and growth factors (IGF-I, IL-6, OPG, RANKL) after 2, 7, and 14 days of culture. Ratios of target genes relative to housekeeping genes (GAPDH, B-actin) were expressed relative to the mean value of the TCP group at day 2, which was set as 100%. Values represent the mean ± SEM. Differences between groups ($n = 6$) were assessed by Student's t-test. $^{\#}P \leq 0.05$ versus TiOblast; $^{*}P \leq 0.05$ versus TCP.

of the cytoskeleton and lead to preferential osteoblastic differentiation [21], which has been found in the present study for the OsseoSpeed surface compared to TiOblast. The increase found in the LDH activity on the TCP surface after 14 days is most probably due to the higher proliferation and/or cellular activity at this later time point on TCP.

MC3T3-E1 osteoblast-like cells undergo a developmental sequence of proliferation and differentiation similar to primary cells in culture [22]. Osteoblast maturation in vitro is characterised by changes in gene expression at each developmental stage [23–26]. Modulation of these expressed genes is subjected to a transcriptional control regulated by growth factors and cytokines [23, 26]. BMP-2 is a highly potent growth/differentiation factor that induces differentiation of progenitor cells into the osteoblast lineage, and exhibits this osteogenic action by activating Smad signaling and by regulating transcription of osteogenic genes. Thus, the higher release of BMP-2 found in the OsseoSpeed group could initiate osteogenic differentiation through the regulation of transcriptional factors.

Runt-related transcription factor 2 (Runx2) is a master regulator of osteogenic gene expression that is necessary for the osteoblast lineage commitment and, as well, regulates osteoblast differentiation [27]. Here, we did not determine Runx2 mRNA levels since, as we have previously reported that Runx2 mRNA expression is constant during osteoblast differentiation [28], probably due to the fact that MC3T3-E1 cells are already committed to the osteoblast lineage. Nevertheless, we have analysed the expression of different transcription factors that have been described to interact with Runx2: Dlx2, a downstream target of BMP-2 that is thought to directly activate Runx2 and Osterix genes [29], and Hes1 that can stimulate the transactivating function of Runx2 [30], although it negatively regulates bone phenotypic maturation and its expression decreases during osteoblast differentiation [31]. We have previously reported that Hes1 and Dlx2 are early responsive genes to roughness and fluoride treatment of titanium implants [32]. In our previous report, both genes were downregulated by fluoride treatment of rough titanium implants after one day in primary human

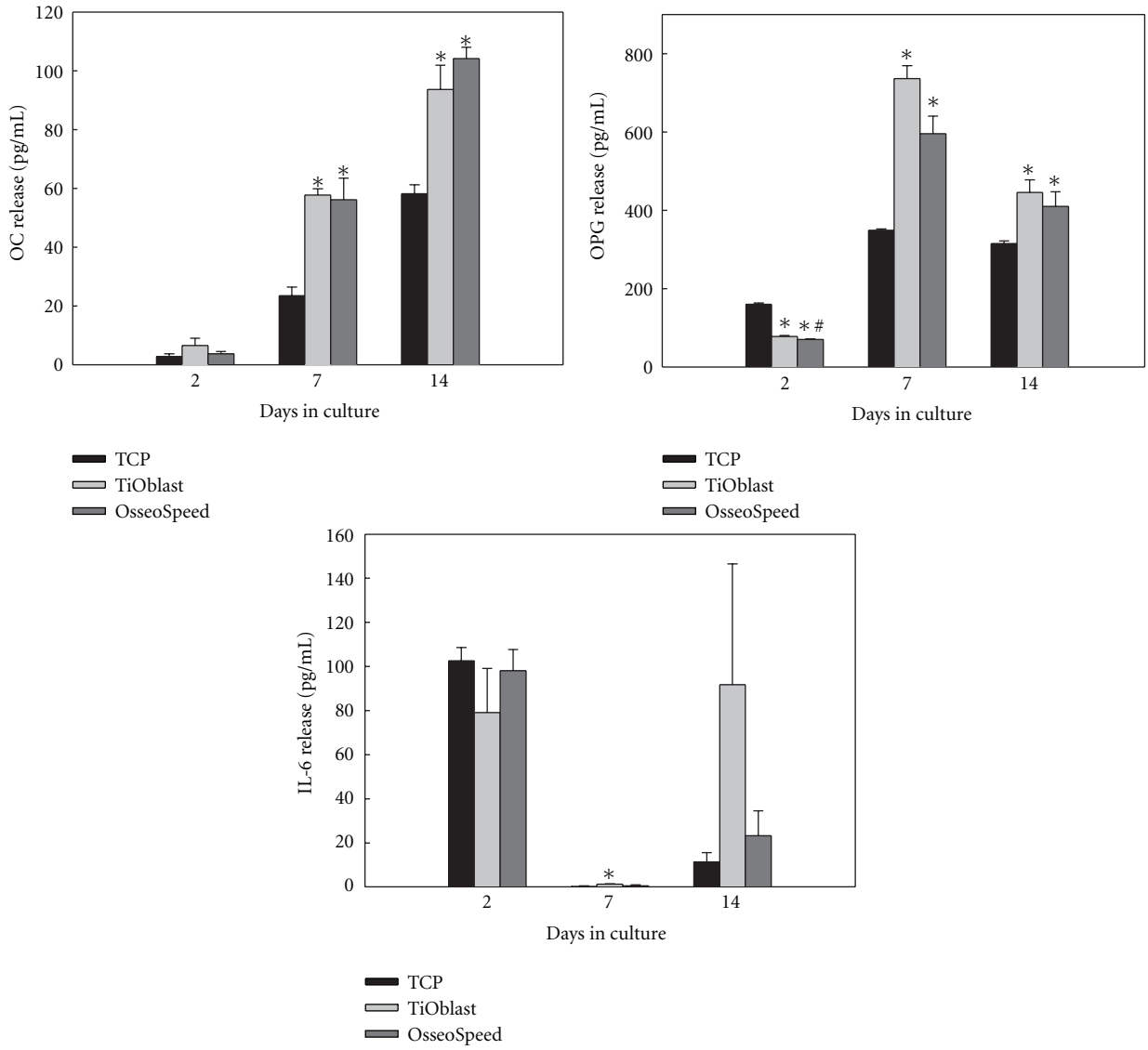

Figure 9: OC, OPG, and IL-6 released to culture media after 2, 7, and 14 days of culture. Values represent the mean ± SEM. Student t-test: $^{*}P \leq 0.05$ versus TCP; $^{\#}P \leq 0.05$ versus TiOblast.

osteoblasts. Here, no differential regulation was found for these two genes among the two surfaces analysed, neither when compared to TCP. The difference between the results may have been caused by differences in the surfaces used for comparison and differences in the cell model.

The Smad family of proteins has been identified as the downstream propagators of BMP signals [33]. BMP-activated Smads induce Runx2 gene expression and Smads interact physically with the Runx2 protein to induce osteoblast differentiation [34]. In particular, Smad1 and Smad5 are necessary for BMP-mediated Runx2 acetylation [35]. We found no important changes on Smad1 and Smad5 at the different time points and groups analysed; only Smad1 showed higher significant levels in OsseoSpeed compared to TCP. Thus, although Smad expression patterns are informative, future studies should investigate their phosphorylation stage to find out whether their activity is regulated in the different surfaces.

Osterix is another transcription factor downstream of Runx2 which is required for the ongoing differentiation within the osteogenic pathway [36], being involved in the differentiation step from preosteoblast to fully functional osteoblast [37]. Here we found higher Osx mRNA levels in cells cultured onto OsseoSpeed implants compared to TiOblast, in agreement with earlier observations [8, 10].

Other osteogenic markers were analysed during osteoblast differentiation. Type I collagen is expressed in high levels in the early proliferation stage, which is gradually decreased as the cell matures. This downregulation was only observed in the TCP group, while TiOblast and OsseoSpeed showed higher coll-1 mRNA levels. In agreement with these results, Masaki et al. [10] also found higher mRNA levels of coll-I in human palatal mesenchymal stem cells cultured on TiOblast and OsseoSpeed than on TCP after 3 days, although these differences were not significant. Alkaline phosphatase increases during extracellular matrix maturation

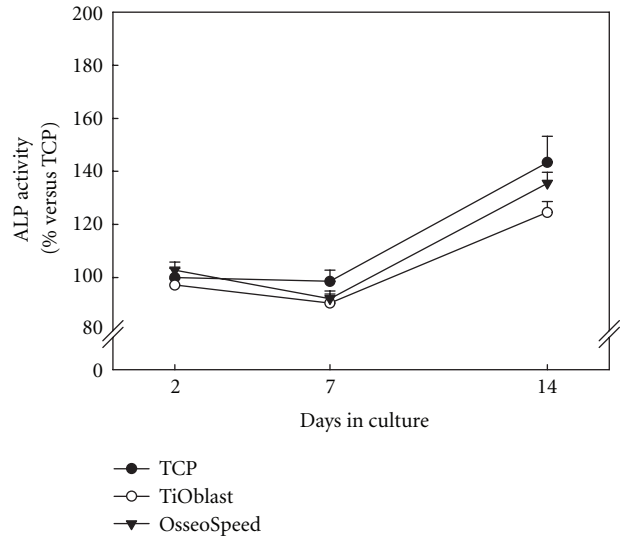

Figure 10: ALP activity measured from culture media collected after 2, 7, and 14 days of culture. Data expressed as a relative to the mean value of the TCP group at day 2, which was set as 100%. Values represent the mean ± SEM. Student t-test: $^{*}P \leq 0.05$ versus TCP; $^{\#}P \leq 0.05$ versus TiOblast.

then decreases when mineralization is well progressed and bone sialoprotein is transiently expressed very early and then upregulated again in differentiated osteoblasts at the onset of mineralization [23, 26]. These two markers, that reflect a more advanced stage of osteoblast differentiation, showed higher mRNA levels on TCP up to the first week, while OsseoSpeed surfaces increased their levels greatly after 14 days, indicating that extracellular matrix of cells seeded on TCP was mature and competent for mineralization after 1 week and on OsseoSpeed surfaces after 2 weeks. This also indicates that differentiation of MC3T3-E1 cells on TiOblast was delayed compared to OsseoSpeed surface. These results are in line with those obtained in the present study for the higher ALP activity and number of crystals deposited in the cell monolayer of OsseoSpeed surface. Using the same in vitro model, another study [8] did not observe significant differences in BSP between the two titanium surfaces, although in this case the roughness was similar, and the titanium particles for grit-blasting¡?bhlt?¿was smaller. Finally, CD44 was analysed as this marker has been indicated to be expressed in higher levels in osteocytes [38]. However, the analysis did not reveal important differences between the two titanium surfaces investigated, only for the TCP group.

Besides these bone-specific markers, the effect of the different titanium implant surfaces on the expression of different growth factors and cytokines involved in bone formation was analysed. IL-6 is a cytokine produced by cells of the osteoblast and osteoclast lineages that not only has a role in inflammation but also increases bone resorption and possibly bone remodeling [39]. Both the mRNA levels and the secretion of IL-6 decreased over the time in cell culture, but in a lesser extent for TiOblast surface. IGF-I induces osteoblast proliferation, bone collagen, and matrix synthesis [40, 41] and stimulates the activity of alkaline phosphatase [42]. Similar to other osteogenic markers commented before, this growth factor was significantly upregulated in OsseoSpeed surface compared to both TCP and TiOblast. Similar results have been found in a previous study in vivo [16], suggesting that IGF-I might play an important role stimulating bone formation when administered in combination with fluoride [43].

Osteoblasts exert a crucial function in osteoclast activation and differentiation, through the production of specific biological mediators such as the activator of nuclear factor k B ligand (RANKL) and its antagonist osteoprotegerin (OPG). In the present work, the total amount of RANKL produced by MC3T3-E1 osteoblasts was below the detection limit of the Luminex assay (3 pg/mL), while OPG was detected in the supernatant during the whole culture period, was similar to the reported results by Guida and coworkers using ELISA [44]. However, OPG production found in this study was similar between TiOblast and OsseoSpeed group in MC3T3-E1 osteoblasts, with higher levels on titanium when compared to TCP. As a trend, TiOblast surfaces showed higher levels than OsseoSpeed, opposite to the results obtained in human bone marrow mesenchymal stem cells [44]. Due to the lack of differences in OPG/RANKL mRNA levels and the secretion of OPG, we conclude that in MC3T3-E1 cells, the levels of OPG/RANKL are not regulated by the different surfaces used in the study. Other authors have reported increased OPG levels in response to rough surfaces [45] and different chemical composition [46].

In conclusion, the results from the present study demonstrate that the gain of using OsseoSpeed surface is an improved osteoblast differentiation and mineralization, without additional effects on cell viability or proliferation. The enhanced in vitro osteogenic properties are in line with the improved osseointegrating properties and clinical performance of fluoride-modified titanium implants [47–49].

Conflict of Interests

The authors declare that they have no conflict of interests. J. E. Ellingsen is the coinventor of the OsseoSpeed surface.

Acknowledgments

The authors wish to thank AstraTech AB (Mölndal, Sweden) for providing the titanium coins. This work was supported by the Norwegian Research Council (Grant no. 171058), and by the Ministry of Science and Innovation of Spain (Torres Quevedo contract to J. M. Ramis and Ramón y Cajal contract to M. Monjo). The authors are especially thankful for the excellent technical support and assistance from Britt Kvam and Aina-Mari Lian (Oral Research Laboratory, Faculty of Dentistry, University of Oslo).

References

[1] J. E. Ellingsen, P. Thomsen, and S. P. Lyngstadaas, "Advances in dental implant materials and tissue regeneration," *Periodontology 2000*, vol. 41, no. 1, pp. 136–156, 2006.

[2] K. Gotfredsen, T. Berglundh, and J. Lindhe, "Anchorage of titanium implants with different surface characteristics: an experimental study in rabbits," *Clinical Implant Dentistry and Related Research*, vol. 2, no. 3, pp. 120–128, 2000.

[3] H. J. Rønold and J. E. Ellingsen, "Effect of micro-roughness produced by TiO_2 blasting-tensile testing of bone attachment by using coin-shaped implants," *Biomaterials*, vol. 23, no. 21, pp. 4211–4219, 2002.

[4] M. Wong, J. Eulenberger, R. Schenk, and E. Hunziker, "Effect of surface topology on the osseointegration of implant materials in trabecular bone," *Journal of Biomedical Materials Research*, vol. 29, no. 12, pp. 1567–1575, 1995.

[5] L. Le Guéhennec, A. Soueidan, P. Layrolle, and Y. Amouriq, "Surface treatments of titanium dental implants for rapid osseointegration," *Dental Materials*, vol. 23, no. 7, pp. 844–854, 2007.

[6] J. E. Ellingsen, "Surface configurations of dental implants," *Periodontology 2000*, vol. 17, no. 1, pp. 36–46, 1998.

[7] L. F. Cooper, Y. Zhou, J. Takebe et al., "Fluoride modification effects on osteoblast behavior and bone formation at TiO_2 grit-blasted c.p. titanium endosseous implants," *Biomaterials*, vol. 27, no. 6, pp. 926–936, 2006.

[8] J. Guo, R. J. Padilla, W. Ambrose, I. J. De Kok, and L. F. Cooper, "The effect of hydrofluoric acid treatment of TiO_2 grit blasted titanium implants on adherent osteoblast gene expression in vitro and in vivo," *Biomaterials*, vol. 28, no. 36, pp. 5418–5425, 2007.

[9] Z. M. Isa, G. B. Schneider, R. Zaharias, D. Seabold, and C. M. Stanford, "Effects of fluoride-modified titanium surfaces on osteoblast proliferation and gene expression," *International Journal of Oral and Maxillofacial Implants*, vol. 21, no. 2, pp. 203–211, 2006.

[10] C. Masaki, G. B. Schneider, R. Zaharias, D. Seabold, and C. Stanford, "Effects of implant surface microtopography on osteoblast gene expression," *Clinical Oral Implants Research*, vol. 16, no. 6, pp. 650–656, 2005.

[11] S. F. Lamolle, M. Monjo, M. Rubert, H. J. Haugen, S. P. Lyngstadaas, and J. E. Ellingsen, "The effect of hydrofluoric acid treatment of titanium surface on nanostructural and chemical changes and the growth of MC3T3-E1 cells," *Biomaterials*, vol. 30, no. 5, pp. 736–742, 2009.

[12] R. Jimbo, T. Sawase, K. Baba, T. Kurogi, Y. Shibata, and M. Atsuta, "Enhanced initial cell responses to chemically modified anodized titanium," *Clinical Implant Dentistry and Related Research*, vol. 10, no. 1, pp. 55–61, 2008.

[13] A. Thor, L. Rasmusson, A. Wennerberg et al., "The role of whole blood in thrombin generation in contact with various titanium surfaces," *Biomaterials*, vol. 28, no. 6, pp. 966–974, 2007.

[14] J. E. Ellingsen, C. B. Johansson, A. Wennerberg, and A. Holmén, "Improved retention and bone-to-implant contact with fluoride-modified titanium implants," *International Journal of Oral and Maxillofacial Implants*, vol. 19, no. 5, pp. 659–666, 2004.

[15] T. Berglundh, I. Abrahamsson, J. P. Albouy, and J. Lindhe, "Bone healing at implants with a fluoride-modified surface: an experimental study in dogs," *Clinical Oral Implants Research*, vol. 18, no. 2, pp. 147–152, 2007.

[16] M. Monjo, S. F. Lamolle, S. P. Lyngstadaas, H. J. Rønold, and J. E. Ellingsen, "In vivo expression of osteogenic markers and bone mineral density at the surface of fluoride-modified titanium implants," *Biomaterials*, vol. 29, no. 28, pp. 3771–3780, 2008.

[17] Y. Li, S. Zou, D. Wang, G. Feng, C. Bao, and J. Hu, "The effect of hydrofluoric acid treatment on titanium implant osseointegration in ovariectomized rats," *Biomaterials*, vol. 31, no. 12, pp. 3266–3273, 2010.

[18] T. Albrektsson and A. Wennerberg, "Oral implant surfaces—part 2—review focusing on clinical knowledge of different surfaces," *International Journal of Prosthodontics*, vol. 17, no. 5, pp. 544–564, 2004.

[19] B. Ellegaard, V. Baelum, and J. Kølsen-Petersen, "Non-grafted sinus implants in periodontally compromised patients: a time-to-event analysis," *Clinical Oral Implants Research*, vol. 17, no. 2, pp. 156–164, 2006.

[20] L. Rasmusson, J. Roos, and H. Bystedt, "A 10-year follow-up study of titanium dioxide-blasted implants," *Clinical Implant Dentistry and Related Research*, vol. 7, no. 1, pp. 36–42, 2005.

[21] S. Lavenus, M. Berreur, V. Trichet, G. Louarn, and P. Layrolle, "Adhesion and osteogenic differentiation of human mesenchymal stem cells on titanium nanopores," *European Cells & Materials*, vol. 22, pp. 84–96, 2011.

[22] H. Sudo, H. A. Kodama, and Y. Amagai, "In vitro differentiation and calcification in a new clonal osteogenic cell line derived from newborn mouse calvaria," *Journal of Cell Biology*, vol. 96, no. 1, pp. 191–198, 1983.

[23] J. E. Aubin, "Advances in the osteoblast lineage," *Biochemistry and Cell Biology*, vol. 76, no. 6, pp. 899–910, 1998.

[24] J. E. Aubin, "Regulation of osteoblast formation and function," *Reviews in Endocrine & Metabolic Disorders*, vol. 2, no. 1, pp. 81–94, 2001.

[25] J. B. Lian, G. S. Stein, J. L. Stein, and A. J. Van Wijnen, "Transcriptional control of osteoblast differentiation," *Biochemical Society Transactions*, vol. 26, no. 1, pp. 14–21, 1998.

[26] G. S. Stein, J. B. Lian, J. L. Stein, A. J. Van Wijnen, and M. Montecino, "Transcriptional control of osteoblast growth and differentiation," *Physiological Reviews*, vol. 76, no. 2, pp. 593–629, 1996.

[27] P. Ducy, R. Zhang, V. Geoffroy, A. L. Ridall, and G. Karsenty, "Osf2/Cbfa1: a transcriptional activator of osteoblast differentiation," *Cell*, vol. 89, no. 5, pp. 747–754, 1997.

[28] M. Monjo, M. Rubert, J. E. Ellingsen, and S. P. Lyngstadaas, "Rosuvastatin promotes osteoblast differentiation and regulates SLCO1A1 transporter gene expression in MC3T3-E1 cells," *Cellular Physiology and Biochemistry*, vol. 26, no. 4-5, pp. 647–656, 2010.

[29] S. E. Harris, D. Guo, M. A. Harris, A. Krishnaswamy, and A. Lichtler, "Transcriptional regulation of BMP-2 activated genes in osteoblasts using gene expression microarray analysis: role of DLX2 and DLX5 transcription factors," *Frontiers in Bioscience*, vol. 8, pp. s1249–s1265, 2003.

[30] K. W. McLarren, R. Lo, D. Grbavec, K. Thirunavukkarasu, G. Karsenty, and S. Stifani, "The mammalian basic helix loop helix protein HES-1 binds to and modulates the transactivating function of the runt-related factor Cbfa1," *Journal of Biological Chemistry*, vol. 275, no. 1, pp. 530–538, 2000.

[31] Y. Zhang, J. B. Lian, J. L. Stein, A. J. Van Wijnen, and G. S. Stein, "The Notch-responsive transcription factor Hes-1 attenuates osteocalcin promoter activity in osteoblastic cells," *Journal of Cellular Biochemistry*, vol. 108, no. 3, pp. 651–659, 2009.

[32] J. M. Ramis, S. F. Taxt-Lamolle, S. P. Lyngstadaas, J. E. Reseland, J. E. Ellingsen, and M. Monjo, "Identification of early response genes to roughness and fluoride modification of titanium implants in human osteoblasts," *Implant Dentistry*, vol. 21, no. 2, pp. 141–149, 2012.

[33] Y. Shi and J. Massagué, "Mechanisms of TGF-β signaling from cell membrane to the nucleus," *Cell*, vol. 113, no. 6, pp. 685–700, 2003.

[34] K. S. Lee, H. J. Kim, Q. L. Li et al., "Runx2 is a common target of transforming growth factor β1 and bone morphogenetic protein 2, and cooperation between Runx2 and Smad5 induces osteoblast-specific gene expression in the pluripotent mesenchymal precursor cell line C2C12," *Molecular and Cellular Biology*, vol. 20, no. 23, pp. 8783–8792, 2000.

[35] E. J. Jeon, K. Y. Lee, N. S. Choi et al., "Bone morphogenetic protein-2 stimulates Runx2 acetylation," *Journal of Biological Chemistry*, vol. 281, no. 24, pp. 16502–16511, 2006.

[36] K. Nakashima, X. Zhou, G. Kunkel et al., "The novel zinc finger-containing transcription factor Osterix is required for osteoblast differentiation and bone formation," *Cell*, vol. 108, no. 1, pp. 17–29, 2002.

[37] A. Ulsamer, M. J. Ortuño, S. Ruiz et al., "BMP-2 induces osterix expression through up-regulation of Dlx5 and its phosphorylation by p38," *Journal of Biological Chemistry*, vol. 283, no. 7, pp. 3816–3826, 2008.

[38] D. E. Hughes, D. M. Salter, and R. Simpson, "CD44 expression in human bone: a novel marker of osteocytic differentiation," *Journal of Bone and Mineral Research*, vol. 9, no. 1, pp. 39–44, 1994.

[39] R. L. Jilka, G. Hangoc, G. Girasole et al., "Increased osteoclast development after estrogen loss: mediation by interleukin-6," *Science*, vol. 257, no. 5066, pp. 88–91, 1992.

[40] E. Canalis, "Effect of insulinlike growth factor I on DNA and protein synthesis in cultured rat calvaria," *Journal of Clinical Investigation*, vol. 66, no. 4, pp. 709–719, 1980.

[41] J. M. Hock, M. Centrella, and E. Canalis, "Insulin-like growth factor I has independent effects on bone matrix formation and cell replication," *Endocrinology*, vol. 122, no. 1, pp. 254–260, 1988.

[42] T. Noda, H. Tokuda, M. Yoshida et al., "Possible involvement of phosphatidylinositol 3-kinase/Akt pathway in insulin-like growth factor-I-induced alkaline phosphatase activity in osteoblasts," *Hormone and Metabolic Research*, vol. 37, no. 5, pp. 270–274, 2005.

[43] P. Ammann, R. Rizzoli, J. Caverzasio, and J. P. Bonjour, "Fluoride potentiates the osteogenic effects of IGF-I in aged ovariectomized rats," *Bone*, vol. 22, no. 1, pp. 39–43, 1998.

[44] L. Guida, M. Annunziata, A. Rocci, M. Contaldo, R. Rullo, and A. Oliva, "Biological response of human bone marrow mesenchymal stem cells to fluoride-modified titanium surfaces," *Clinical Oral Implants Research*, vol. 21, no. 11, pp. 1234–1241, 2010.

[45] S. Lossdörfer, Z. Schwartz, L. Wang et al., "Microrough implant surface topographies increase osteogenesis by reducing osteoclast formation and activity," *Journal of Biomedical Materials Research Part A*, vol. 70, no. 3, pp. 361–369, 2004.

[46] P. Spyrou, S. Papaioannou, G. Hampson, K. Brady, R. M. Palmer, and F. McDonald, "Cytokine release by osteoblast-like cells cultured on implant discs of varying alloy compositions," *Clinical Oral Implants Research*, vol. 13, no. 6, pp. 623–630, 2002.

[47] M. Rödiger, H. Schliephake, E. McGlumphy, and K. Phillips, "Early loading of fluoride-modified implants in the posterior mandible—5-year-results," in *IADR*, San Diego, Calif, USA, 2011.

[48] C. Mertens and H. G. Steveling, "Early and immediate loading of titanium implants with fluoride-modified surfaces: results of 5-year prospective study," *Clinical Oral Implants Research*, vol. 22, no. 12, pp. 1354–1360, 2011.

[49] O. Geckili, E. Mumcu, and H. Bilhan, "Radiographic evaluation of narrow diameter implants after 5 years of clinical function a retrospective study," *Journal of Oral Implantology*. In press.

Hindawi Publishing Corporation
International Journal of Biomaterials
Volume 2012, Article ID 381535, 5 pages
doi:10.1155/2012/381535

Review Article

Effects of Surface Charges on Dental Implants: Past, Present, and Future

Cecilia Yan Guo, Jukka Pekka Matinlinna, and Alexander Tin Hong Tang

Department of Dental Materials Science, Faculty of Dentistry, University of Hong Kong, 34 Hospital Road, Sai Ying Pun, Hong Kong

Correspondence should be addressed to Jukka Pekka Matinlinna, jpmat@hku.hk

Received 20 March 2012; Accepted 12 September 2012

Academic Editor: Carlos Nelson Elias

Osseointegration is a major factor influencing the success of dental implantation. To achieve rapid and strong, durable osseointegration, biomaterial researchers have investigated various surface treatment methods for dental subgingival titanium (Ti) implants. This paper focuses on surface-charge modification on the surface of titanium dental implants, which is a relatively new and very promising methodology for improving the implants' osseointegration properties. We give an overview on both theoretical explanations on how surface-charge affects the implants' osseointegration, as well as a potential surface charge modification method using sandblasting. Additionally, we discuss insights on the important factors affecting effectiveness of surface-charge modification methods and point out several interesting directions for future investigations on this topic.

1. Introduction

A major factor that determines the success of dental implantation is *osseointegration*, which is the stable anchorage of an implant in living bone achieved by direct bone-to-implant contacts [1, 2]. Osseointegration derives from the Greek *osteon* (*bone*) and the Latin verb *integrare* (to make whole). The term refers to the direct structural and functional connection between living bone tissues and the surface of a load-bearing dental subgingival implant. Per-Ingvar Brånemark (b. 1929), a Swedish orthopaedic surgeon and research professor acknowledged as the "father" of modern dental implantology, proposed that titanium (Ti) implants integrate such that the bone is laid very close to the implant without any intervening connective tissue. It was shown that the titanium dioxide, TiO_2, layer permanently fuses with the bone, as Brånemark et al. showed in 1950s [3].

High-quality osseointegration stand for an accelerated healing process, high stability, and durability of the dental implant. This paper focuses on dental implants made of titanium and its alloys, which are commonly used due to their superior mechanical and biological properties. Using current materials and techniques, a titanium dental implant requires several months to osseointegrate with its adjacent bone. Moreover, the osseointegration is incomplete: analysis of retrieved titanium implants shows that the bone-to-implant attachment is far from perfect; in particular, the percentage of bone-to-implant contact area averages 70%–80%, with a minimum of 60%, even for successful implants that had lasted for up to 17 years [4]. Therefore, much room remains for the improvement of the surface quality of a titanium dental implant, in terms of the rate and strength of its osseointegration.

In light of this goal, it is crucial to understand the interactions between the host bones and the titanium implant in a living body which occurs mostly in the bone-implant interface. Both *in vitro* and *in vivo* studies showed that such interactions depend mainly upon the implant's surface characteristics [5]. Major aspects of the implant's surface characteristics include, but not limited to, surface morphology, surface chemistry, and surface energy, which significantly affect the initial bone cells' response to the implant at the bone-implant interphase [6].

Based on this theory, considerable work has been done to investigate various surface modification methods to improve the osseointegration of a titanium dental implant, such as surface-roughening (e.g., sandblasting and/or acid-etching) and coating, for example, with hydroxyapatite (HA),

$Ca_{10}(PO_4)_6(OH)_2$, to improve the implant's bioactivity [5]. However, most existing methods incur some drawbacks. For instance, surface roughening methods often lead to increased soft-tissue growth onto the bone-implant interface [5], which negatively affects the contact between the implant and its host bone. On the other hand, the HA coating layer tends to disintegrate under certain circumstances, which causes cracks on the implant's surface [5]. Hence, researchers are still searching for new surface-treatment methods that avoid the above drawbacks. For instance, the use of direct silanization of polished Ti has been studied and proposed as a coating method [7].

The surface energy of a biomaterial is determined by the material's surface-charge density and the net polarity of the charge. Compared to an electrically neutral surface, a surface with net positive or negative charge may be more hydrophilic [8]. The surface-charge of a dental implant is known to be a key factor to guild bone cells adhesion and early stage bone mineralization in the bone-implant interface. Thus, surface-charge modification seems to be a promising new direction for improving the osseointegration of a titanium dental implant. Although surface-charge modification is a relatively new methodology, it has been rapidly gaining research attention in recent years. The main challenge, however, lies in effective modification of the surface-charge of the dental implant material. The main objective, hence, is to develop effective and practical techniques that create a long-lasting electric field on the implant's surface, in order to promote the implant's osseointegration without incurring the drawbacks of existing surface-treatment methods.

1.1. Titanium Surface: Oxides. Titanium (Ti) is the most widely used metallic material for dental subgingival implants, due to its invaluable and outstanding biomedical and biomechanical properties. These are its availability, high biocompatibility, high strength and stiffness and, relatively low density. More importantly, titanium implants are known to osseointegrate with living bone tissues. Ti is recognized for its high strength-to-weight ratio. Titanium is a strong metal with low density, and especially in oxygen-free circumstances it is also quite ductile. Ti is lustrous, metallic-white in color and it is paramagnetic, having fairly low thermal and electrical conductivity [9]. Ti is also a material of choice in prosthetic dentistry and Ti resin bonding is promoted using silica-coating methods [10].

Although the so-called commercially pure Ti has acceptable mechanical properties and has been used for orthopaedic and dental subgingival implants, for most applications titanium is alloyed with small amounts of Al and V, typically 6 wt-% and 4 wt-%, respectively. Such Ti alloy is Ti-6Al-4V (a.k.a Ti6Al4V or Ti 6–4), is the most commonly used Ti-alloy. It has a chemical composition of 6% Al, 4% V, ≤0.25% Fe (maximum), ≤0.2% O_2, and the balance Ti. Commercially pure (c.p. Ti) is available in four grades where the oxygen content varies between 18 wt-% and 0.40 wt-% and Fe content between 0.20 wt-% and 0.50 wt-%. The apparently slight concentration differences have, however, a substantial effect on the physical and mechanical properties of c.p. Ti. At RT c.p. Ti has a hexagonal close-packed (h.c.p.) crystal lattice and is called the α-Ti (*so-called* α-phase). On heating, an allotropic phase transformation occurs: at 883°C, it forms a body-centered cubic (b.c.c.) lattice, labeled as β-phase. Ti is a reactive metal: in air and aqueous electrolytes, it forms spontaneously a dense oxide film at its surface.

Ti is a dimorphic metal: the α-form has a hexagonal structure below 882.5°C, while the β-form stays body-centered cubic above 882.5°C. Ti is brittle when cold, and malleable when hot, however, it can be ductile only when it is free of oxygen. On the other hand, traces of nitrogen or oxygen increase its strength. It is attacked by acids only on heating, and nitric acid, HNO_3, oxidized Ti to TiO_2. Melting Ti is cumbersome because at 800°C it combines with nitrogen which sets high requirements for casting Ti—a protective atmosphere is vital. Ti forms alloys with Al, Cr, Co, Cu, Fe, V, Fe, Ni and Sn [11].

Titanium is highly biocompatible, as a result of low-toxicity and a low rate of ion release from its surface non-toxic, and it is not rejected by the body [5]. Such properties are unanimously understood to be the consequence of an inert surface oxide film. When pure titanium or its alloys are exposed to air, a layer of titanium dioxide, TiO_2, with a thickness of approximately 2–5 nm can often be formed in a few seconds. This thin film also protects the titanium materials, making the latter highly resistant to corrosion. TiO_2 is insoluble in water and dilute acids but slowly dissolves in concentrated sulphuric acid. Several phases containing between 63.6–65.5 atom-% of oxygen have been indentified: these Ti oxides are of formulae $TiO_{1.752}$ to $TiO_{1.902}$. Titanium (III) oxide, Ti_2O_3, behaves as a basic oxide, and is prepared by heating TiO_2 with carbon. Ti_2O_3 is a violet powder. Interestingly, Ti oxide with the valence +2, TiO, shows marked nonstoichiometry in its composition. At elevated temperatures, at around 1400°C, TiO has a defect crystal lattice over the composition range $TiO_{0.64}$ to $TiO_{1.27}$ and electrical neutrality is preserved in the crystal by changes in the charges on the Ti ions. Also oxides, such as Ti_3O_5 and Ti_2O, have been detected and identified in special circumstances at elevated temperatures [9, 12].

2. Surface-Charge Modification for Titanium Dental Implants

2.1. Surface-Charge and Apatite-Layer Formation. A special group of biomaterials, including bioactive glass and glass-ceramics, have the ability to form direct bonding with bone. When such materials are inserted into living body, an intermediate biologically active bone-like apatite layer starts to form in the material-bone interface, through which the material can bond to bone [13]. Several previous studies conjecture that the formation this apatite layer on the implant's surface is a prerequisite for the implant to bond to living bone in a biological environment [14, 15]. Metals, including titanium and its alloys, cannot directly bond effectively to living bone. In order to build such bonds, various methods have been proposed to coat ceramic materials onto titanium dental implants, which help to form

a biologically active bone-like apatite layer [16]. Bioactive retention can be achieved in cases where the implant is coated with bioactive materials such as hydroxyapatite. These bioactive materials stimulate bone formation leading to a physicochemical bond: the implant is anchylosed with the bone. However, as we mentioned before, the coating layer (e.g., HA) may easily peel off from its underlying titanium alloy. An alternative approach overcomes this problem by enabling titanium materials themselves to form a bone-bonding layer. Using TiO_2 gel, Li et al. successfully induced bone-like apatite formation on titanium-based material in simulated body fluid [13]. This result shows that it is possible for titanium and its alloys to form an apatite layer though appropriate treatments.

It has also been shown that NaOH-etched and subsequently heat-treated titanium possesses the ability to directly form an apatite layer, which has been applied to artificial hip joints, and clinically used in Japan since 2007 [17]. This phenomenon is explained by the electrostatic interactions of sodium titanate, $Na_2Ti_3O_7$, on the titanium material's surface with ions in the living body [16, 18]. The above treatment produces a negatively charged sodium titanate layer on the surface of the titanium material, which attracts positively charged Ca^{2+} ions. Ca^{2+} ions exhibit higher binding affinity compared to other cations such as K^+, Na^+, and Mg^{2+}; consequently, Ca^{2+} are predominantly absorbed on a negatively charged biomaterial surface in a biological environment. After Ca^{2+} ions accumulate on the biomaterial's surface, the surface becomes positively charged; hence, the surface starts to attract negatively charged phosphate ions, which react with the Ca^{2+} ions to form a calcium phosphate (i.e., a type of apatite) layer [17]. This calcium phosphate layer takes an amorphous structure after its formation, and it subsequently transforms into more stable crystalline apatite.

Ever since the invention of surface-treatment methods for inducing the apatite-forming ability of titanium materials, it is believed that a negatively charged surface is essential to obtain a bioactive material with good osseointegration properties [19]. A large number of research papers have emphasized the importance of surface-charge in the formation of the apatite layer, as well as in the surface interactions between the titanium material and the biologic environment [13, 20–24]. Li et al. illustrate that a successful apatite inducer for titanium implants could be a material which has and/or develops both negative surface-charge and abundant OH^- groups in physiologically related fluid; such materials can thus be considered as candidates to serve for bone-bonding materials [13].

While it is widely agreed that negative surface-charge is more effective for promoting bone-implant interaction of titanium dental implants, some researchers hold the view that positive surface-charge may also be of help. For instance, it is reported that a positively charged titanium implant can develop a bone-like apatite layer [25].

2.2. Surface-Charge and Cell Reactions. The osseointegration of a dental implant material depends upon the cell reactions of the material, especially cell adhesion onto its surface. Cell attachment, adhesion, and spreading are the first phase of the interactions between the host cells and the implant. These reactions affect the cells' capacity to stay and proliferate on the implant's surface, and subsequently generate bone tissues surrounding the implant [26]. Cell-implant interactions depend upon the implant's surface topography, chemistry and surface energy. These properties do not only determine the adhesion of cells, but also the orientation of adsorbed molecules [8]. As described in Section 2.1, the surface energy of a material is related to the material's surface-charge. Thus, previous research has investigated the influence of the effect of implant's surface-charge on the cell reactions to the implant. It was found that on a negatively charged biomaterial surface, cells proliferate more actively; meanwhile, multiple layers of cells and enlarged colonies of osteoblast-like cells were also observed [27]. In contrast, cell adhesion and proliferation on positively charged biomaterial were found to be subdued [27].

When a biomaterial is inserted into living body, it absorbs proteins before cells adhere to its surface [28, 29]. Once attached on the material's surface, proteins can mediate cell-implant interactions [28, 29]. Cells, such as osteoblasts and fibroblasts, mainly interact with the adsorbed proteins, rather than with the implant material itself. For such cells, the implant's surface-charge influences their reactions to the implant, by affecting the type and amount of proteins attached on its surface [30].

In a biological environment, all chemical substances surrounding an electrically neutral implant, including organic and inorganic ions, proteins, ionic groups, and amino acids, have equal opportunity to contact and accumulate on implant's surface. On the other hand, a charged implant surface can induce electrical attraction or repulsion between the implant's surface and the surrounding chemical species, depending on their polarity. For example, as explained in Section 2.1, Ca^{2+} ions have superior binding affinity to a negatively charged biomaterial surface and accumulate on them [31]. Besides the effect on crystal nucleation, another significant role of Ca^{2+} is to attract cell-adhesion proteins (e.g., integrins, fibronectin, and osteonectin), which are characterized by their capacity to interact with a specific ligand [27]. These proteins significantly affect the attachment, adhesion, and spreading of osteoblasts, the cells that form bony tissues [26]. Consequently, osteoblasts attach and proliferate on a matrix grown on the bone-like apatite layer formed with Ca^{2+} ions [27], which may result in faster and stronger bone-to-implant bonding. In contrast, a positively charged implant surface attracts anionic groups which act as antiadhesive molecules, which negatively affect osteoblast adhesion [27].

Titanium naturally has a dense layer of TiO_2 of several nanometers thick on its surface. In a biological environment (typical with pH = 7.4), the surface-charge of this TiO_2 layer appears to be only slightly negative. Hence, researchers have devoted efforts to create a long-lasting, negative electric field on the titanium dental implant's surface.

2.3. Sandblasting and Titanium Surface-Charge. Sandblasting is a simple and commonly used surface-treatment method for titanium dental implants, and it has been shown

to accelerate osteoblast attachment in a biological environment [26, 32], thereby enhancing the osseointegration of the treated titanium implants. Until recently, these desirable effects of sandblasting have been exclusively attributed to its roughening effect on the implant's surface. Guo et al.'s experiment reveals that current sandblasting techniques also generate a small amount of negative electric charge on the titanium material's surface [33]. Because negative surface-charge is commonly believed to promote osseointegration of a titanium material, this experiment suggests that sandblasting's favorable effects may, at least, be partially explained by this electrical phenomenon.

In Guo et al.'s experiment [33], Al_2O_3 grits were blasted using compressed air onto different groups of titanium plates. After the sandblasting, an electrostatic meter were place adjacent to each titanium plate to measure for static voltage on titanium plants, which is proportional to the amount of electrical charge on the plate's surface. The results show that immediately after sandblasting, the titanium plate exhibits negative static voltage, meaning that negative charge is present on the plate. The value of the static voltage (i.e., the amount of charge) is affected by the sandblasting duration, as well as environmental factors, such as atmospheric humidity.

The static charge generated by sandblasting, however, decays with time. In this study, immediately after sandblasting finishes, the static voltage of a titanium plate quickly decreases [33]. This voltage drop gradually slows down, until reaching a stable value, which is often a fraction of the initial voltage obtained by sandblasting. These findings suggest that there is abundant room for refinement of sandblasting's effect on the generation of surface-charge on titanium implants, which may promise significant improvement of the osseointegration properties of sandblasted titanium dental implants.

2.4. Future Research Work to Improve Surface-Charge Generation. As a simple and economical technique to generate surface-charge s on titanium surface, it may be of industrial interest to look into the research issues of sandblast-induced surface-charge. Although exploratory work has been done for enhancing the osseointegration of dental implants through sandblast-induced surface-charge modification, there remain several interesting directions of work that are worth of further investigations. On the theoretical side, better understanding of the underlying mechanism for charge generation during sandblasting is important. To be more precise, it is crucial to understand where the electrical charge comes from, why and how the charge remains on the titanium surface, how much charges are needed, and the factors that affect the amount of charge generated during the sandblasting process. Such insights help us design and develop better techniques for sandblast-induced surface-charge generation.

On the practical side, since a typical dental implant takes the complex shape of a screw, it is of major interest to study the distribution of charge on the dental implant's surface. This information is critical for targeted charge strengthening on a screw. Another critical task is to retain the negative charge on the implant's surface, in order to further improve its osseointegration property. As reviewed in previous sections, the electrical charge that remains on the sandblasted titanium materials' surface gradually dispersed into the atmosphere. Therefore, two possible methodologies for the retention of the negative charge on the implant's surface are (i) generation of a higher amount of sufficient initial negative charges to allow for natural decay of charges up to the expiration date of the implant product, and/or (ii) to retain the surface-charge of the implant after an initial charging step. These approaches must, at the same time, be compatible to the therapeutic level of charges present at the moment of implant insertion to the patient.

Regarding the specific technique of generating charge through sandblasting-induced surface-charge, yet another industrial interesting direction for further study is to investigate the major parameters for the sandblasting that influence the generation of surface-charge for on the titanium dental implant. Example of such factors includes the materials used in blasting the implant, the size of the grits, and the blasting speed. Furthermore, it is interesting to study whether acid etching, which is commonly applied together with sandblasting, can help improving the surface-charge of the titanium implant.

3. Conclusion

This paper has summarized our current knowledge about the role of surface-charge on the osseointegration properties of titanium dental implants, and reviewed the state-of-the-art surface-charge modification methods for such implants. Specifically, we have described two known mechanisms for surface-charge to affect the implants' osseointegration, that is, by forming an apatite layer, and by attracting certain types of proteins with desirable reactions from bone-forming cells. Regarding surface-charge modification methods, we have presented a recently proposed original work on the modification of the surface-charge of titanium materials through sandblasting, and pointed out several important directions on this topic for further investigations to enable this technique practically.

Acknowledgments

The authors would like to thank the Graduate School of the University of Hong Kong and the Prince Philip Dental Hospital for their continuous support.

References

[1] T. Albrektsson and C. Johansson, "Osteoinduction, osteoconduction and osseointegration," *European Spine Journal*, vol. 10, no. 2, pp. S96–S101, 2001.

[2] S. Kakuta, K. Miyaoka, S. Fujimori, W. S. Lee, T. Miyazaki, and M. Nagumo, "Proliferation and differentiation of bone marrow cells on titanium plates treated with a wire-type electrical discharge machine," *The Journal of oral implantology*, vol. 26, no. 3, pp. 156–162, 2000.

[3] P. I. Brånemark, G. A. Zarb, and T. Albreksson, "Tissue-integrated prostheses. osseointegration in clinical dentistry,"

Plastic & Reconstructive Surgery, vol. 77, no. 3, pp. 496–497, 1986.

[4] T. Albrektsson, A. R. Eriksson, B. Friberg et al., "Histologic investigations on 33 retrieved nobelpharma implants," *Clinical Materials*, vol. 12, no. 1, pp. 1–9, 1993.

[5] C. Y. Guo, A. T. H. Tang, and J. P. Matinlinna, "Insights into surface treatment methods of titanium dental implants," *Journal of Adhesion Science & Technology*, vol. 26, pp. 189–205, 2012.

[6] I. F. Amaral, A. L. Cordeiro, P. Sampaio, and M. A. Barbosa, "Attachment, spreading and short-term proliferation of human osteoblastic cells cultured on chitosan films with different degrees of acetylation," *Journal of Biomaterials Science, Polymer Edition*, vol. 18, no. 4, pp. 469–485, 2007.

[7] J. P. Matinlinna, S. Areva, L. V. J. Lassila, and P. K. Vallittu, "Characterization of siloxane films on titanium substrate derived front three aminosilanes," *Surface and Interface Analysis*, vol. 36, no. 9, pp. 1314–1322, 2004.

[8] B. D. Boyan, T. W. Hummert, D. D. Dean, and Z. Schwartz, "Role of material surfaces in regulating bone and cartilage cell response," *Biomaterials*, vol. 17, no. 2, pp. 137–146, 1996.

[9] C. F. Bell and K. A. K. Lott, *Modern Approach To Inorganic Chemistry*, Butterworths, London, UK, 3rd edition, 1972.

[10] J. P. Matinlinna and P. K. Vallittu, "Silane based concepts on bonding resin composite to metals," *Journal of Contemporary Dental Practice*, vol. 8, no. 2, pp. 001–008, 2007.

[11] R. B. Heslop and P. L. Robinson, *Inorganic Chemistry*, Elsevier, Amsterdam, The Netherlands, 3rd edition, 1967.

[12] R. J. H. Clark, *The Chemistry of Titanium and Vanadium*, Elsevier, Amsterdam, The Netherlands, 1968.

[13] P. Li, C. Ohtsuki, T. Kokubo, K. Nakanishi, N. Soga, and K. De Groot, "The role of hydrated silica, titania, and alumina in inducing apatite on implants," *Journal of Biomedical Materials Research*, vol. 28, no. 1, pp. 7–15, 1994.

[14] L. L. Hench, "Bioceramics: from concept to clinic," *Journal of the American Ceramic Society*, vol. 74, no. 7, pp. 1487–1510, 1991.

[15] T. Kokubo, "Bioactive glass ceramics: properties and applications," *Biomaterials*, vol. 12, no. 2, pp. 155–163, 1991.

[16] H. M. Kim, F. Miyaji, T. Kokubo, and T. Nakamura, "Preparation of bioactive Ti and its alloys via simple chemical surface treatment," *Journal of Biomedical Materials Research*, vol. 32, no. 3, pp. 409–417, 1996.

[17] D. K. Pattanayak, T. Kawai, T. Matsushita, H. Takadama, T. Nakamura, and T. Kokubo, "Effect of HCl concentrations on apatite-forming ability of NaOH-HCl- and heat-treated titanium metal," *Journal of Materials Science*, vol. 20, no. 12, pp. 2401–2411, 2009.

[18] S. Nishiguchi, S. Fujibayashi, H. M. Kim, T. Kokubo, and T. Nakamura, "Biology of alkali- and heat-treated titanium implants," *Journal of Biomedical Materials Research A*, vol. 67, no. 1, pp. 26–35, 2003.

[19] T. Kokubo, D. K. Pattanayak, S. Yamaguchi et al., "Positively charged bioactive Ti metal prepared by simple chemical and heat treatments," *Journal of the Royal Society Interface*, vol. 7, no. 5, pp. S503–S513, 2010.

[20] P. Ducheyne, P. Bianco, S. Radin, and E. Schepers, "Bioactive materials: mechanisms and bioengineering considerations," in *Bone Bioactive Biomaterials*, P. Ducheyne, T. Kokubo, and C. A. van Blitterswijk, Eds., pp. 1–12, Reed Healthcare Communications, Leiderdorp, The Netherlands, 1993.

[21] P. Ducheyne and J. M. Cuckler, "Bioactive ceramic prosthetic coatings," *Clinical Orthopaedics and Related Research*, no. 276, pp. 102–114, 1992.

[22] L. L. Hench and E. C. Ethridge, *Biomaterials: An Interfacial Approach*, Academic Press, New York, NY, USA, 1982.

[23] T. Kokubo, "Bioactivity of glasses and glass ceramics," in *Bone-Bonding Materials*, P. Ducheyne, T. Kokubo, and C. A. van Blitterswijk, Eds., pp. 31–46, Reed Healthcare Communications, Leiderdorp, The Netherlands, 1992.

[24] P. Li and F. Zhang, "The electrochemistry of a glass surface and its application to bioactive glass in solution," *Journal of Non-Crystalline Solids*, vol. 119, no. 1, pp. 112–118, 1990.

[25] D. A. Puleo and A. Nanci, "Understanding and controlling the bone-implant interface," *Biomaterials*, vol. 20, no. 23-24, pp. 2311–2321, 1999.

[26] K. Anselme, "Osteoblast adhesion on biomaterials," *Biomaterials*, vol. 21, no. 7, pp. 667–681, 2000.

[27] M. Ohgaki, T. Kizuki, M. Katsura, and K. Yamashita, "Manipulation of selective cell adhesion and growth by surface charges of electrically polarized hydroxyapatite," *Journal of Biomedical Materials Research*, vol. 57, no. 3, pp. 366–373, 2001.

[28] J. D. Andrade, "Principles of protein adsorption," in *Surface and Interfacial Aspects of Biomedical Polymers*, J. D. Andrade, Ed., pp. 1–80, Plenum Press, New York, NY, USA, 1985.

[29] J. L. Brash and T. A. Horbett, "Proteins at interfaces: current issues and future prospects," in *Proteins at Interfaces: Physicochemical and Biochemical Studies*, J. L. Brash and T. A. Horbett, Eds., pp. 1–33, American Chemical Society, Washington, DC, USA, 1987.

[30] K. A. Hing, "Bone repair in the twenty-first century: biology, chemistry or engineering?" *Philosophical Transactions of the Royal Society A*, vol. 362, no. 1825, pp. 2821–2850, 2004.

[31] S. Shimabayashi, C. Tamura, and M. Nakagaki, "Adsorption of hydroxyl ion on hydroxyapatite," *Chemical & Pharmaceutical Bulletin*, vol. 29, no. 11, pp. 3090–3098, 1981.

[32] S. K. Nishimoto, M. Nishimoto, S. W. Park et al., "The effect of titanium surface roughening on protein absorption, cell attachment, and cell spreading," *International Journal of Oral and Maxillofacial Implants*, vol. 23, no. 4, pp. 675–680, 2008.

[33] C. Y. Guo, J. P. Matinlinna, and A. T. H. Tang, "A novel finding of sandblasting's effect on titanium surface—static charges generation," *Journal of Adhesion Science & Technology*, vol. 26, no. 23, pp. 2603–2613, 2012.